THE EFFECT OF ELECTRON BEAM RADIATION ON THE DEGRADATION OF BIOPOLYMERS

LOO SAY CHYE, JOACHIM

SCHOOL OF MATERIALS ENGINEERING AND SCIENCE

NANYANG TECHNOLOGICAL UNIVERSITY

2005

THE EFFECT OF ELECTRON BEAM RADIATION ON THE DEGRADATION OF BIOPOLYMERS

Loo Say Chye, Joachim

School of Materials Science and Engineering

A thesis submitted to the Nanyang Technological University in fulfillment of the requirement for the degree of Doctor of Philosophy

2005

Abstract

The study of the effects of electron beam (e-beam) radiation on PLGA and PLLA and their subsequent hydrolytic degradation characteristics were reported in this thesis. The objective is to investigate the use of e-beam radiation as a means to control and fine-tune the hydrolytic degradation time of these biopolymers. The results obtained show conclusive evidence that PLGA and PLLA degrade through chain scission when exposed to e-beam irradiation in the presence of air, through two main degradation mechanisms of backbone main chain scission and hydrogen abstraction. The presence of a crystalline phase could however arrest this radiation-induced degradation process. The decrease in average molecular weights results in changes in the physiochemical properties of these biodegradable polyesters. The decrease in average molecular weights were observed to follow a linear relationship with radiation dose. Irradiated samples of PLGA and PLLA, when hydrolytically degraded, were observed to degrade faster than the non-irradiated samples. This was due to a higher water uptake, resulting from a lower T_g and the formation of more hydrophilic hydroxyl end groups, with irradiation. The increase in water uptake leads to an increase in osmotic pressure and subsequently an increase in mass loss due to microcavitation and osmotic cracking. A modeled relationship between radiation dose and the hydrolytic degradation time, through their molecular weights, was established for both PLGA and PLLA. This relationship allows for a more accurate and precise control of the rate of hydrolytic degradation of PLGA and PLLA with e-beam radiation. It is concluded that e-beam radiation could therefore be used to control the hydrolytic degradation times of PLGA and PLLA.

Acknowledgements

The author would like to express his sincere gratitude to the following people who have played an important role in the author's accomplishments and completion of his PhD research and thesis:

My heart felt thanks to my supervisor, Professor Freddy Boey Yin Chiang, who is also the main initiator behind this research project. His key involvement saw the materializing of this research work; and his guidance and advice rendered were indeed indispensable for the completion of my PhD research.

Special thanks to my co-supervisor, Assistant Professor Ooi Chui Ping, for her relentless support, help and guidance throughout my PhD research work. Her invaluable advice and encouragement throughout my candidature is greatly appreciated.

I would like to thank Ms. Tan Hui Tong for her help in printing and compiling my thesis, on my behalf, during my 3 months attachment at Mayo Clinic.

Not forgetting the school manager (Ms Loreen Tan) all the technical staff (Nelson Ng, Serene Kok, Wilson Lim, Choo Yong Cheong, Samsudin), friends and colleagues of Biomaterials Lab and Advanced Materials Research Center (AMRC-B3) who have in one way or other contributed to the completion of my PhD research work.

Table of Contents

List of Figures

List of Tables

Chapter 1 Introduction

1.1 Background

The development of technology has always revolved around man's ability to use different materials at different eras and ages. Starting from the Stone Age, man has evolved through the Iron Age, the Bronze Age, till today, perhaps, the Polymer Age. With exciting developments surrounding polymers and its uses, man is now able to tap on the versatility of polymers, without compromise, and create new technology from it.

In the biomedical field, medical doctors are now working closely with engineers and scientists to create, invent and improve on existing medical facilities and to discover novel ways for the treatment of diseases, such as cancer and coronary heart diseases. Medical development is often hampered by the lack of understanding in materials science and now many see the need to tap on the potential of biomaterials for their use in the human body, or even for tissue engineering. With this in mind, research into biomaterials becomes inevitable for the advancement of medical science.

Biomaterials may be defined as synthetic materials used to replace part of a living system or to function in intimate contact with living tissue [1]. Biopolymers, a class of biomaterials, have been extensively studied for decades to meet such a function in the human body, and have become a very important material for many

applications in the biomedical field. Some of the more commonly known biopolymers include polyesters [2-6], such as the lactic/glycolic acid polymers.

More specific examples of such polyesters are poly(lactide-co-glycolide) (PLGA) and poly(L-lactide) (PLLA). They have been extensively used in biomedical and pharmaceutical applications for controlled drug delivery purposes [7], which include both sustained delivery and targeted delivery on a one time or sustained basis [7]. They have generated immense interest due to their favorable properties [7-11] such as excellent biocompatibility, biodegradability and good mechanical strength. PLGA and PLLA are biodegradable polymers because they degrade through hydrolysis of their ester bonds, into lactic and glycolic acids [8, 12-16]. As a result, they can be used as temporary implants or as drug carriers where they will eventually, through time, metabolized into water and carbon dioxide in vivo, making them to be potentially useful biomaterials, or more specifically, biopolymers. The rate of hydrolytic degradation of PLGA and PLLA is dependent on their physiochemical properties, such as molecular weight, degree of crystallinity and glass transition temperature (T_g) [8, 17-18].

Besides hydrolytic degradation of biopolymers, radiation has also been known to alter the physiochemical properties of polymers, through main-chain scission (degradation) or cross-linking (polymerization) [19, 20]. Although both processes will take place simultaneously in many polymers during irradiation, the dominance of chain scission over cross-linking will result in a reduction in molecular weight [21]. Whether the process will be characterized predominantly by either scission or

cross-linking depends on several factors [22, 23], which includes the chemical structure of the polymer, the amount of dosage and the environment of the material during irradiation. As a result, ionizing radiation, through polymerization and degradation, affects the service life of products [24, 25]. Therefore, radiation besides being a tool for sterilization can be used as a possible means to alter the properties of biodegradable polymers to control their hydrolytic degradation rate and time. This is extremely important for applications such as temporary implants (heart and urinary stents) and for controlled drug release.

1.2 Problem statement

There are numerous journal papers that discuss about the effects of radiation on polymers [23-33], which includes polyethylene [26, 27], polypropylene [28-30], poly(methyl methacrylate) [21], polycarbonates [31, 32], isobutylene-isoprene rubber [33] and even polyesters [23]. However, there are very few papers that report about the effects of radiation on biodegradable polymers [34-36]. Besides, these papers have also failed to discuss the radiation-induced degradation mechanisms during irradiation. One of the gaps of research is therefore the lack of an extensive research work conducted on the effects of radiation on biodegradable polymers, such as PLGA and PLLA. With regards to the papers that discussed the effects of radiation on biodegradable polyesters [34-36], very few have discussed the effects of radiation on the subsequent hydrolytic degradation behaviour of PLGA and PLLA.

Another gap of research is that most of these papers [26-30, 32-36], focused their work mainly on gamma irradiation, while ignoring the possible use of electron beam (e-beam) radiation, which this thesis aims to study. Gamma radiation is potentially harmful and requires stringent conditions and training for its usage. The choice of e-beam radiation over gamma radiation is that it is much safer and as a result, has been even widely used industrially for other applications, such as polymer curing [37-39]. Electron beam accelerators are also adequately shielded and provide better versatility in controlling the radiation dose. E-beam has lower penetration depths, making it more viable for irradiation of drug encapsulated polymers, where the irradiation of the encapsulated drugs can be prevented. It can also be delivered in a matter of seconds, saving time and costs and is thus an excellent choice for commercial usage.

The problem in the degradation of biodegradable polymers such as PLGA and PLLA can therefore be summarized as ‘the inability to control the degradation and life span of these polymers in an accurate manner’. The ability to do so would be especially useful for controlled drug release applications, where an accurate release of drugs can be achieved. It would also be useful in temporary implants, such as heart and urinary stents, where a complete degradation of the polymer after a specific known time period is desired. Though *Chu et al.* has done a comprehensive study describing the effects of radiation on the hydrolytic degradation behaviour of poly(glycolic acid) [40], the work conducted on poly(glycolic acid) is also not representative of other lactic/glycolic acid polymers, such as PLGA and PLLA. This thesis therefore aims to fill this gap by studying the hydrolytic degradation of

irradiated PLGA and PLLA. Since there are also currently no papers that explore the use of radiation as a means to control the rate of hydrolytic degradation and degradation time of biopolymers (PLGA and PLLA), it is therefore of interest to find a predictable and precise method to control the degradation time of these biopolymers, through the use of e-beam radiation.

1.3 Objectives

The focus of this thesis is to study the hydrolytic degradation of e-beam irradiated biopolymers, and the main objective is to investigate the use of e-beam radiation as a means to control and fine-tune the degradation time of biopolymers. In fulfilling this main objective, the research work was divided into three major parts.

The first part is to conduct an in-depth study on the radiation-induced degradation of PLGA and PLLA, using e-beam radiation. Here, it is first required to investigate the changes in the physiochemical properties of these biopolymers with radiation dose. A thorough understanding of the changes to the properties of these polymers would then allow a deeper appreciation of how radiation may affect their hydrolytic degradation behaviour. The radiation-induced degradation mechanisms will also be thoroughly studied, to support the observations made and to provide additional information on the possible hydrolytic degradation behaviours of irradiated polymers. Further studies will also be done to examine how crystals can be used to retard the radiation-induced degradation of PLGA.

The second part is to study the hydrolytic degradation behavior of irradiated PLGA and PLLA. This will be achieved, firstly, by analyzing the rate of hydrolytic degradation of the irradiated biopolymers, through their water uptake, mass loss and degradation rate constants. The changes to the physiochemical properties of these polymers after hydrolytic degradation will also be further investigated.

The third part is to model the hydrolytic time and life span of PLGA and PLLA to radiation dose. This will be achieved by combining the results obtained from the first and second parts. At the end of this thesis, it would then be determined if radiation can be used as a means to control and fine-tune the hydrolytic degradation time of biopolymers.

1.4 Scope

In this work, only the following lactic/glycolic acid polymers will be studied, namely PLGA and PLLA. These polyesters were chosen because of their favorable properties such as good biocompatibility, biodegradability and mechanical strength [8, 9], resulting in their extensive use in various biomedical applications [5, 6, 9, 10, 16, 17, 41-42]. They are also promising candidates for controlled drug release applications [2-11].

E-beam radiation will be studied and the radiation dose will range from 2.5 Mrad to 50 Mrad, to provide a sufficiently broad dose spectrum of the effects of radiation on

the polymers. The study by *Birkinshaw et al.* on the hydrolytic degradation of irradiated poly-D-L-lactide only conducted the study up to a maximum dose of 10 Mrad [36], which is certainly insufficient in determining the use of radiation to control the hydrolytic degradation of these polymers.

The research will be restricted to only polymeric thin films of PLGA and PLLA, since e-beam radiation is depth dependent and the sample thickness is critical. It is also noted that most biomedical applications are in the form of polymeric thin films, such as heart and urinary stents; and for drug encapsulated polymers, the polymer is usually thin-walled. Thus, the use of thin films is substantiated in view of these applications.

The physiochemical properties that are of interests in this study are the average molecular weights, the thermal properties, and the morphological properties. These properties will be studied since the hydrolytic degradation rates and behaviour of these polymers is highly dependent on these physiochemical properties [8, 17-18].

The study of crystals in the retardation of radiation-induced degradation will be conducted only on amorphous PLGA, since PLLA is a semi-crystalline polymer and annealing has little changes on the degree of crystallinity for PLLA. Amorphous PLGA and semi-crystalline PLGA can be prepared, and the varying degree of crystallinity of semi-crystalline PLGA can be easily controlled. The effects of crystals in retarding radiation-induced degradation will then be investigated.

The irradiated PLGA and PLLA would then undergo in-vitro hydrolytic degradation. For the in-vitro hydrolytic degradation, the irradiated films will be incubated at 37°C in phosphate buffer solution (PBS) for over a period of 12 weeks for PLGA and 26 weeks for PLLA, to allow for complete degradation of these biopolymers.

Chapter 2 Literature Review

2.1 Background

2.1.1 Lactic/glycolic acid polymers

Lactic/glycolic acid polymers are generally classified as polyesters [2-4] or aliphatic polyesters [5, 6]. The homo-polymers or co-polymer of lactic/glycolic acid polymers are usually named poly(lactic acid), poly(glycolic acid) and poly(lactic-co-glycolic) acid. Lactic/glycolic acid polymers can be categorized into low molecular weight polymers or oligomers and high molecular weight polymers. The difference between the high and low molecular weight polymers arises from their methods of synthesis. The low molecular weight lactic/glycolic acid polymers are synthesized by condensation polymerization, whereas high molecular weight lactic/glycolic acid polymers are synthesized by ring-opening polymerization [8]. The advantages of this ring-opening polymerization method are, there is no dehydration needed in the polymerization system, the polymers can be readily purified, and the stoichiometry of monomers to repeat units of the polymer is guaranteed [8]. These high molecular weight lactic/glycolic acid polymers are often named poly(lactide-co-glycolide) (**Figure 2.1**), poly(lactide) (**Figure 2.2**) and poly(glycolide).

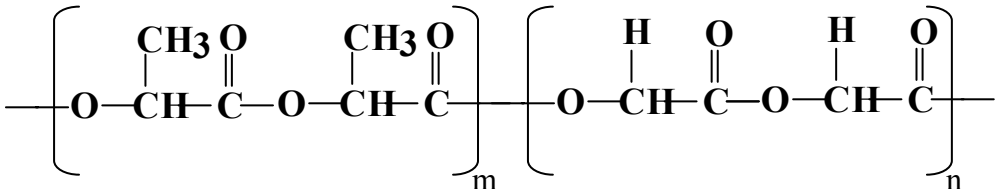

Figure 2.1 - Chemical structure of poly(lactic-co-glycolic acid) (PLGA)

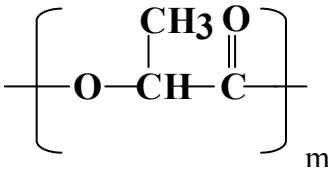

Figure 2.2 – Chemical structure of poly(L-lactic acid) (PLLA)

2.1.2 Physiochemical properties of lactic/glycolic acid polymers

(a) Composition of lactic acid to glycolic acid

Unlike glycolic acid, which contains only symmetric carbon atoms, lactic acid has one asymmetric carbon atom and is thus, a chiral molecule that exists as two optical isomers, namely D-lactic acid and L-lactic acid. When two lactic acid molecules combine to form the cyclic lactide dimer, three possible stereoisomers can be formed: D-lactic acid, L-lactic acid, and meso-lactide, which is made of a D-lactic acid moiety and an L-lactic acid moiety, as illustrated in **Figure 2.3**. In addition, an equimolar mixture of D-lactic and L-lactic forms D,L-lactic acid [43]. Each of these polymers has their own distinct properties and can even differ in their ability to

crystallize. The polymers derived from the optically active D-lactide or L-lactide are semi-crystalline, whereas those derived from the optically inactive meso-lactide or D,L-lactide are amorphous [8]. Poly(D-lactic acid), poly(L-lactic acid) and poly(glycolic acid) are semi-crystalline due to the high regularity of their polymer chains. Of the three, poly(glycolic acid) has the highest crystallinity because it does not have a methyl side group of the poly(lactic acids). This makes packing easier and thus, promotes crystallinity.

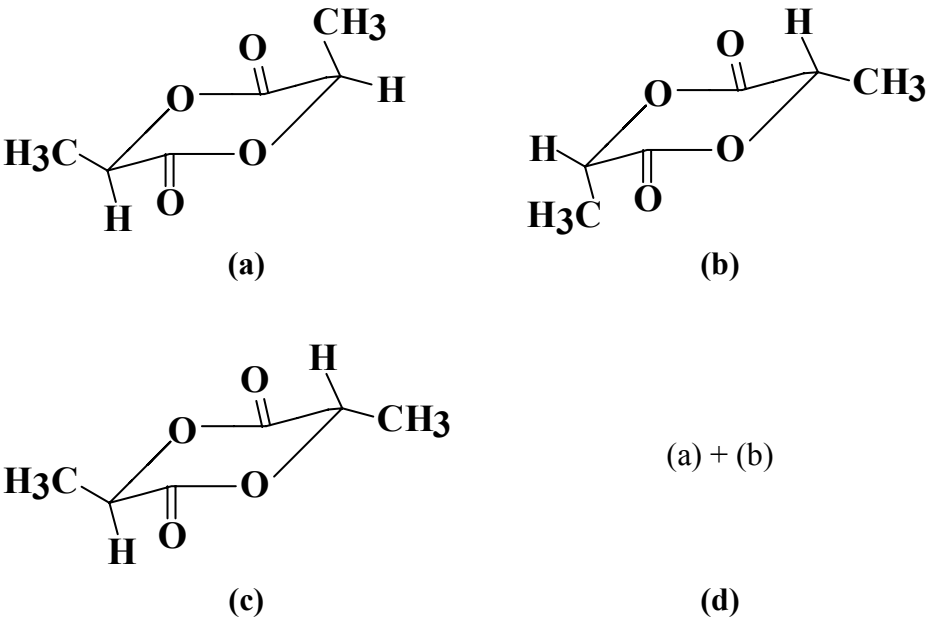

Figure 2.3 – Stereostructure of lactide isomers: (a), D-lactide; (b), L-lactide; (c), meso-lactide; (d), D,L-lactide

(b) Molecular weight and polydispersity

Molecular weight is used essentially in characterizing lactic/glycolic acid polymers. The molecular weight and polydispersity affects the mechanical strength and its degradation rate [8, 44, 45]. Factors that affect the molecular weight of the polymer include monomer purity, polymerization temperature, polymerization time, catalyst concentration and addition of chain transfer agents [8]. Since the molecular weight of PLGA and PLLA affects their rate of hydrolytic degradation, the ability to accurately control their molecular weights may be a means to control their degradation rates and behaviours.

The molecular weight of polymers is usually expressed as the number average (M_n) and weight average (M_w) molecular weight. The ratio of M_w to M_n is a useful indicator of the molecular weight distribution or polydispersity. This polydispersity index indicates the polymerization termination reaction [46] and can also monitor the rate of polymer hydrolysis [8]. For many polymers, a narrower molecular distribution or a smaller polydispersity index yields better properties [47].

(c) Crystallinity and melting point

Crystallinity is another important property in the characterization of lactic/glycolic acid polymers, and is affected by several factors, including chain regularity [44] and molecular weight [48]. Apart from the intrinsic susceptibility of a given polymer to have crystalline region, the processing history of a polymer, such as its heating and

cooling rate, also has significant effects on its crystallinity [49]. The percentage or degree of crystallinity (DOC) reflects the extent of formation of crystalline regions within a polymer matrix, and can affect the mechanical strength of the polymer, which can determine the end applications of the polymer [40]. The DOC also affects the swelling behaviour of a polymer and its capability to undergo hydrolysis, and consequently, its rate of degradation [8, 17-18].

X-ray diffraction (WAXD) and the differential scanning calorimetry (DSC) are two most frequently used techniques in the determination of the extent of polymer crystallinity. The melting temperature (T_m) of semi-crystalline polymers can be determined by DSC. The melting points of lactic/glycolic acid polymers change with the monomer ratios of L-lactic acid to glycolic acid, as illustrated in **Figure 2.4** [8]. It is also noted by *Jamshidi et al.* that the increase in molecular weight also result in an increase in T_m [50].

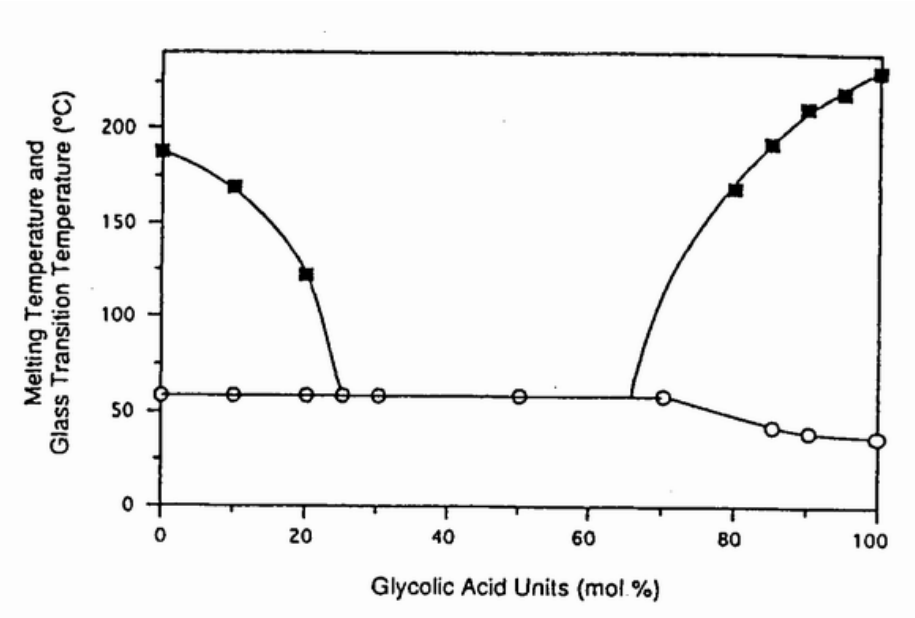

Figure 2.4 – Melting points (■) and glass transition temperatures (o) as a function of glycolic acid units composition for poly(L-lactic-co-glycolic acid) [8]

(d) Chain mobility and glass transition temperature

Both homo- and co-polymers of lactic/glycolic acid polymers normally have glass transition temperature (T_g) above physiological temperature (37°C). Thus, they have fairly rigid chain structure, which gives them significant mechanical strength. Generally, the lower the T_g the higher is the permeability of a given type of polymer [51]. As a result, the T_g affects the rate of hydrolysis and degradation [8, 17-18].

The T_g of the polymer is related to its molecular weight through a theoretical analysis of *Fox and Flory* [52].

$$T_g = T_{g,\infty} - K/M \qquad \textbf{(Eq. 2.1)}$$

where M is the molecular weight, $T_{g,\infty}$ is the glass transition temperature at infinite molecular weight, and K is a constant depending on the polymer. The T_g of lactic/glycolic acid polymers therefore, increases with the increase in molecular weight [8, 52], as illustrated in **Figure 2.5** [8]. The increase in the lactic acid content was also found to increase T_g [8]. In general, a polymer with higher T_g has lower chain mobility [8].

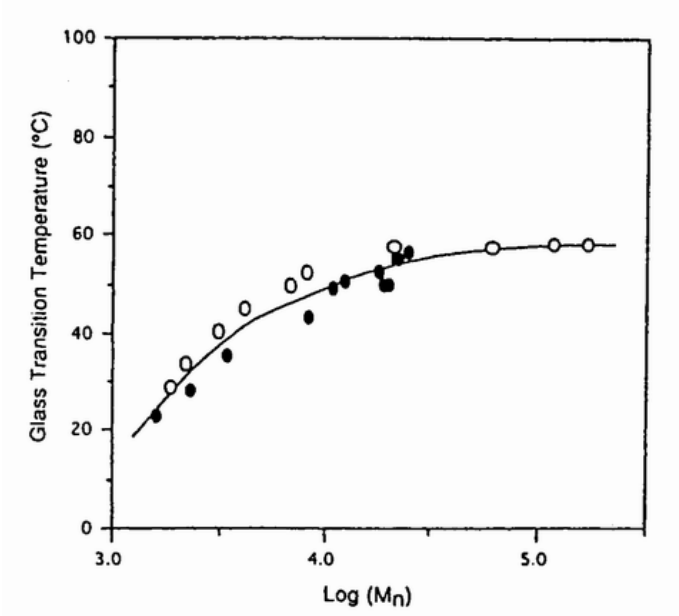

Figure 2.5 – Effect of molecular weight on the glass transition temperature of poly(L-lactic acid) (o) and poly(D,L-lactic acid) (●) [8]

(e) Thermal stability

Lactic/glycolic acid polymers degrade into the cyclic dimer, lactide and/or glycolide, when heated above 200°C for a prolonged time under vacuum or in a nitrogen environment [41]. Thermal degradation at lower temperatures mainly results in a reduction of the molecular weight or intrinsic viscosity of the polymer [53]. *Jamshidi et al.* [50] suggested that the decrease in thermal stability of lactic/glycolic acid polymers maybe due to several factors. These factors include polymer hydrolysis caused by trace amount of water contained in the polymer, depolymerization, oxidative, random chain scission caused by trace amount of oxygen and inter- and intramolecular transesterification with the formation of monomers and oligomers. The thermal stability of lactic/glycolic acid polymers can be determined by thermogravimetric analysis (TGA).

(f) Solubility

Lactic/glycolic acid polymers are linear, hydrophobic polyesters. They can dissolve in many common organic solvents. Ethyl acetate and methylene chloride (dichloromethane) are commonly used because they are less toxic [54]. The solubility of lactic/glycolic acid polymers is affected by factors such as polymer composition and crystallinity [8]. Generally, a polymer with high degree of crystallinity, such as poly(glycolic acid), has low solubility in common organic solvents.

2.2 Degradation of lactic/glycolic acid polymers

2.2.1 Background

Lactic/glycolic acid polymers are hydrolytically unstable and undergo degradation in an aqueous environment. Although insoluble in water, they degrade by hydrolytic attack of its ester bond, with possible enzyme catalytic effects [8, 14]. This hydro-degradation is also referred to as bio-erosion. Through this hydrolytic attack, random chain scission occurs in the lactic/glycolic acid polymer, causing it to degrade into lactic and glycolic acids [8, 14-18, 42]. In vivo, lactic and glycolic acids enter the tricarboxylic acid cycle and is metabolized and subsequently eliminated from the body as carbon dioxide and water [8, 15, 17, 42, 55]. **Figure 2.6** depicts a suggested scheme for the in vivo fate of these products [56].

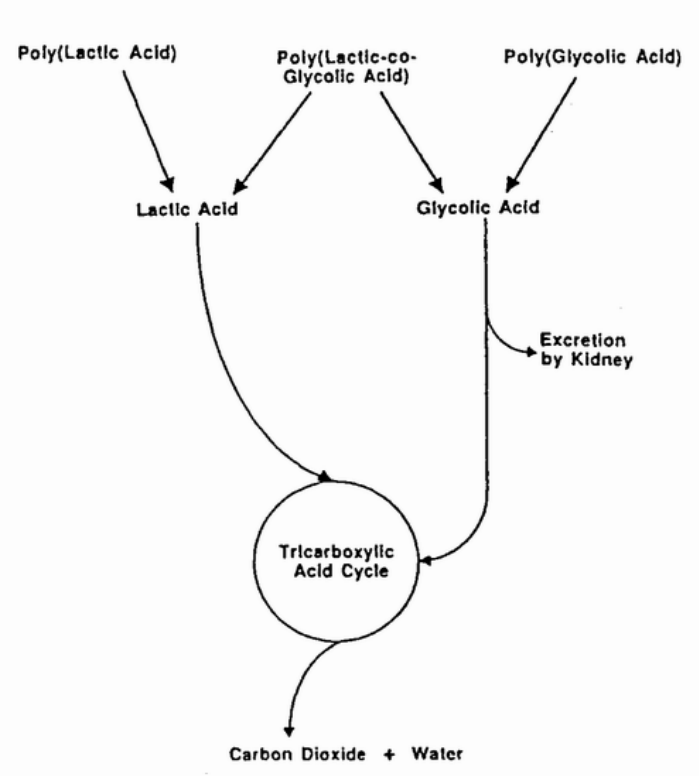

Figure 2.6 – Metabolism and excretion of degradation by-products of lactic/glycolic acid polymers in vivo [56]

2.2.2 Degradation mechanisms

Biodegradable polymers can be categorized into two groups on the basis of the mechanism or process by which they degrade. These processes are bulk degradation and surface degradation [8]. The lactic/glycolic acid polymers belong to the category of polymers that undergo bulk degradation [8]. Studies of this process have shown that not only there is degradation at the lactic/glycolic acid polymer surface, but the polymer matrix also swells and degrades at the same time [57]. The

degradation of lactic/glycolic acid polymers in vitro and in vivo is through random chain scissions of the swollen polymer [58].

The degradation of lactic/glycolic acid polymers can be characterized in terms of change in molecular weight and molecular weight distribution, weight loss, water uptake and change in morphology of the degraded polymers. A three-phase mechanism for degradation has been proposed by *Raghuvanshi et al.* [12]. The first stage involves random chain scission, where the molecular weight of the biopolymer decreases significantly, but with no appreciable weight loss or soluble monomer products formed. In the second stage, a decrease in molecular weight accompanied by a rapid loss of mass will be observed. Soluble oligomeric fragments and monomer products are formed in this stage. The final stage is where soluble monomer products are formed from soluble oligomeric fragments. This phase is attained when the biopolymer is completely soluble.

On the other hand, *Wu et al.* has proposed a four-phase degradation mechanism [8]. In the first stage, the polymer absorbs water and undergoes little swelling. During this step, some covalent bonds in the backbone will be cleaved and there is no weight lost. In the second stage, cleavage of the covalent bonds in the polymer backbone by hydrolysis begins. As a result, more carboxylic end groups are formed, which may cause auto-acceleration of the hydrolysis reaction. A loss of mechanical strength is also observed. The third step involves massive cleavage of the backbone covalent bonds and at some critical molecular weight, significant weight loss begins

to occur. In the fourth step, solubilization of the oligomers into the surrounding medium occurs, and the polymer loses mass and disappears.

Generally, the mechanisms proposed by *Raghuvanshi et al. and Wu et al.* are almost similar. Both are agreeable to the three main mechanisms stages of cleavage of covalent bonds, polymer mass loss and solubilization of oligomers, as summarized by *Raghuvanshi et al*. However, *Wu et al.* has included an additional stage in the beginning of the degradation process, which is water absorption, an imperative step for hydrolysis to occur in all biodegradable polyesters.

However, *Chu et al.* has proposed a different degradation mechanism with regards to the morphology of the polymer [40]. The model that was proposed was through two main stages: in the amorphous region and then in the crystalline region. *Chu et al*. believed that water molecules diffuse through the polymer and accommodate in the amorphous regions and not at all in the crystalline region. *Chu et al.* argued that this occurs because the amorphous zone is more open of the two and as a result, water penetrates easily. Therefore, degradation starts in the amorphous region and a loss of amorphous material results, leaving behind cracks. After which, subsequent degradation then occurs in the crystalline regions. This model is biased towards semi-crystalline polymers, such as poly(glycolic acid), and has not taken into account polymers that are amorphous in nature, for example PLGA. The two degradation stages that *Chu et al.* proposed is also not sharply defined, and some crystalline regions could also be destroyed during amorphous degradation. This

model failed to take into account that some crystallization could have also occurred during hydrolytic degradation.

Therefore, there is a lack of a definitive model that can be applied to both amorphous and semi-crystalline polymers. A more general degradation mechanism model that can be applied to any biopolymer system with regards to degradation is required. The degradation mechanisms as proposed by *Raghuvanshi et al.*, *Wu et al.* and *Chu et al.* would be reviewed and further discussed in later sections.

2.2.3 Kinetics of degradation

For biopolymers to be extensively used for biomedical and pharmaceutical applications, the understanding of their hydrolytic degradation rate and behaviour are of significant importance. The ability to control the rate of degradation will certainly enhance their usage in many applications, which may include as a drug carrier or a temporary implant. Nevertheless, it is generally accepted [59-62] that the hydrolysis of most polyesters proceeds according to the reaction:

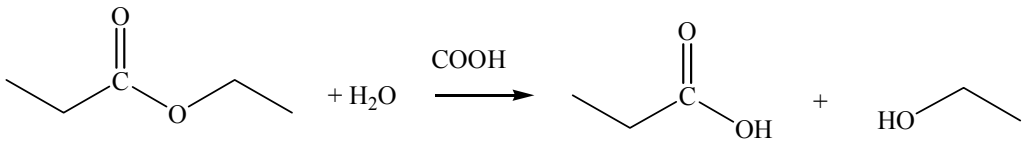

The kinetics of this reaction are given by

$$\frac{d[COOH]}{dt} = k'[ester][H_2O][COOH] = k[COOH] \qquad \textbf{(Eq. 2.2)}$$

where [COOH], [ester] and [H_2O] are the concentrations of carboxyl end groups, ester and water in the polymer matrix respectively, and it is assumed that in the early stages of the reaction the concentration of water and ester are constant. By assuming that [COOH] = $1/M_n$, it can thus be shown that

$$\ln M_n = \ln M_{n,0} - kt \qquad \textbf{(Eq. 2.3)}$$

where $M_{n,0}$ is the initial number-average molecular weight of the polymer, and k is the rate constant of the degradation process. However, *Farrar et al.* reported that degradation rate constant, k, is independent of initial molecular weight [62]. The observation by *Farrar et al.* was still inconclusive since the author excluded several graphical points from their results and there was no explanation given for this conclusion.

2.2.4 Factors affecting rate of degradation

The degradation rate of a polymer is dependent on the intrinsic properties of the polymer [63], such as its wettability, molecular weight, ratio of lactide to glycolide for the co-polymer, degree of crystallinity, glass transition temperature (T_g) and, if microparticles are used, the microparticle structure [8, 17-18, 45]. Other

environmental factors, such as mechanical stresses, solar radiation, atmospheric oxygen and moisture, also affect the rate of degradation of biopolymers [64].

(a) Lactide/glycolide polymer composition

It is known that the lactic/glycolic acid polymer composition, ratio of lactide to glycolide, has an effect on the rate of degradation [8, 45]. The methyl group makes the lactic acid moieties in the polymer more hydrophobic and provides steric hindrance to attack by water molecules. Therefore, glycolic acid polymers degrade faster than lactic acid polymers. In general, co-polymers with a low lactic acid content tend to degrade more rapidly. According to a study conducted by *Reed et al.*, the increased in chain regularity towards a more homogenous polymer will also decrease the rate of hydration and hydrolysis by enhancing crystallization [65]. Though it is agreed that the lactide/glycolide polymer composition determines the rate of degradation, there is little literature that reports on how other factors, such as radiation, may affect or change the rate of hydrolytic degradation of different lactide/glycolide polymer composition. In this thesis, the effect of radiation on the hydrolytic degradation of PLGA and PLLA will therefore be studied.

(b) Molecular weight

The molecular weight of the polymer also affects the rate of degradation [8, 45, 66], as shown in **Figure 2.7** [8]. Biodegradability increases as molecular weight decreases. The main reason is because low molecular weight polymers are more

hydrophilic, due to the higher percentage of end groups [8, 66]. *Schliecker et al.* also observed an increase in water uptake with time because degradation increases polymer hydrophilicity [66], resulting in an autocatalytic effect. Though many papers agree to the fact that higher molecular weight polymers have lower rate of degradation, there is a lack of papers that model the initial molecular weight of a polymer to its degradation rate. It would therefore be of interest to model the molecular weight of a polymer to its degradation rate and time.

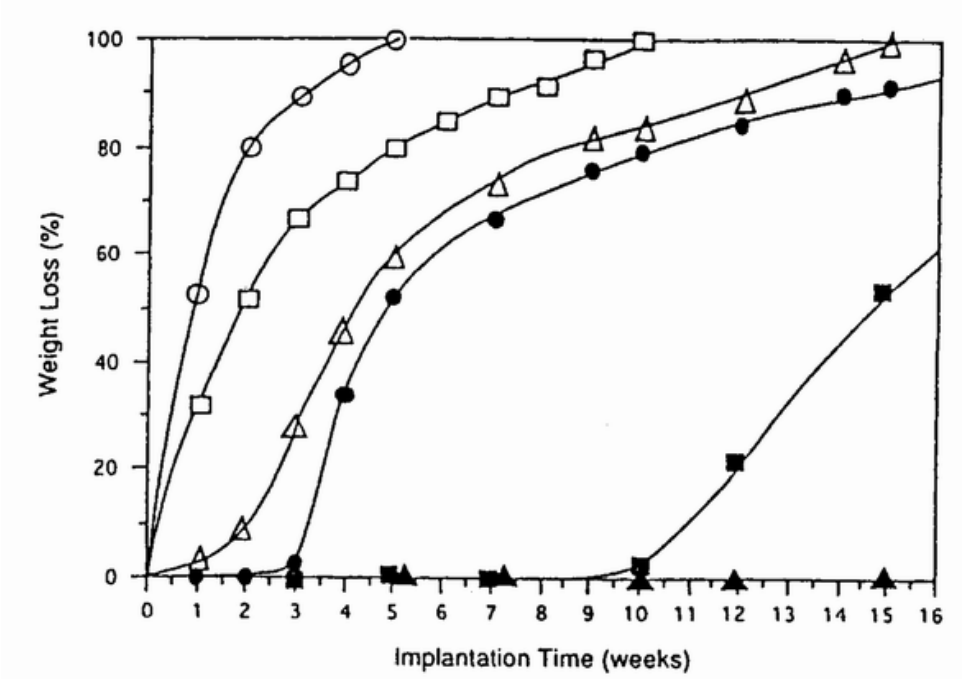

Figure 2.7 – Effect of molecular weight on the degradation rate of poly(D,L-lactic acid) M_n: (o), 1400; (□), 1600; (Δ), 2000; (●), 4300; (■), 11500; (▲), 16900 [8]

(c) Crystallinity

The rate of degradation is also dependent on the permeability of the polymer to water. Water will readily penetrate amorphous regions, but a semicrystalline nature of a polymer will tend to limit water accessibility, as proposed by *Chu et al.* [40]. This is because the crystalline region is highly packed, and results in a slower hydrolysis of the polymer chains in the crystalline regions. *Wu et al.* also concluded that amorphous polymers will degrade faster than semi-crystalline polymers, and a higher degree of crystallinity in a polymer slows polymer degradation [8]. *Chu et. al.* and *Eldsater et al.* studied the effects of crystals in retarding the hydrolytic degradation of semi-crystalline polymers, such as poly(glycolic acid) [40] and poly(ε-caprolactone) [67] respectively. However, there is hardly any work done to compare the rate of degradation between an amorphous and semi-crystalline morphology of the same polymer, which this thesis aims to investigate.

In the studies conducted by *Schliecker et al.* and *Eldaster et al.*, it was observed that crystallinity in the polymer increased with degradation time [66, 67]. *Schliecker et al.* noted that a lower molecular weight polymer had a greater ease in forming crystals during hydrolytic degradation [66]. However, there was no mention about the effects of crystallization on the subsequent hydrolytic degradation rate in both the studies. It was also inconclusive whether a lower molecular weight or higher crystallinity as a result of degradation, would have a greater influence on the hydrolytic degradation rate.

(d) Other physiochemical properties

Other physiochemical properties that affect the rate of hydrolytic degradation include the glass transition temperature (T_g) [8]. The T_g of a polymer reflects its chain mobility [8], and directly determines the ease of water diffusion and chemical attack and thus, the rate of degradation [8, 17-18]. It is well accepted, as reviewed by *Wu et al.*, that a lower Tg would have a higher rate of degradation [8].

2.2.5 Degradation characteristics

(a) Homogeneous and heterogeneous degradation

There are many papers that report about the degradation characteristics of lactic/glycolic acid polymers [68-71]. *Vert et al.* [68], *Grizzi et al.* [69] and *Li et al.* [71] all reported that lactic/glycolic acid polymers undergo heterogeneous degradation, which is contrary to the report by *Grijmpa et al.* [70] who argued against heterogeneous degradation. The paper by *Li et al.* [71] counter argued the results obtained by *Grijmpa et al.*, stating that the Size Exclusion Chromatography (SEC) chromatograms obtained by *Grijmpa et al.* showed bimodal distribution, which could be the consequence of heterogeneous degradation [57]. It is however noted that in all of their work, the samples were large (above 1.5 mm in thickness). It was concluded by *Grizzi et al.* that small-sized devices, such as thin films and microspheres, degraded homogeneously without internal autocatalysis [69].

(b) Osmotic cracking

Another degradation characteristic of lactic/glycolic acid polymers is the phenomenon of surface cracking [40, 72]. *Chu et al.* has reported the formation of surface cracks on PGA sutures with hydrolytic degradation. It was also noted that this surface cracks were not observed on irradiated sutures that had not been subjected to hydrolytic degradation [40]. *Gautier et al.* reported similar observations with hydrothermal-aged polyester matrix, and had attributed this to osmotic cracking [72]. *Gautier et al.* suggested that water entering the microcavities, due to osmosis, results in the increase of osmotic pressure in the microcavities. This would have caused osmotic cracking, as what was observed by *Chu et al.* on the scanning electron microscope (SEM) [40].

2.3 Radiation

2.3.1 Background

Radiation has been used for many purposes, and its used include in a variety of applications in medical [73, 74], industrial [39, 75], research, and national security or military situations. In medical applications, radiation helps with both diagnosis, such as medical imaging in computerized tomography (CT) scan [76], and treatment of patient's illness, such as in the treatment of cancer through radiotherapy [73]. Industrial applications include quality control tests and inspections. Other applications of radiation also include sterilization [75, 77-78], in the treatment of food [56] and also in the generation of electric power at nuclear reactors. However, not all forms of radiation can serve the same purpose. For example, alpha rays and beta rays are sub-atomic particles that travel at close to the speed of light; and alpha rays can be stopped by a piece of paper, while beta rays can be stopped by one or two centimeters of human tissue. Gamma rays and X-rays are waves of energy similar to visible light, except they have more energy and are invisible. They travel at the speed of light and penetrate matter more easily than the particulate radiations. Therefore, for the practical value of radiation for certain purposes and applications, the chosen radiation must meet certain requirements [79], such as:

- Be available with sufficient output at acceptable cost.
- Be able to sufficiently penetrate the material or product.
- Be capable of producing the desired effect with reasonable efficiency
- Be safe.

- Should not produce undesirable radioactivity.
- Should be capable of reliable control and economical shielding if required.

For these reasons, each form of radiation can only be used for certain specific applications. For example, X-ray is commonly used in medical imaging, whereas, electron beam (e-beam) radiation is more commonly used for the sterilization of drugs and for cross-linking polymerizations. The use of e-beam is now more widespread in the medical industry because it is safe and the electron penetration is, or can be made, adequate [79].

(a) Electron beam radiation

E-beam radiation is a form of ionizing radiation that can be used as an effective means of destroying microorganisms and their reproductive cells [78]. E-beam irradiation, generally characterized by its low penetration and high dose rates, is a process by which products are exposed to a concentrated, highly charged stream of electrons produced through the acceleration and conversion of electricity. As the product or material passes beneath or in front of the electron beam, it absorbs energy from the electrons. This absorption of the electron energy alters various chemical and biological bonds within the product or material. The energy that is absorbed per unit mass of product or material is referred to as the absorbed dose. Electron beams are very fast, and can deliver the required radiation in seconds. However, they penetrate matter much less than gamma or X-ray sources [79].

2.3.2 Radiation on materials

Radiation causes changes to both organic and inorganic materials. This is especially so for organic materials, such as polymers, where radiation usually causes polymer degradation [19, 20]. Polymers are the most vulnerable to significant damage from irradiation, as compared to other inorganic materials. The large quantities of energy deposited by ionizing radiation, such as x-rays and e-beam radiation, onto the target material leads through the formation of ions, activated atoms and molecules, and free radicals, to a complex series of chemical reactions. These can have a very significant effect on the chemical and physical properties of the irradiated compounds, especially polymers. These effects can be even more enhanced if the irradiation takes place in a regular atmospheric environment where reactive species such as ozone, $O^{\bullet}$ and $OH^{\bullet}$ radicals are formed [80]. In the presence of these reactive species, the reactions of concern are chain scission, cross-linking, and oxidation [19-20, 80]. As such, it would be of interests to study the effect of radiation on polymers, and observe how radiation can change the properties of polymers through polymerization [81, 82] or degradation [28, 31].

2.3.3 Irradiation of non-biodegradable polymers

Radiation can result in drastic changes to the properties of polymers, and there are many journals written about the effects of radiation on non-biodegradable polymers; such as polyethylene [26, 27], polypropylene [28-30], poly(methyl methacrylate)

[21], polycarbonates [31, 32], isobutylene-isoprene rubber [33] and polyesters [23]. The main effects of radiation on these polymers are degradation [26-33], though there are some polymers that undergo cross-linking under the influence of radiation [37-39, 81, 83]. Many polymers, on exposure to high-energy radiation may also give off gases such as hydrogen, carbon dioxide, carbon monoxide, methane and ammonia. As a result, the effects of these various reactions are depolymerization, loss of strength, embrittlement, acidification and discolorations, and a greatly enhanced rate of subsequent aging deterioration [80].

Most of these papers that study the effects of radiation on polymers, focus their work with regards to gamma radiation [27-30, 32-33]. There is hardly any work done on the effects of e-beam radiation on these polymers. E-beam processing effectively and efficiently creates useful changes in material properties and performance, through polymer cross-linking and even chain scission [19, 20]. As mentioned, e-beam radiation is known to be safe, and can deliver the required radiation in seconds [79]. Electron beam accelerators, as shown in **Figure 2.8**, are also adequately shielded and are capable of reliable control for commercial usage, producing the desired effects with reasonable efficiency. These advantages make the use of e-beam radiation more attractive, as compared to the more harmful and destructive gamma radiation. It would therefore be of interests to study the effects of e-beam radiation on polymers in this thesis.

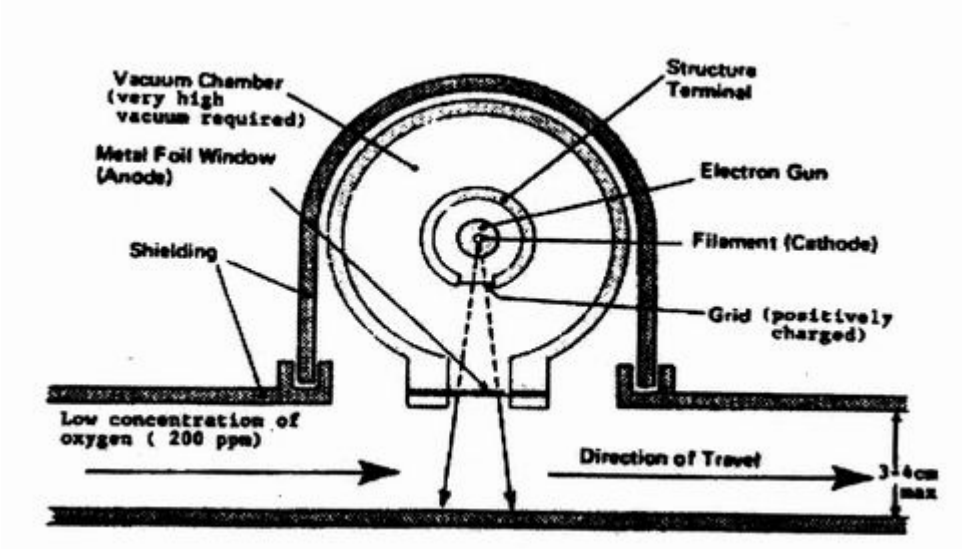

Figure 2.8 – Schematic diagram of electrocurtain electron beam accelerator [79]

(a) Radiation chemical yields for chain scission and cross-linking

Ionizing radiation causes the formation and breaking of polymer bonds as a result of intermolecular cross-linking and scission in the polymer. The radiation chemical yields for chain scission (G_s) and cross-linking (G_x), which is defined as the number of such reactions per 100 electron volts of absorbed energy, therefore determines the extent of chain scission or cross-linking during irradiation. There are several papers that have reported the calculation of G_s and G_x in their irradiation study [21, 33, 83]. The papers by *Ichikawa et al.* [21] and *Janik et al.* [83] obtained their calculations from the work of *Charlesby et al.* [22]. However, the equations used by *Ichikawa et al.* failed to consider the cross-linking effect in the calculations, and the equations used by *Janik et al.* were for aqueous solution. *Sen et al.* obtained the

calculations for the radiation chemical yields from a more recent study by *Schnabel et al.* [84]. The equations are as follows [33],

$$1/M_w = 1/M_{w,0} + (G_s/2 - 2G_x) \times D \times 1.038 \times 10^{-6} \quad \textbf{(Eq. 2.4)}$$

$$1/M_n = 1/M_{n,0} + (G_s - G_x) \times D \times 1.038 \times 10^{-6} \quad \textbf{(Eq. 2.5)}$$

where $M_{w,0}$ and $M_{n,0}$ are the weight and number average molecular weights of non-irradiated samples. M_w and M_n are the corresponding values following exposure to irradiation dose, D. *Sen et al.* highlighted in the paper that a ratio of G_s/G_x greater than 4 would indicate that chain scission is more dominant.

(b) Radiation-induced degradation of polymers

Degradation of polymers from irradiation can occur in two ways. When the energy from electron beam radiation exceeds the attractive forces between the atoms or the bond dissociation energy, chain scission occurs [85]. This happens because the excited states dissipate some of the excess energy by bond scission, and this result in the formation of free radicals [86]. These free radicals can then cause chain transfer and the subsequent splitting of polymer chains [19]. The other way is through oxidative degradation, where peroxyl free radicals interact with the polymeric bonds to cause chain scission [35, 80].

The radiation energy is usually high enough to cause chain scission in most polymeric materials. Chain scission from high energy radiation results in the formation of free radicals, which will cause further radiochemical reactions. According to *Carlsson et al.*, the scission of C-H bonds, in polymers, is usually favoured over C-C backbone scission [86]. This is attributed to energy migration along the backbone by an exciton mechanism, minimizing energy localization in specific C-C backbone bonds, whereas energy deposited in C-H bonds cannot migrate [87]. An alternative suggestion, by *Tsuda et al.*, is that in highly excited states, C-C bonds are in fact more stable than C-H bonds, contrary to the ground-state situation [88]. In addition, the recombination of two macroalkyl radicals resulting from backbone scission is facilitated by a solid matrix [89].

The oxidative degradation of polymers is a free radical chain reaction. This reaction consists of five steps, instead of the usual three steps of initiation, propagation and termination [80]. The two additional important steps are conversion of the formed polymer radicals to peroxyl radicals (main oxygen consuming reaction) and degenerate chain branching (responsible for the auto-acceleration character of the process). The formation of these peroxyl radicals due to the presence of oxygen is expected to initiate a chain hydro-peroxidative process, which will result in chain scission.

(c) Crystals in retarding radiation-induced degradation

A study conducted by *Franck et al.* mentioned about the ability of crystals in retarding the degradation of polymers during irradiation [90]. The crystalline regions formed consist of chains that are more oriented and closely packed compared to the amorphous regions. Therefore, the close proximity of the polymer chains in the crystalline structure encourages the trapped free radicals to recombine, thus reducing the number of effective chain scission. According to *Franck et al.*, this effect is also known as the "cage effect" [90], a concept which involves the recombination of initial radicals before they can diffuse out of the active region and undergo chain scission reactions other than recombination elsewhere. *Williams et al.* also agreed, stating that the close-packed structure of the crystalline regions excludes oxygen, stabilizers and specific active radical species from this region [30]. As a result, *Williams et al.* concluded that peroxyl free radicals are unlikely to be formed within the crystalline regions, thus reducing the number of effective chain scissions. However, more work is needed to verify the "cage effect" in lactic/glycolic acid polymers, since the work conducted by *Franck et al.* and *Williams et al.* are on non-biodegradable polymers. The effect of crystals in retarding radiation-induced degradation for PLGA would be thoroughly investigated in this thesis.

2.4 Irradiation of lactic/glycolic acid polymers

There are several papers that described about the effects of radiation on lactic/glycolic acid polymers, such as poly(lactic acid) [34], poly(lactide-co-glycolide) [35, 91], poly(glycolic acid) [40], and composites of poly(L-lactide) and hydroxyapatite [92]. As with the papers on the irradiation of non-biodegradable polymers, most of the authors again focus their work mainly on gamma irradiation. This was with the exception for the study conducted by *Montanari et al.*, who did a comparison between gamma and beta irradiation effects on PLGA [93]. The study showed that microspheres of PLGA were more stable against beta radiation as compared to gamma radiation; with respect to the drug release rate, where gamma irradiated PLGA had a faster rate of release than beta irradiated PLGA. However, *Montanari et al.* also noted that the main interactions of either radiation with matter are basically the same, except for only minor differences, such as the high penetration depths, low dose rate of gamma irradiation and a low penetration depth, high dose rate of beta irradiation.

2.4.1 Radiation-induced degradation of lactic/glycolic acid polymers

Montanari et al. conducted extensive studies on the effects of radiation on PLGA [35, 91, 93], with the objective of using radiation for sterilization purposes. The studies showed that PLGA degrades under the influence of gamma irradiation, with significant effects on the drug release behaviour of PLGA. The degradation studies

were conducted by observing the changes to the molecular weight and T_g of PLGA with respect to days after post-irradiation [91]. It was concluded that the molecular weight of PLGA decreased with time (days) after initial irradiation at day 0, with the T_g remaining unchanged with time. Since these studies concentrated on the use of radiation for sterilization, the radiation dose used in the studies was only 25 kGy (2.5 Mrad). There was however no data on the irradiation of PLGA at higher radiation dose, for example at 50 Mrad. The dose range used in these studies was too narrow and was therefore insufficient to study the use of radiation as a means to control the rate of hydrolytic degradation in PLGA. Sufficient study needs to be conducted over a larger dose range to evaluate the behaviour of PLGA and PLLA under e-beam radiation.

Gupta et al. discussed his work on the effects of increasing gamma radiation dose on PLLA up to 500 kGy (50 Mrad) [34]. It was reported that at low radiation dose, chain scission is dominant, whereas at higher radiation dose (above 25 Mrad), there is a relative increase in cross-linking to chain scission. *Gupta et al.* proposed that at lower radiation doses, the dissolved oxygen in the polymer act as free radical scavengers, thus increasing the incidences of chain scission. However, at higher radiation dose, the amount of oxygen dissolved in the sample would have probably been used up and no further scavenging of free radicals can occur, thereby increasing the incidences of cross-linking. It was also observed that crystallinity decreased and chain flexibility increased with radiation dose. This observation was also confirmed by *Kantoglu et al.* [94], where a significant decrease in crystallinity and damage in the crystalline region due to irradiation was observed.

Radiation damage also result in the decrease in mechanical properties of poly-D-L-lactide as observed by *Birkinshaw et al.* [36]. It was noted in the study of compression-moulded samples of poly-D-L-lactide that the molecular weight and mechanical strength decreased as a result of random chain scission. Substantial embrittlement occurred at radiation doses of 10 Mrad. However, contrary to the results from *Montanari et al.* who observed a decrease in molecular weight with post-irradiation ageing [91], *Birkinshaw et al.* observed that the molecular weight and mechanical strength of irradiated poly-D-L-lactide remained relatively stable over time. The explanation given by *Birkinshaw et al.* was that meta-stable peroxyl or hydroperoxyl groups were not formed on irradiation, thus the absence of an ageing effect. *Montanari et al.*, on the other hand, used electron paramagnetic resonance (EPR) to validate the formation of peroxyl groups during the irradiation of PLGA [35, 91, 93], which would have provided stronger evidence of the existence of peroxyl free radicals during the irradiation of PLGA in the presence of oxygen.

The work done by *Montanari et al.* certainly concentrated more on the drug release rate of drugs from PLGA after irradiation sterilization [35, 93]. There was however no mention of the hydrolytic degradation rate and time of PLGA upon irradiation in their work. A comprehensive study on the hydrolytic degradation of irradiated PLGA and PLLA was therefore lacking in this field of research.

2.4.2 Radiation-induced degradation mechanisms

In a separate paper, *Montanari et al.* did a comprehensive study on the effect of gamma radiation on PLGA microspheres [35, 91], describing the degradation of PLGA. A radiolysis mechanism was suggested, through the use of the EPR, where the structures of the free radicals formed at room temperature and in the presence of oxygen were determined. The formation of peroxyl free radicals was due to the diffusion of oxygen into PLGA, and the structures of peroxyl free radicals formed are shown in **Figure 2.9** [35].

The radiolysis mechanism that was proposed however was not substantiated with other spectroscopy characterization techniques, such as the Fourier-transformed infra-red (FTIR), Raman and H^1 nuclear magnetic resonance (H^1 NMR) spectroscopy, on the irradiated polymers. These characterization techniques would have confirmed the chemical structures of irradiated PLGA and PLLA and provide a stronger basis in proposing the radiation-induced degradation mechanisms that occur during the irradiation of PLGA and PLLA. This aspect of the work would therefore be covered in greater detail in this thesis.

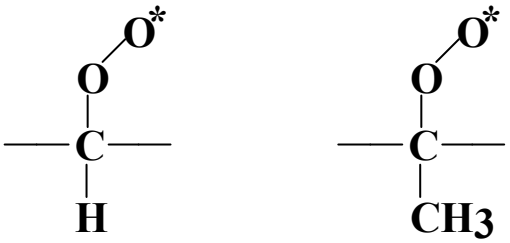

Figure 2.9 – Chemical structures of peroxyl free radicals formed during irradiation of PLGA

2.4.3 Hydrolytic degradation of irradiated lactic/glycolic acid polymers

It would be of importance to study the hydrolytic degradation behaviour of irradiated lactic/glycolic acid polymers, since these polymers would be used in vivo and their main advantages lie in their excellent biodegradability. Few papers have discussed about the effects of radiation on the hydrolytic degradation of lactic/glycolic acid polymers [36, 40, 95].

Chu et al. has done a comprehensive study describing the effects of radiation on the hydrolytic degradation behaviour of poly(glycolic acid) [40], but not on other lactic/glycolic acid polymers, such as PLGA and PLLA. It was concluded in the study that irradiation increases the rate of hydrolytic degradation of poly(glycolic acid). The kinetics of degradation conducted was through the observation of the decrease in the mechanical and physical properties of the polymer over 10 days. It would have been a more substantial if *Chu et al.* had modeled the kinetics of hydrolytic degradation to the molecular weight of the polymer as described by several authors [59, 60].

Chu et al. noted an increase in water uptake with irradiation [95], contrary to *Birkinshaw et al.* where a lower water uptake for irradiated samples of poly-D-L-lactide was observed [36]. It would have been an interesting study to verify the contradictory results obtained from both authors, since it is widely known that radiation would have resulted in a lower molecular weight polymer, and thus, a

higher water uptake. This thesis would therefore seek to verify whether irradiation would enhance water uptake and hydrolysis.

2.5 Summary

Lactic/glycolic acid polyesters undergo hydrolytic degradation through the hydrolysis of their ester bonds. Two main hydrolytic degradation mechanisms had been proposed. It is, however, generally agreed that the kinetics of degradation observes a linear trend when plotted in logarithmic form. Factors, such as molecular weight and degree of crystallinity, that affect the rate of degradation have been reported and discussed. A review of the journal papers has shown that there is a dearth of data on the e-beam radiation of PLGA and PLLA on their subsequent hydrolytic degradation rate. There are numerous journal papers that discuss about the effects of radiation on polymers, but few discussed the effects of radiation on PLGA or PLLA in great depth and detail. Most of these papers of radiation on polymers would examine the use of gamma radiation, but none studied the effects of electron beam radiation. Therefore, the effects of electron beam radiation on biopolymers, such as PLGA and PLLA, would be extensively discussed in this thesis, where a discussion on their radiation chemical yields, radiation-induced degradation mechanisms, changes in their physiochemical properties, and subsequent hydrolytic degradation rates and behaviour would be conducted in greater depth.

Chapter 3 Materials and Methods

3.1 Lactic/glycolic acid polymers

The lactic/glycolic acid polymers used in this research study were biomedical grade co-polymer PLGA (80:20) (80% lactide and 20% glycolide), and homo-polymer PLLA. Both PLGA (80:20) and PLLA were purchased from Purac Far East, Singapore, and manufactured by Purac Holland. Their intrinsic viscosity is 4.8 and 4.37 for PLGA (80:20) and PLLA respectively. Their number average molecular weight was measured using gel permeation chromatography (GPC) to be about 5.6 $x10^5$ g/mol and 4.8 $x10^5$ g/mol for PLGA and PLLA respectively.

3.2 Electron beam accelerator

The electron beam accelerator works by emitting electrons from the cathode. The electron beam accelerator used is the Energy Sciences Inc. (ESI) Electron Beam Accelerator model CB175. This low energy electron accelerator employs a cylindrical vacuum chamber in which a longitudinal heated tungsten filament is raised to a negative potential typically of 175 kV. The electrons emitted from the "linear" cathode are accelerated in a single step to the exit window. The exit window as part of the vacuum chamber is kept at ground potential, and this causes the electrons to accelerate towards the window. The electrons accelerating to the window then penetrate the thin titanium foil and enter the process zone. The

underlying process material will then be irradiated by the electron beam, as shown in schematic diagram in **Figure 2.8**.

3.2.1 Polymer film thickness

Due to the attenuation and low penetration depths of e-beam radiation, it is important to achieve adequate irradiation dose during electron beam processes. There are basically three methods that can be used to ensure that the whole irradiated material receives at least the minimum dose requirement:

1. A suitable voltage level can be chosen to ensure 100% irradiation. It is noted that a higher accelerating voltage will result in a deeper penetration.
2. If the voltage has to be pre-set at a standardized volt, then to ensure 100% irradiation, the material has to be overdosed.
3. If the voltage has to be pre-set and no over dose is allowed, then the thickness of the irradiated material has to be controlled to the desirable thickness.

For this work, the e-beam accelerator would be operated at its maximum accelerating voltage of 175 kV. The thickness of the polymer film had to be limited to a maximum thickness to ensure a 100% radiation dose throughout the film. The depth-dose distribution, for unit density material, for a family accelerating voltage from 125 to 300 kV is shown in **Figure 3.1**.

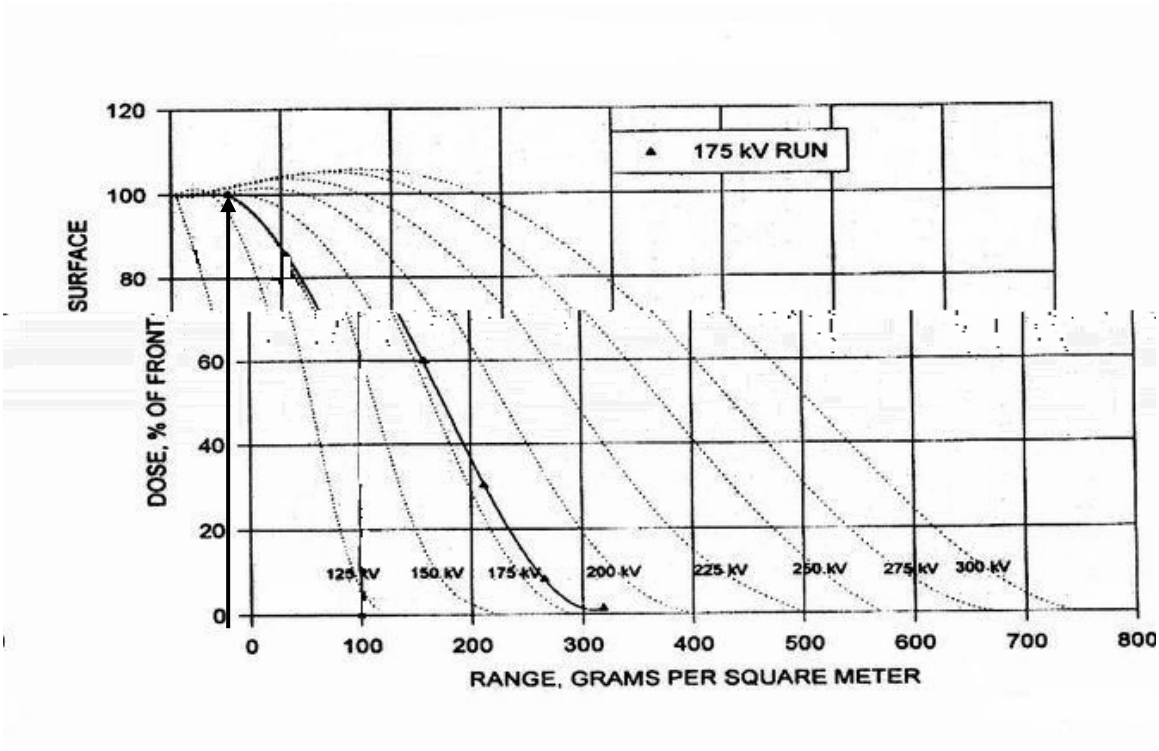

Figure 3.1 – Attenuation curve for a family of accelerating voltage for a material of unit density

From **Figure 3.1**, for a polymer to be entirely exposed to 100% from the front surface and throughout the thickness at 175 kV, its maximum thickness has to be approximately 50 μm thick or within a range of 50 g/m^2, for a unit density material. Therefore the thickness of the non-unit density PLGA and PLLA films can be calculated using the ratio:

$$t_p / \rho_p = t_u / \rho_u \qquad \textbf{(Eq. 3.1)}$$

where t_p is the thickness of the polymer film, ρ_p is the density of the polymer, t_u and ρ_u is the thickness and density of the unit density material respectively. ρ_u is taken to be 1 g/cm^3 for a unit density material. The appropriate thickness of PLGA and

PLLA films can then be calculated, with the knowledge of their respective densities [96], as tabulated in **Table 3.1**.

Table 3.1 – Tabulation of the density and maximum thickness acceptable for PLGA and PLLA films for e-beam irradiation at 175 kV

Polymer	Polymer density (gcm^{-3})	Maximum thickness (μm)
PLGA	1.319	66
PLLA	1.275	64

3.3 Preparation of PLGA and PLLA films

Films of PLGA and PLLA were prepared by a solvent casting method. Each of the biopolymers was first dissolved in HPLC grade dichloromethane [9, 54] of purity 99.99%, which was purchased from E. Merck, Germany, at a weight ratio of 1:12 (ratio weight of polymer to weight of dichloromethane). Dichloromethane was chosen as the solvent in this work because it is approved by the Food and Drugs Administration (FDA), and it is less toxic [54] than chloroform.

The polymer solution was then spread over a glass plate to give a film of approximately 0.7 mm in wet thickness, as according to the height of the film applicator. The solvent was then evaporated slowly in air at room temperature for 48 hours to prevent the formation of air bubbles. The films were next placed in an oven at 40°C for a week to evaporate any remaining solvent, leaving behind dried

PLGA and PLLA films. Thermogravimetric analysis (TGA) conducted on the films showed no significant amount of DCM present in the films after drying. The dry thickness of the films were then measured, using the film thickness measurement device (Elcometer, model 456) that employs ultrasound technique, to be about 55 μm ± 3 μm; which were less than their limited maximum thickness, as shown in **Table 3.1**. It is critical that the maximum thickness of the films were not exceeded and careful measures were taken to exclude thick films (>60 μm) from the experiment. This is to ensure a depth of e-beam penetration at 175 kV for all PLGA and PLLA films is kept constant. The polymer films were cut then into rectangular strips of dimensions 8 cm x 3 cm before irradiation. The dimension of the polymer strips were smaller than the processing area of the radiation chamber (10 cm x 10 cm), thus ensuring uniform irradiation throughout the sample.

3.4 Electron beam irradiation

PLGA and PLLA films were e-beam irradiated at room temperature and humidity (~70%), and in the presence of oxygen. The films were irradiated at radiation doses of 2.5, 5, 10, 20, 30 and 50 Mrad. The absorbed dose is defined by the quantity of ionizing radiation energy imparted per unit mass of a specified material [97]. The SI unit of absorbed dose is the gray (Gy), where 1 Gy is equivalent to the absorption of 1 joule per kilogram of the specified material (1 Gy = 1 J/kg) [91]. The discontinued unit for absorbed dose is the rad (1 rad = 100 erg/g = 0.01 Gy) and is determined by the beam current [98-100]. For the ESI Electron Beam Accelerator, the electron

beam current determines the treatment dose delivered according to this relationship [101],

$$I = \frac{D \times V}{k} \qquad \textbf{(Eq. 3.2)}$$

where I is the electron beam current in milliamperes (mA), D is the dose in Mrad, V is the line speed in meter per minute (mpm) and k is the yield factor, which is given as 19.3 Mrad.mpm/mA for the ESI Electron Beam Accelerator [101].

The accelerating voltage of the electron beam accelerator was maintained at 175 kV, with a beam current of 2.5 mA and the conveyor or line speed was kept at 19.3 m/min. This will deliver a radiation dose of 2.5 Mrad dose per pass, as according to **Eq. 3.2**. Films were then irradiated to the appropriate dose by performing multiple passes. Since irradiation is carried out continuously with multiple passes, the radiation chain reactions that occur are assumed to mainly occur during irradiation and the changes that occur between passes, though insignificant, would be taken as part of the degradation process.

3.5 Crystallization of PLGA

The effects of crystals in the retardation of radiation-induced degradation and hydrolytic degradation were studied using PLGA films. The crystallization temperature of PLGA was reported to be around 115^{o}C [102], which is within a

range, (T_m – 10K) and (T_g + 30K), where thermal motion of the polymer chains is conducive for the formation of stable ordered regions [103]. Amorphous films of PLGA were therefore isothermally annealed at 115^oC in an oven from 15 min to 1 day to obtain different degree of crystallinity of PLGA. The degree of crystallinity was measured using wide angle x-ray diffraction (WAXD) and differential scanning calorimetry (DSC). Polarizing optical microscope was also used to monitor the crystallization process of PLGA.

3.6 In vitro hydrolytic degradation

The in vitro hydrolytic degradation studies of PLGA and PLLA films were conducted by first measuring and recording the initial mass (m_0) of each film sample to be hydrolytically degraded. The samples were then placed in 10ml screw top bottles containing phosphate buffered saline (PBS) solution (pH 7.4) and incubated at 37.0°C for various lengths of time. Samples were removed once every 3 days for the first two weeks to observe the changes in water uptake, and subsequently once weekly for characterization. The pH of the solution was monitored over time to ensure a stable pH of 7.4 is maintained at all times.

At the designated time, the films were removed from the PBS solution, rinsed with distilled water and surface dried using water-absorbent paper. The wet mass was then measured immediately (m_w). The samples were then dried in an oven at 37.0°C for 5 days to a constant weight, and after which the dry mass was recorded (m_d). All

mass measurements were done on the Mettler Toledo mass balance, of an accuracy of 0.01 mg. Mass measurements were recorded only when a stable mass measurement, of up to 0.01 mg accuracy, is obtained. The water uptake was then calculated by subtracting the dry mass (m_d) from the wet mass (m_w), and taken as a percentage over the dry mass. Mass loss was taken as the difference in the dry mass (m_d) with respect to the initial mass (m_0) of sample. Since there are slight differences in the initial masses of each film, all parameters were normalized by dividing by their initial masses and reported in terms of percentage.

3.7 Characterization techniques

The following characterization techniques were used in the course of study of the effects of radiation on PLGA and PLLA, and their subsequent hydrolytic degradation rates and behavior. The techniques used were for both radiation hydrolytic degradation studies.

3.7.1 Gel permeation chromatography (GPC)

The gel permeation chromatography (GPC) makes use of the size exclusion principle and it is directly used to determine the molecular weight of polymers. The number and weight average molecular weight (M_n & M_w respectively) were determined using the Agilent GPC 1100 series. GPC was performed at 30°C with

80%-tetrahydrofuran and 20%-DCM as solvents, and using RID (Reflective Index Detector) as the detector. The calibration is done in accordance to polystyrene standards and the flow rate used was 1 $mLmin^{-1}$.

(a) Radiation study

The changes in the average molecular weights of PLGA and PLLA with radiation dose were studied, by plotting average molecular weights with increasing radiation dose. The radiation chemical yields were calculated by the plot of inverse average molecular weight with radiation dose [33].

(b) Hydrolytic degradation study

In this study, the results from the GPC were used to study the rate of degradation. Here, the natural logarithmic number average molecular weight (ln M_n) would be plotted against degradation time in days, as according to **Eq 2.3**. The degradation rate constant, k would then be used to model to the initial average molecular weight of the polymer before hydrolysis.

3.7.2 Differential Scanning Calorimetry (DSC)

Differential Scanning Calorimetry (DSC) measurements were performed on a TA Instrument DSC 2920 Modulated DSC apparatus. The use of the modulated mode allows the heat capacity of the sample to be measured in one run with an error of 1% or less. To avoid oxidative degradation, the sample and reference pans were purged with nitrogen at a constant flow rate of 48 $mLmin^{-1}$. The samples were heated from -40°C to 250°C at a scan rate of 5°C min^{-1}, with approximately 5 mg of each sample used in the analysis. For the measurement of the degree of crystallinity, the total area under the endothermic peak (ΔH_f) was taken, and the degree of crystallinity was then calculated as the percentage of ΔH_f over $\Delta H_{f\,(100\%)}$, which is the enthalpy heat of fusion for a 100% crystalline polymer. For incidences when a crystallization peak was observed, the difference (ΔH) between the enthalpy of fusion (ΔH_f) and the enthalpy of crystallization (ΔH_c) [104] was used as a measurement of the level of sample crystallinity. Since the $\Delta H_{f\,(100\%)}$ of PLGA is not to be found in literature reviews, its ΔH will be taken as the measurement of DOC. The $\Delta H_{f\,(100\%)}$ for PLLA is taken as 95 J/g [105]. The DSC was also used to measure the thermal properties, i.e. glass transition temperature (T_g), melting temperature (T_m) and crystallization temperature (T_c). The melting and crystallization temperature was taken as the temperature corresponding to the minimum and maximum of the endothermic and exothermic peaks respectively. For the radiation and hydrolytic degradation studies, the degree of crystallinity and thermal properties of PLGA and PLLA were plotted against radiation dose and degradation time respectively.

3.7.3 Wide-angle x-ray diffraction (WAXD)

Wide-angle x-ray diffraction (WAXD) was performed using the Shimadzu XRD-6000 employing CuKα radiation (λ = 1.5406 A°), with a thin-film attachment that rotates at a speed of 50 rpm. A scan axis of 2θ was used to obtain diffraction patterns of a scan range between 5° and 40°, with a scan rate of 0.2 °min^{-1}. The θ-fixed angle was kept at 0.5°, and the voltage and current used was 40 kV and 30 mA respectively.

The degree of crystallinity was calculated as the percentage of the scattered intensity of the crystalline phase over the scattered intensity of the crystalline and amorphous phase. The FWHM (Full-width at half maximum), B, is also related to the mean dimension of crystallites perpendicular to the hkl planes, t, by Scherrer's equation [106],

$$B = \frac{0.9\lambda}{t\cos\theta} \qquad \textbf{(Eq. 3.3)}$$

where B is the broadening of diffraction line on the 2θ scale (radians) measured at its half maximum intensity. The FWHM is strongly affected by crystal defects and distortions, which cause line broadening. In this report, the variation in the FWHM was used as a rough indication of the changes in crystal size.

3.7.4 Small angle x-ray scattering (SAXS)

Small angle x-ray scattering (SAXS) was conducted using a Bruker AXS Inc. Nanostar system, with CuKα radiation source (λ = 1.5418 A°). An X-ray tube voltage of 40 kV and a current of 35 mA were used. A scan axis of 2θ was used to obtain diffraction patterns of a scan range between 0° and 2.8°, with a scan time of 12000 seconds. A vacuum chamber for the incident beam path and scattered beam path was used, and a two-dimensional multiwire proportional HI-STAR area detector was used to detect the SAXS signals. One-dimensional diffraction profiles were calculated by averaging the two-dimensional patterns. Corrections were made for sample thickness and sample transmission, and background scattering was subtracted from the SAXS data. The channel numbers of the area detector were calibrated with the use of silver behenate and a rat-tail collagen.

The results obtained were analyzed for changes in the SAXS invariant. The SAXS invariant is taken as the area under the scattering pattern. In a 2-phase system with no voids, the invariant is related to the square difference between the electron densities of the amorphous and crystalline phase, as shown [107],

$$I = \omega_a \omega_c (\rho_a - \rho_c)^2 \qquad \textbf{(Eq. 3.4)}$$

where ω_a and ω_c are the weight fractions of the amorphous and crystalline phase respectively, and ρ_a and ρ_c are their electron densities. The invariant would be used for measuring the amount of oxygen uptake of the films during irradiation.

3.7.5 Thermogravimetric analysis (TGA)

Thermogravimetric analysis (TGA) was carried out on a TA Instrument Hi-Res 2950 TGA. Experiments were performed under nitrogen atmosphere at a constant flow rate of 48 $mLmin^{-1}$. The samples were heated from 40°C to 400°C at a heating rate of 15°C/min. The decomposition temperature was taken as the point of inflexion of the graph when mass loss begins.

3.7.6 Polarized optical microscope (POM)

The polarized optical microscope was used to qualitatively verify the presence of crystals during isothermal annealing. It was also used for observing the changes in the crystal morphology after irradiation. The crystals in the films were observed using the LabOPhot-2/2a Nikon polarized microscope and the pictures taken were viewed on this optical microscope between crossed polarizers at a magnification of x420.

3.7.7 Scanning electron microscopy (SEM)

The surface morphology was analyzed for evidence of degradation, irradiation and hydrolytic, using the field emission scanning electron microscope (FESEM). The SEM used was the JOEL, model JSM-6340F, and was operated at a voltage of 5 kV. Before SEM analysis, the samples were first coated with gold using a sputter coater model SPI-Module. The samples were coated for 40 s, with the gas pressure set at 20 mbar and the current adjusted to approximately 18 mA. Signs of surface cracking due to irradiation and osmotic cracking and formation of microcavities due to hydrolytic degradation were observed using the FESEM.

3.7.8 Spectroscopy techniques

In the study of the radiation-induced degradation mechanism, it would be important to understand the changes to the chemical structures of PLGA and PLLA after irradiation. The changes to the chemical structures were verified using FTIR, Raman and NMR spectroscopy. These techniques used were complementary to one another, which provide a more rigorous study of the degradation mechanism involved.

(a) Fourier-transformed infrared spectroscopy (FTIR)

FTIR spectra were obtained using the Perkin Elmer system 2000 FTIR with 16 scans per sample over the range of 4000 - 400 cm^{-1}. For irradiation studies, polymeric films were used in the characterization process. Changes to the peaks with radiation dose were studied and these peaks were compared against FTIR handbooks [108].

For hydrolytic degradation studies, KBr discs were used for the characterization process. The hydrolytically degraded samples were first dissolved in $CDCl_3$ (chloroform-d) solution and then dripped onto dried KBr (potassium bromide) discs using polyethylene droppers. The wetted discs were then placed in a vacuum oven to be dried for an hour before characterization. Any changes to the peaks with hydrolytic degradation were examined.

(b) Raman spectroscopy

Raman spectroscopy analysis was employed, using the Renishaw ramascope. The main purpose of using the Raman spectroscopy was to identify changes to the C–C skeletal backbone, below 1300 cm^{-1} [108], of PLGA and PLLA after irradiation, since FTIR is a poor technique for this purpose. The spectroscope uses an Olympus BH2-UMA microscope having an objective lens of magnification 20. The Raman spectra obtained were stimulated by a laser light of 663 nm with a total of 5 scans per sample.

(c) ^{1}H NMR spectroscopy

The ^{1}H NMR spectra of irradiated PLGA films were acquired at room temperature using a Bruker 400 MHz NMR Spectrometer and $CDCl_3$ was used as the solvent. Chemical shift (δ) was measured in ppm using tetramethylsilane (TMS) as an internal reference. The chemical shifts were compared to references obtained from *Bruice et al.* and *Bakhtiar et al.* [109, 110]. Each of the peaks obtained were then identified accordingly.

Chapter 4 Results and Discussion

4.1 Electron beam irradiation of PLGA and PLLA

This section of the chapter reports on the investigation into the effects of e-beam radiation on the morphological, thermal and radiation-induced degradation behaviours of both PLGA (amorphous) and PLLA (semi-crystalline) films. It also establishes a relationship between the changes in their molecular weights and radiation dose and suggests the possible radiation degradation mechanisms involved.

4.1.1 Chain scission of PLGA and PLLA

PLGA and PLLA films were irradiated with the e-beam accelerator, and the films became brittle to touch with increasing radiation dose. This embrittlement process was presumably due to the degradation of the films as a result of e-beam irradiation. The dominance of chain scission or cross-linking during irradiation can be observed from the changes in the molecular weights of PLGA and PLLA. **Figure 4.1** plots the changes in the molecular weights (M_n and M_w) of PLGA with radiation dose. It can be observed from **Figure 4.1** that the molecular weights of PLGA decrease with increasing radiation dose. This indicates that chain scission is more dominant than cross-linking during e-beam irradiation of PLGA. The plot of the changes in molecular weights of PLLA with radiation dose is shown in **Figure 4.2**.

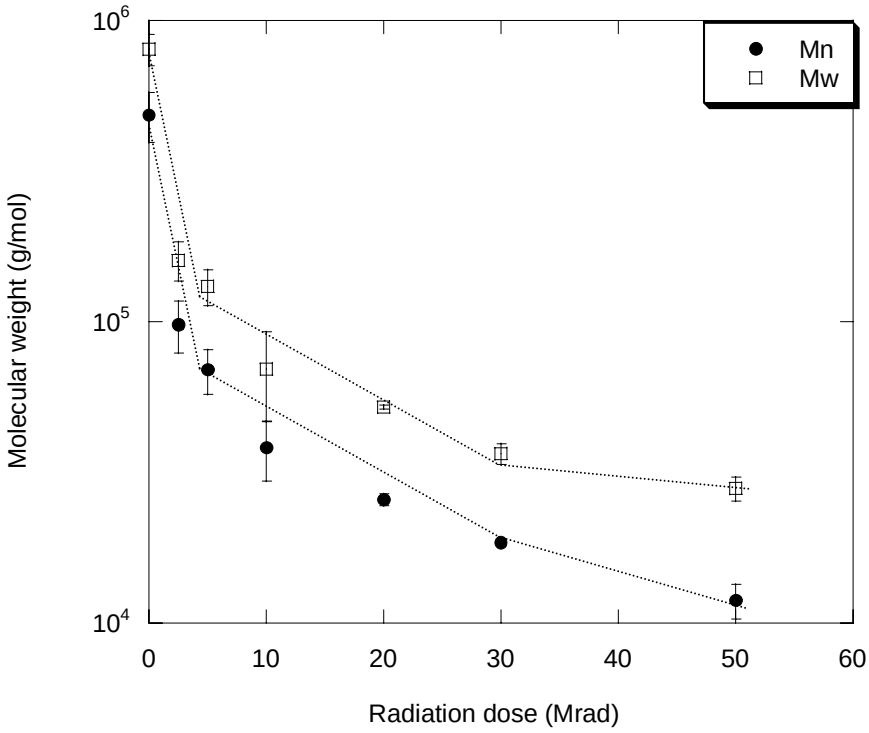

Figure 4.1 – Change in molecular weights of PLGA with radiation dose

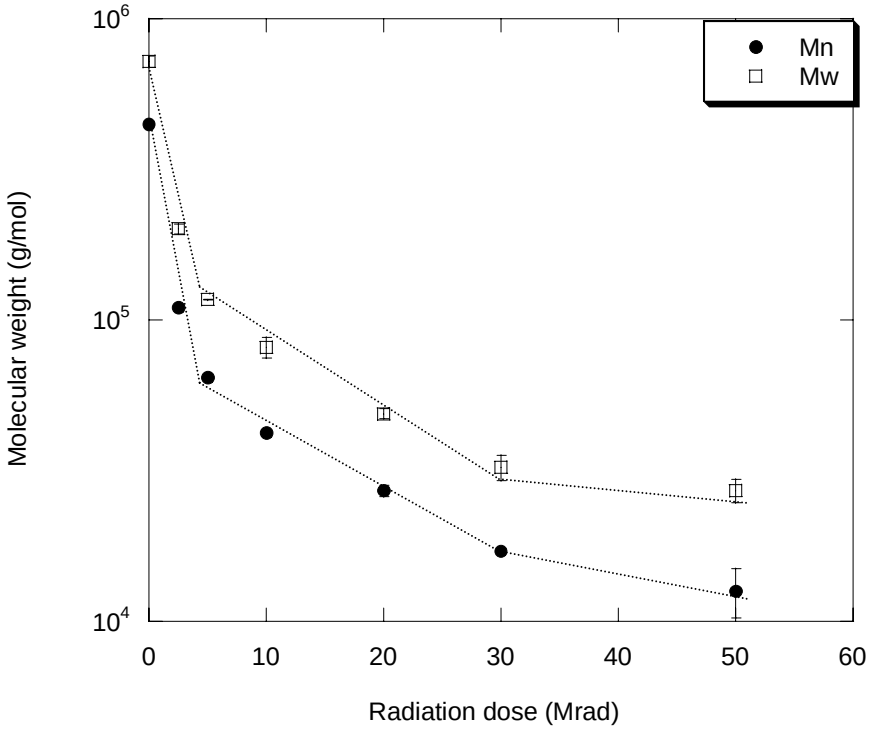

Figure 4.2 – Change in molecular weights of PLLA with radiation dose

It can be observed from **Figure 4.2** that the molecular weights of PLLA, similarly, decrease with increasing radiation dose, indicating scission of the PLLA chains. During irradiation, PLGA and PLLA molecules are excited, to form active species, such as free radicals. Since irradiation is carried out in the presence of oxygen, these free radicals, being highly reactive with oxygen, will react to form peroxyl free radicals. They will then react with one another and initiate reactions among the polymeric chains, causing chain scission through chain transfer and the splitting of the polymer chains. The high energy from the e-beam radiation may at the same time disrupt the molecules and cause the breaking of chemical bonds between monomers. The chemical bonds with the lowest bond dissociation energy will therefore be the first to be broken by the high energy radiation, thereby lowering the molecular weight of these polyesters.

It can be observed from **Figure 4.1** and **Figure 4.2** that there are three empirical stages to the decrease in molecular weights. In the first stage, below 5 Mrad, a drastic decrease in molecular weight was observed, followed by a more steady decrease in the second stage, between 5 Mrad and 30 Mrad. In the third stage, between 30 Mrad and 50 Mrad, the molecular weight decrease is minimal. There are a few reasons to this observed phenomenon; firstly, the difference in radiation-induced degradation mechanisms at each stages, secondly the increase in incidences of free radical recombinations with increasing radiation dose and thirdly the formation of a crystalline phase upon irradiation, which would all be further discussed.

(a) Radiation-induced degradation mechanisms

One of the reasons for this observation is due to the difference in radiation-induced chain scission mechanisms at each of the three stages. The study of the radiation-induced degradation mechanisms is one of the novel contributions to scientific knowledge in this thesis. This study is of interest not only because of the dearth of journal papers on the radiation mechanisms of PLGA and PLLA, but it will also allow a better understanding of how radiation may affect the rate of hydrolytic degradation of these biodegradable polyesters.

It is believed that the radiation-induced degradation mechanism of both PLGA and PLLA, from 0 Mrad to 50 Mrad, follows a 3-stage process. The first stage results in the initial drastic decrease in molecular weight, below 5 Mrad, due to a dominance of backbone main chain scission, where long polymeric backbone chains break into shorter chains. Random chain scission of the polymer backbone and side-groups occurs uniformly both in the crystalline and amorphous regions, forming alkyl free radicals. This happens because the energy from the radiation exceeds the attractive forces between the atoms. The excited states along the polymer backbone dissipate some of the excess energy through bond scission, which results in massive formations of alkyl free radicals. However, *Carlsson et al.* [86] and *Tsuda et al.* [88] mentioned that the scission of C-H bonds is usually favoured over C-C backbone scission; where in highly excited states, C-C bonds are more stable than C-H bonds, contrary to the ground-state situation. *Partridge et al.* [87] attributed this to energy migration along the backbone by an exciton mechanism, thus

minimizing energy localization in specific C-C backbone bonds, whereas energy deposited in C-H bonds cannot migrate. However, for polyesters such as PLGA and PLLA, the C-C backbone is interrupted by intermittent oxygen atoms along the polymer backbone, as shown from their chemical structures in **Figure 2.1** and **Figure 2.2**. This irregularity along the backbone will weaken the skeletal backbone and increase the ease of backbone chain scission. The irregularity also prevents the migration of energy and results in the localization of radiation energy at the C-C and C-O bonds along the polyester backbone, causing scission at these locations of the backbone.

The breaking of the backbone results in the formation of carbon dioxide gas, as observed from the formation of a carbon dioxide FTIR peak at frequency 2340 cm^{-1} [108], from **Figure 4.3**. It is to be noted that the formation of carbon dioxide gas was observed for all irradiated samples from 2.5 Mrad to 50 Mrad, proving that backbone chain scission occurs through 50 Mrad. This carbon dioxide peak was only detected for freshly irradiated samples. Carbon dioxide is formed probably due to the removal of the ester group from the polyesters and from the decomposition of the peroxyl free radical in the peroxidation radical phase, as shown in **Figure 4.4**. **Figure 4.5** shows the schematic diagram of the various possible locations of chain scission occurring. The formation of carbon dioxide from the removal of the ester group can also be seen from **Figure 4.5**.

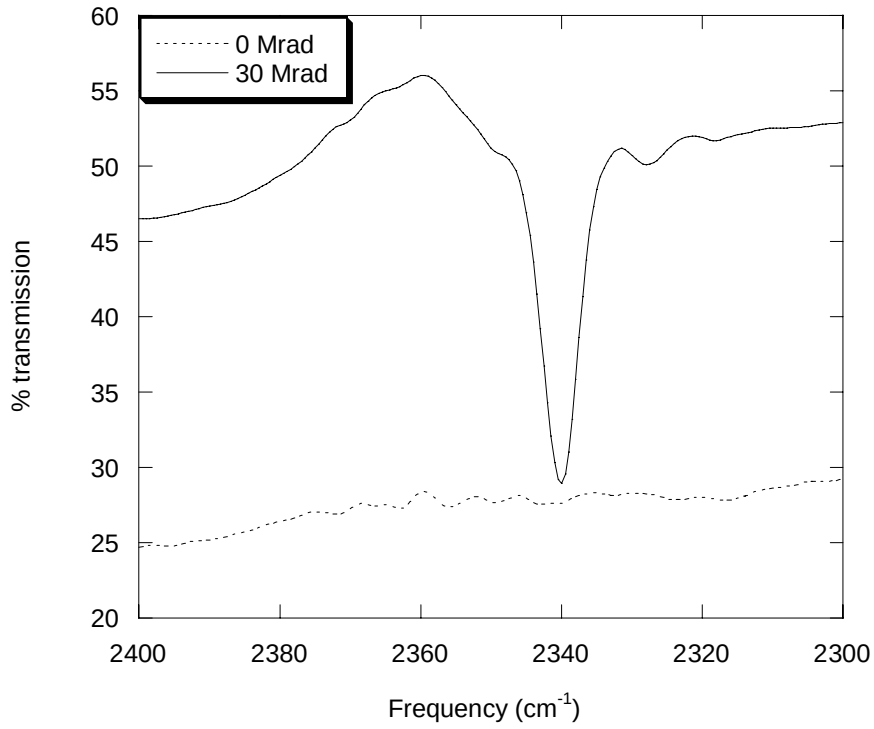

Figure 4.3 – FTIR spectra of PLGA showing carbon dioxide peak at frequency 2340 cm^{-1} after irradiation

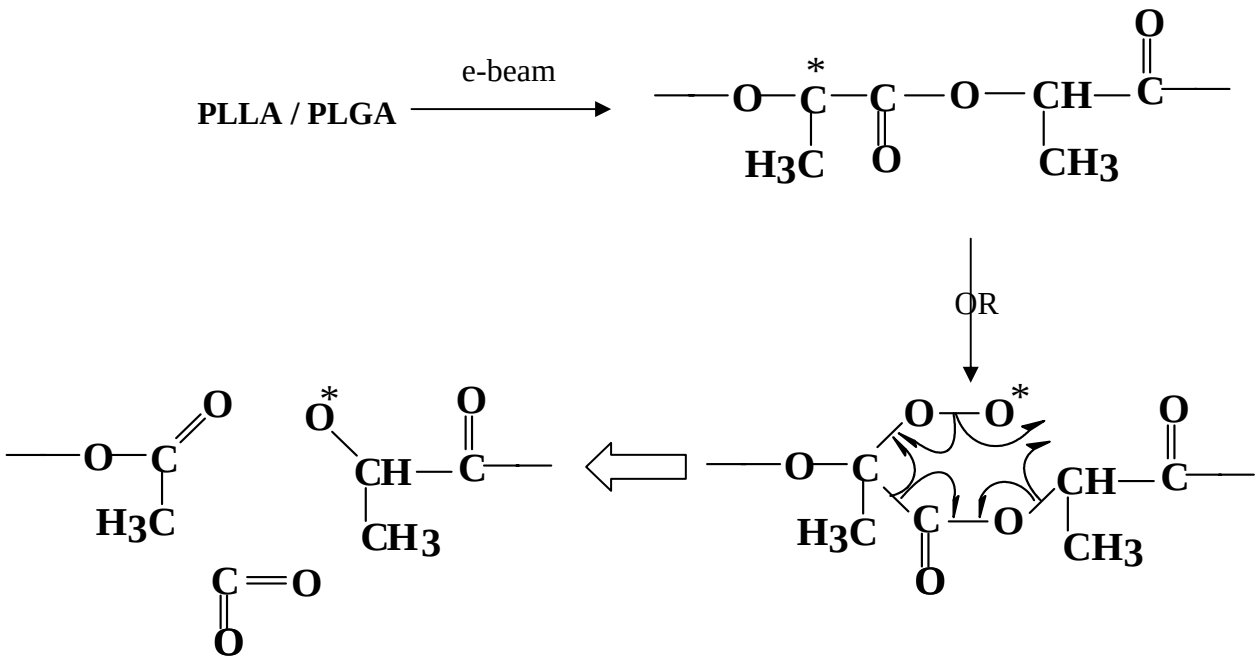

Figure 4.4 – Schematic diagram of decomposition of peroxyl free radical releasing carbon dioxide

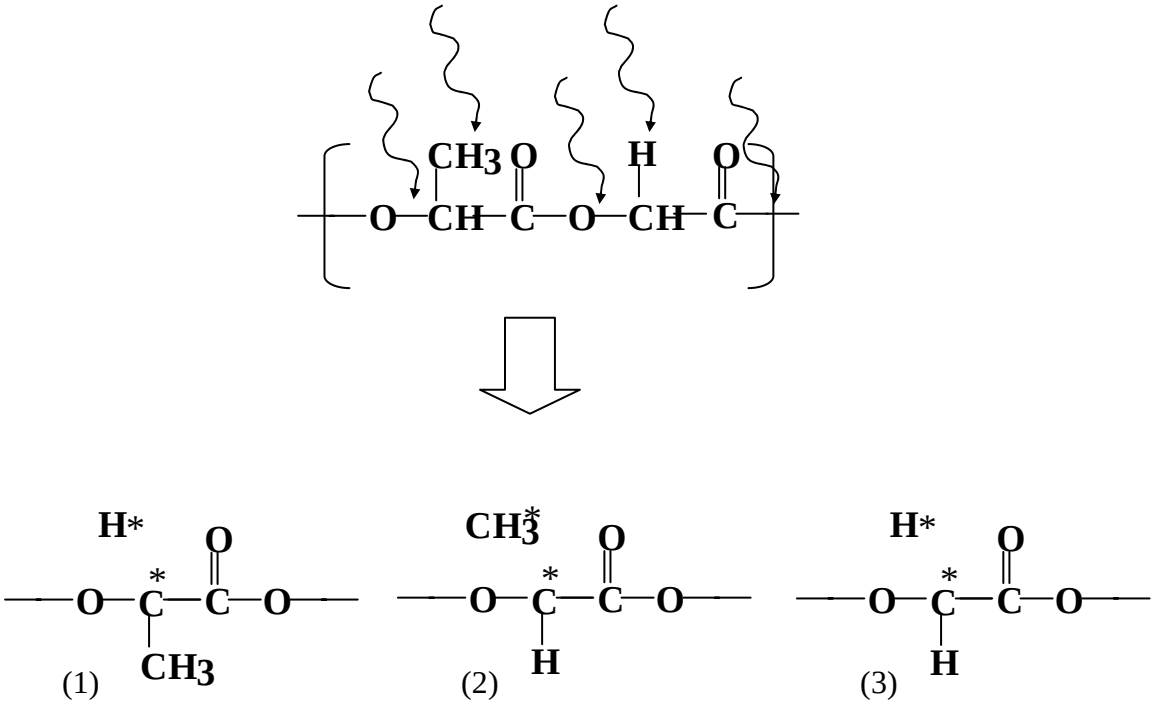

(a) Polymer side-chain scission

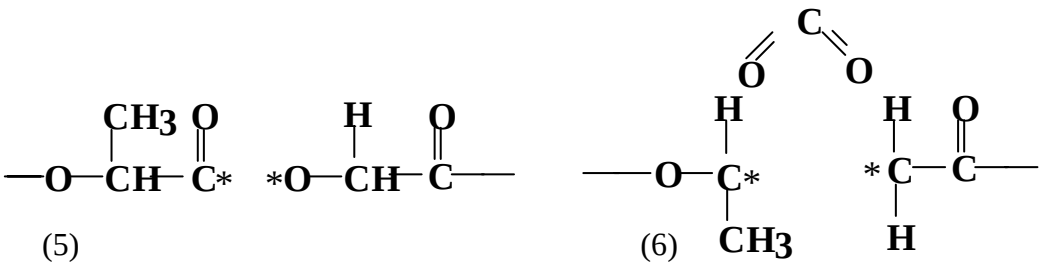

(b) Polymer backbone main-chain scission

Figure 4.5 – Schematic diagram of the various locations of statistically possible chain scissions

Figure 4.6 and **Figure 4.7** plots the SAXS invariant of the irradiated films with radiation dose for PLGA and PLLA respectively. The results show an initial increase in the invariant, which subsequently remain relatively constant. The increase in invariant in irradiated PLGA and PLLA can be interpreted as an increase in the difference in electron densities between the amorphous and crystalline phases. This increase in electron density difference is due to the formation of peroxyl free radicals, when oxygen enters the amorphous region, as also observed by *Goldman et al.*, in the irradiation of UHMPE [27], and also during the irradiation of polypropylene [29] and polycarbonate [32]. *Williams et al.* reported that oxygen is excluded from the crystalline regions due to their close-packed structure [30]. The electronegativity of oxygen increases the electron density of the amorphous phase, thus increasing the invariant. This will result in a difference in bond structures of the amorphous and crystalline chains [111]. It is therefore noted that during the first stage of the degradation mechanism, oxygen enters into the amorphous region of the polymer.

Oxygen molecules act as alkyl free radical scavengers, resulting in radical conversion and the formation of peroxyl free radicals. There are several possible structures of peroxyl free radicals that may be formed during irradiation, as shown in **Figure 4.8**. Peroxyl free radicals cause chain scission, within the amorphous region and at the crystal interface, through hydrogen abstraction [80]. This is the second stage of the degradation mechanism, where backbone chain scission and hydrogen abstraction occurs simultaneously at equal rates, contrary to the first stage where backbone chain scission is more dominant.

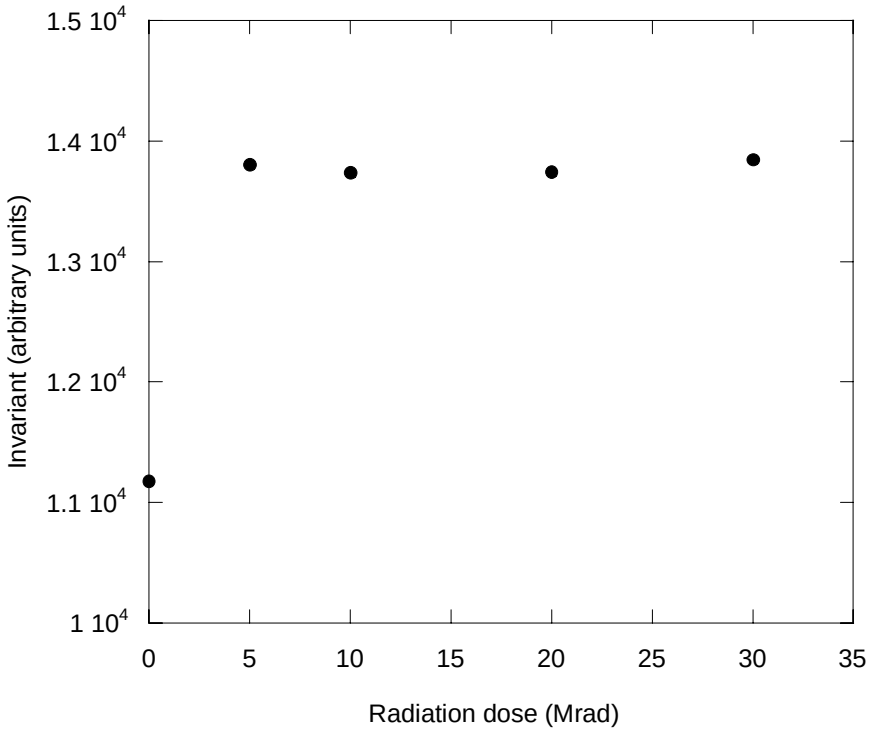

Figure 4.6 – Plot of PLGA SAXS invariant with radiation dose

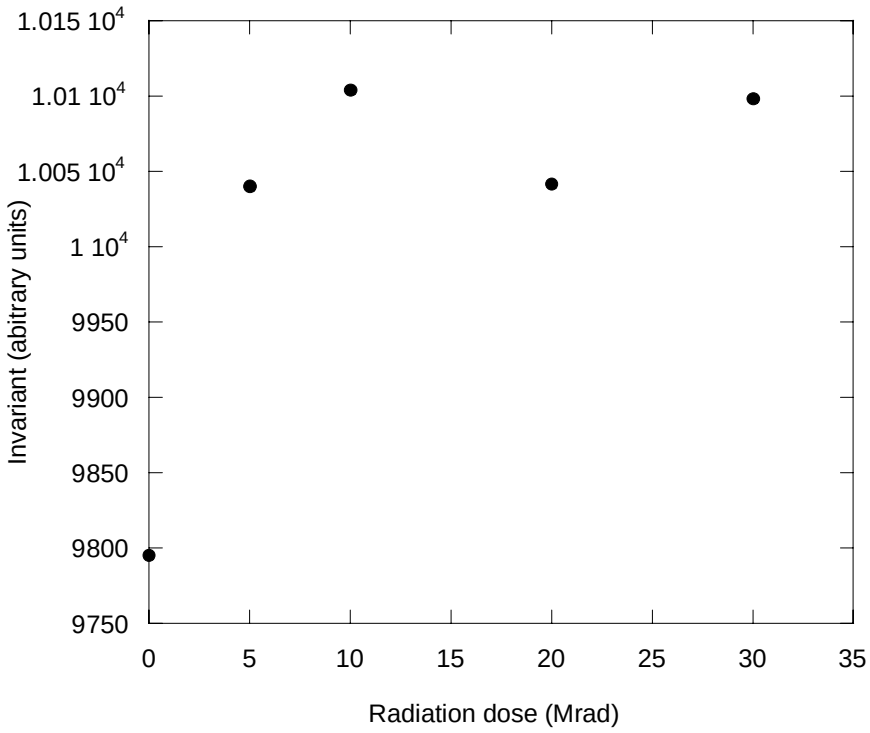

Figure 4.7 – Plot of PLLA SAXS invariant with radiation dose

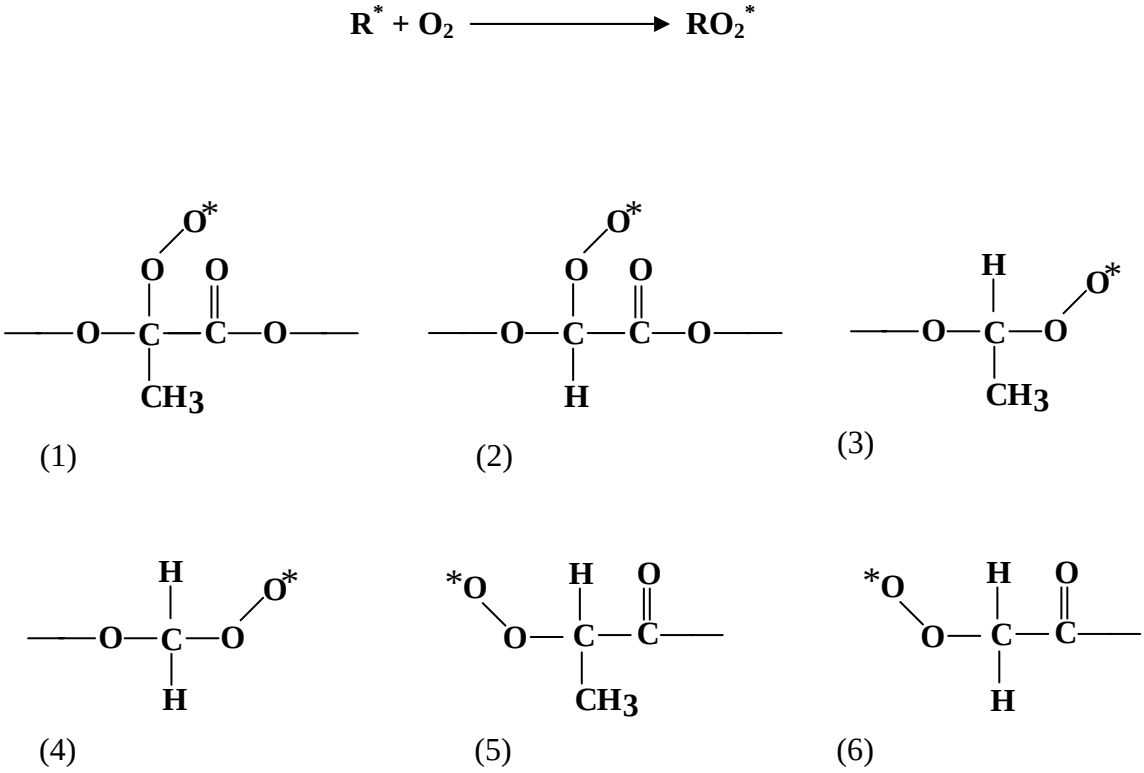

Figure 4.8 – Possible chemical structures of peroxyl free radicals in PLGA

At higher radiation doses (above 30 Mrad), hydrogen abstraction becomes the main dominant radiation-induced scission mechanism, though minimal backbone chain scission may also occur [111]. This is the third stage of the radiation-induced degradation mechanism. Unlike a combination of main-chain scission and hydrogen abstraction in the second stage, hydrogen abstraction alone had less pronounced effect on the decrease in molecular weight [111]. The evidence of hydrogen abstraction taking place more dominantly at higher radiation dose can be verified using Fourier-transformed infrared (FTIR) and Raman spectroscopy. The following describes the results obtained from these spectroscopy techniques.

(i) FTIR spectroscopy

Irradiation of PLGA and PLLA results in similar changes in their FTIR spectra; and therefore, only the results of PLGA will be discussed. **Figure 4.9** plots the % infrared transmittance against the infrared frequency (3800 cm^{-1} to 3100 cm^{-1}) for the non-irradiated and 50 Mrad irradiated PLGA films. **Figure 4.9** shows two distinct differences between the non-irradiated and irradiated samples; firstly, the formation of a new peak at frequency 3320 cm^{-1} and secondly, the increase in peak intensity at frequency 3505 cm^{-1}. **Figure 4.10** plots the increase in peak intensity for 3505 cm^{-1} relative to the peak intensity of 3650 cm^{-1}. The formation of a peak at frequency 3320 cm^{-1} and the increase in peak intensity at 3505 cm^{-1} corresponds to an increase in the hydroxyl (OH) groups formed during irradiation, though a small contribution could also be from water and hydro-peroxides produced in the course of oxidation [102]. The formation of these OH groups, as the termination product, is therefore the result of the hydro-peroxides undergoing degenerate chain branching, resulting from hydrogen abstraction [80]. It can be observed from **Figure 4.10** that the more OH groups are formed at 30 Mrad and above.

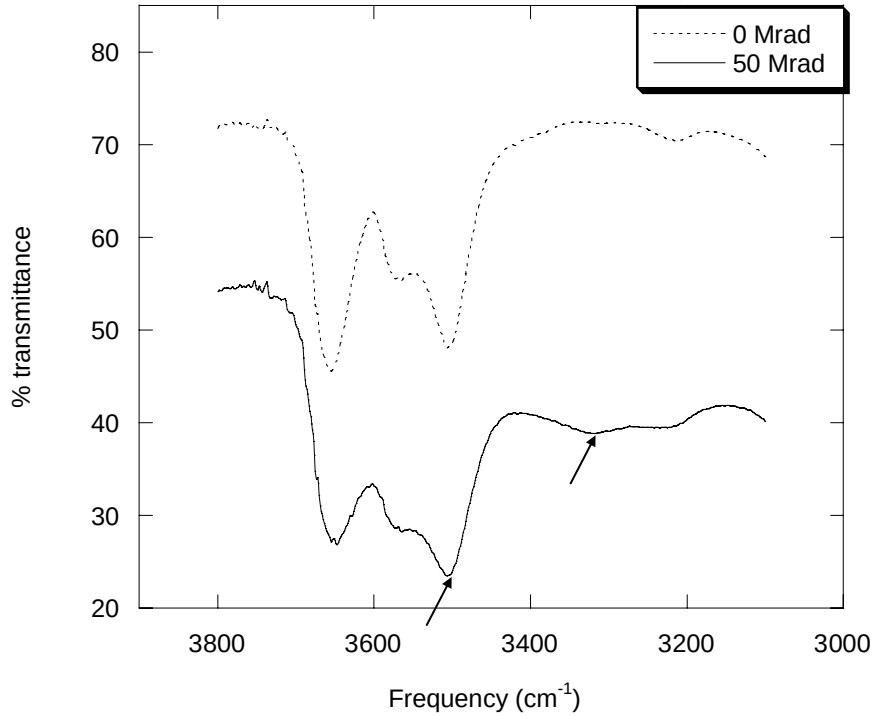

Figure 4.9 – FTIR plot of % transmittance against infrared frequency (3800 cm^{-1} to 3100 cm^{-1}) of PLGA (Arrows indicate peaks with changes)

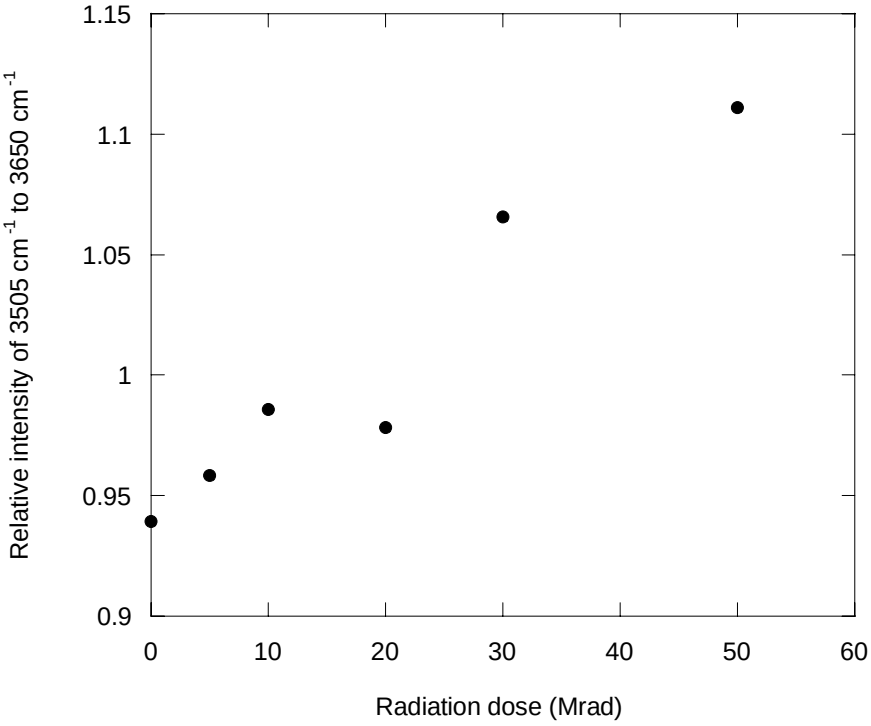

Figure 4.10 – Relative increase in peak intensity of peak 3505 cm^{-1} to peak 3650 cm^{-1}

(ii) Raman spectroscopy

The Raman spectroscopy was used as a complement to the FTIR spectroscopy, in which certain bonds that could not be observed on the FTIR may be seen using the Raman spectroscopy. The Raman was therefore used to observe changes to the C–C skeletal backbone of the biopolymers after irradiation, since FTIR is a poor technique for this purpose [108]. The Raman spectroscopy identifies molecular bonds that can be polarized (more frequently symmetric vibrational mode), by detecting a change in polarizability during vibration.

As the C–C skeletal backbone is of interest to our study from the Raman spectroscopy, only the spectrum below 1400 cm^{-1} will be highlighted. It was also noted that the changes in the Raman spectra for PLGA and PLLA were the same, and thus only the results for PLGA would be used in the discussion. The Raman spectra (from 1400 cm^{-1} to 400 cm^{-1}) of the non-irradiated and irradiated (50 Mrad) PLGA films are shown in **Figure 4.10**. It can be observed that no new peaks were formed after irradiation. However, there was an increase in peak intensity for the irradiated film at frequencies 1250 cm^{-1}, 705 cm^{-1}, 490 cm^{-1} and 430 cm^{-1}. These peaks correspond to OH bending coupled to CH_2 or CH group, possible CC–OH stretch, and the skeletal bending of primary and secondary alcohols respectively. The increase in the intensities of these peaks therefore indicates the formation of hydroxyl (OH) groups. The results obtained from the Raman spectroscopy reinforced the observations made on the FTIR, where an increase in OH groups was observed at higher radiation dose, or during the third stage of degradation.

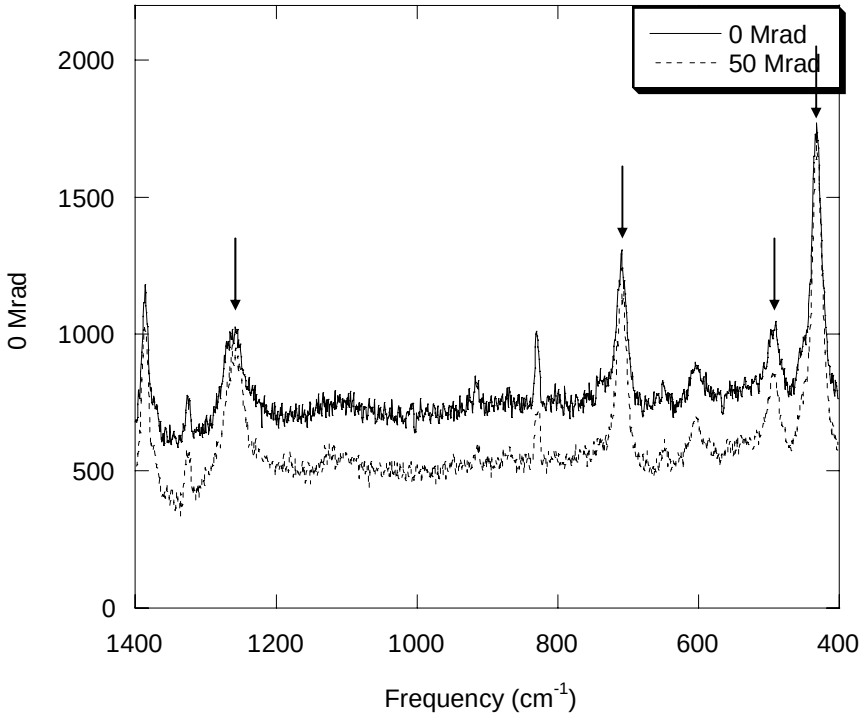

Figure 4.11 – Raman spectroscopy of non-irradiated and 50 Mrad irradiated PLGA film (1400 cm^{-1} to 400 cm^{-1}) (Arrows indicate peaks with changes)

Hydrogen abstraction through these peroxyl free radicals result in the formation of hydro-peroxides and subsequently more alkyl free radicals, as shown in the schematic diagram from **Figure 4.12**. The hydro-peroxides subsequently undergo chain degeneration to form OH groups as the main end-product constituent, as verified from the FTIR (**Figure 4.10**) and Raman (**Figure 4.11**) and shown from the schematic diagram in **Figure 4.13**. It had been observed that the more highly irradiated samples (30 and 50 Mrad) showed a more significant increase in OH groups, verifying that hydrogen abstraction is more dominant at these radiation doses. Hydroxyl free radicals formed will also recombine to form alcohol side groups, peroxides or water [102], further increasing the number of OH groups.

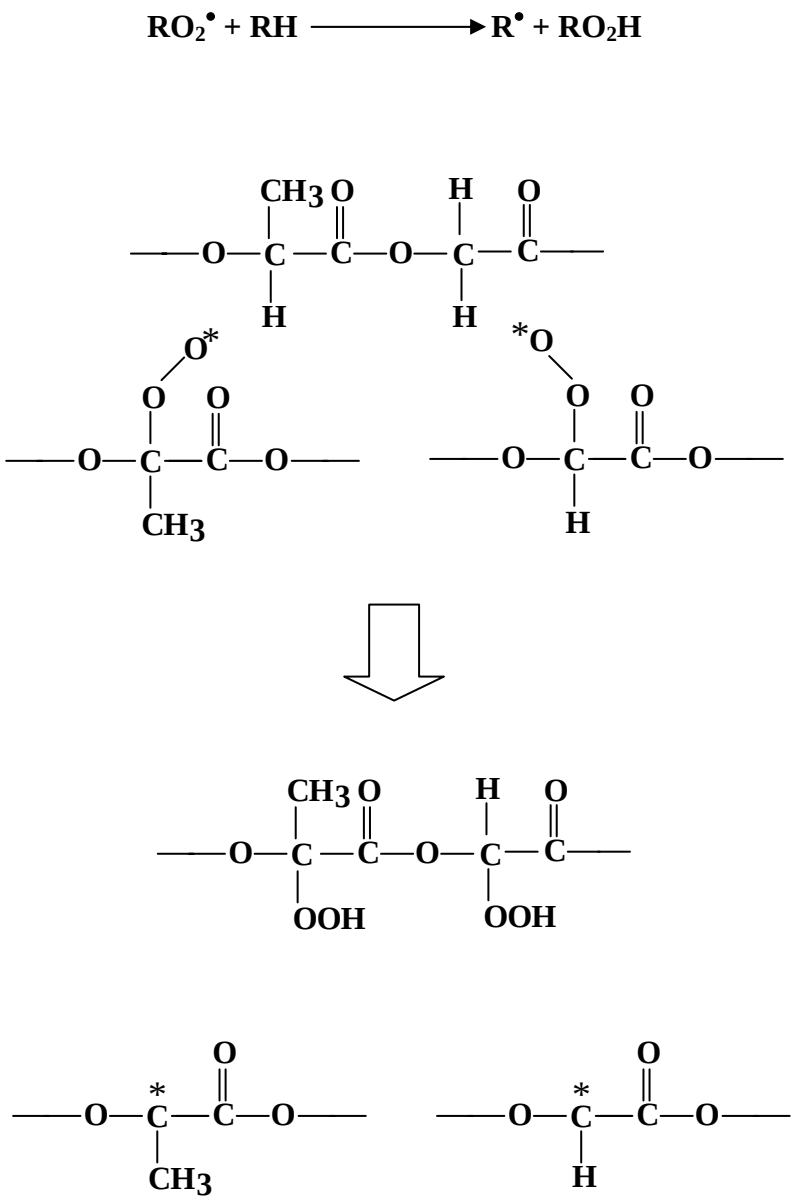

Figure 4.12 – Schematic diagram showing hydrogen abstraction of PLGA in forming hydro-peroxides

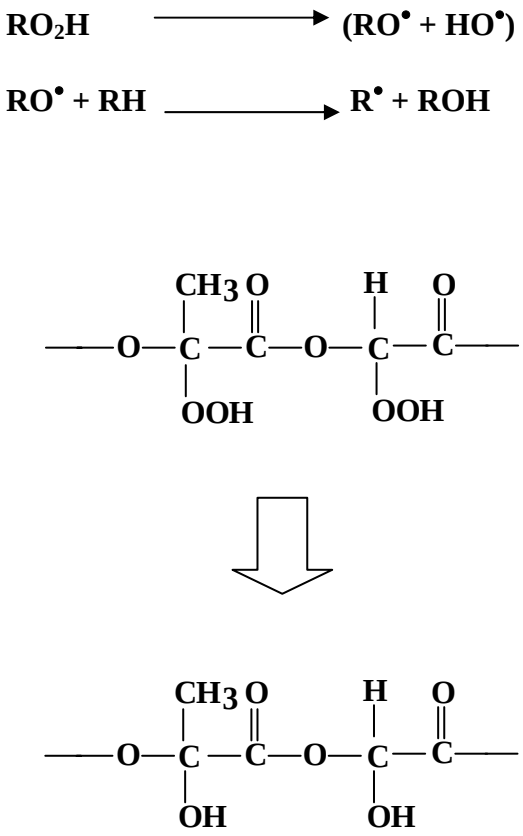

Figure 4.13 – Diagram showing the formation of hydroxyl groups

The 3-stage degradation process can therefore be summarized as dominant backbone chain scission, followed by simultaneous backbone scission and hydrogen abstraction, and lastly, dominant hydrogen abstraction. It was noted from the results that although some hydrogen abstraction reactions are occurring at low radiation dose, it is more dominant at higher radiation dose. Hydrogen abstraction alone could not have caused the initial drastic decrease in molecular weight, which can only be explained by backbone chain scission. This explains the difference in molecular weight decrease as observed from **Figure 4.1** and **Figure 4.2**.

(b) Free radical recombination

Another reason for the difference in the decrease in molecular weight is that at higher radiation doses, there is a relative increase of free radical recombination to free radical-induced chain scission. At high radiation dose, the number of alkyl free radicals formed could have been larger than the number of peroxyl free radicals present, due to the continuous formation of alkyl free radicals, as seen from **Figure 4.12**. Alkyl free radicals being less effective in causing chain scission are therefore more likely to recombine. The recombination effect can be observed from the ^{1}H NMR spectroscopy.

The ^{1}H NMR of a non-irradiated and 50 Mrad irradiated PLGA is shown in **Figure 4.14** and **Figure 4.15** respectively. The difference between the two ^{1}H NMR spectra is shown in **Figure 4.16**, where a magnification of the ^{1}H NMR region from 1.0 ppm to 2.7 ppm is highlighted. It can be seen that new overlapping multiplets were formed at 1.76 ppm, doublets at 1.45 ppm, a singlet at 1.28 ppm, triplets at 1.18 ppm and various multiplets and singlets within the range of 2.15 ppm to 2.50 ppm. The existence of these peaks arises from the formation of new bonds as a result of recombination of the backbone. This recombination process therefore explains for the reduction in molecular weight decrease with increasing radiation dose. **Table 4.1** summarizes the possible chemical structures for each of these ^{1}H NMR peaks due to free radical recombination.

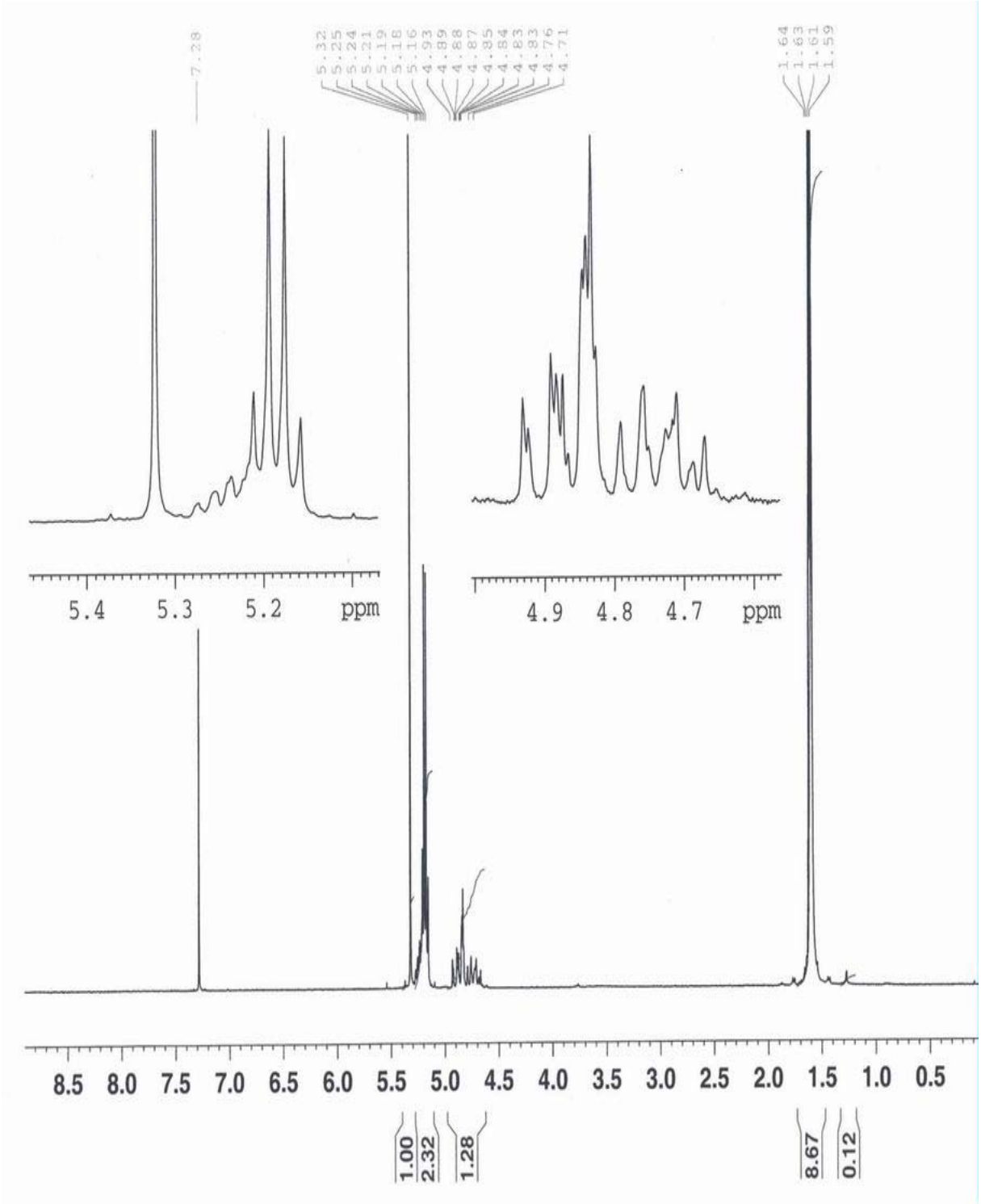

Figure 4.14 – ^{1}H NMR of non-irradiated PLGA

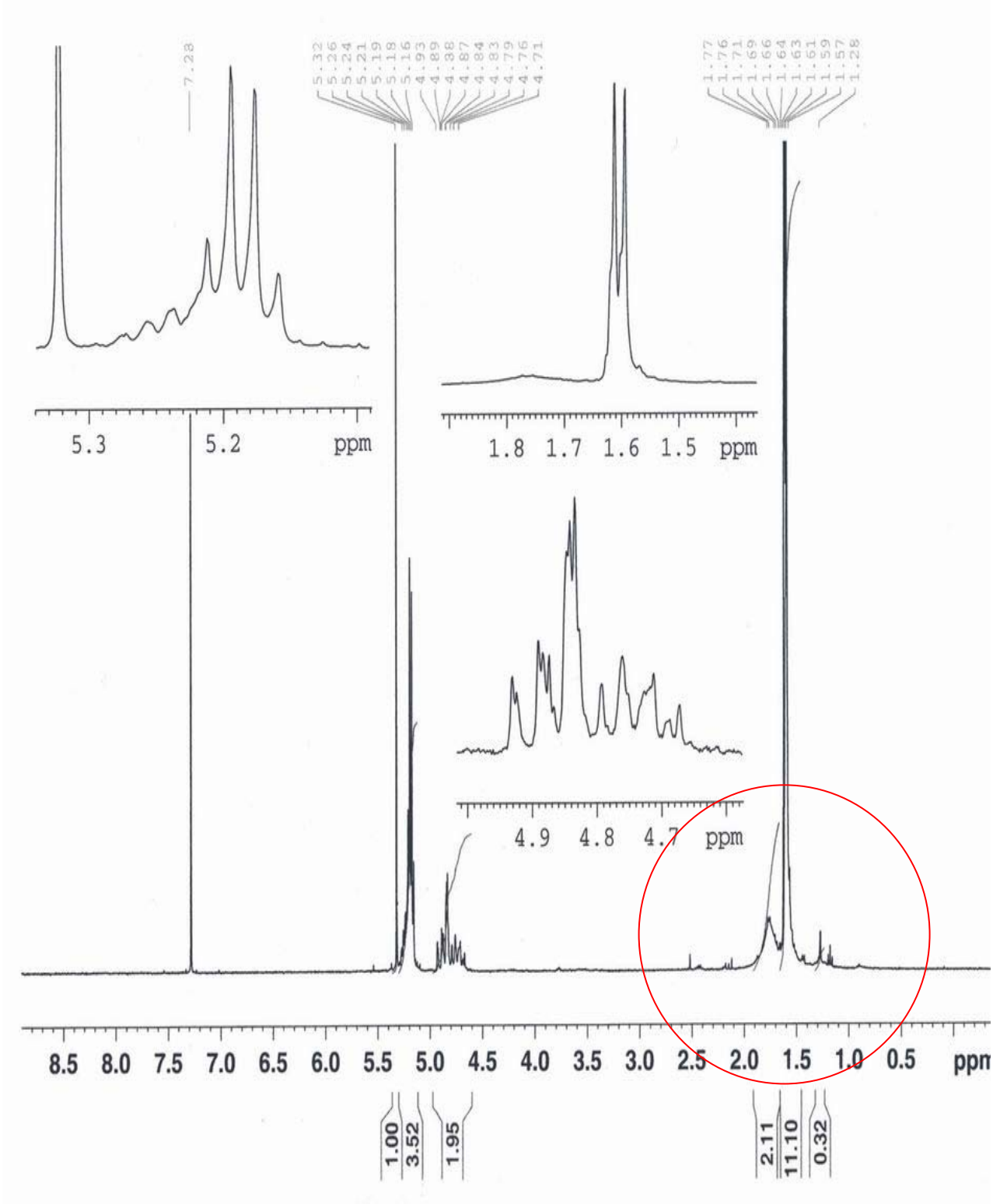

Figure 4.15 – ^{1}H NMR of 50 Mrad irradiated PLGA

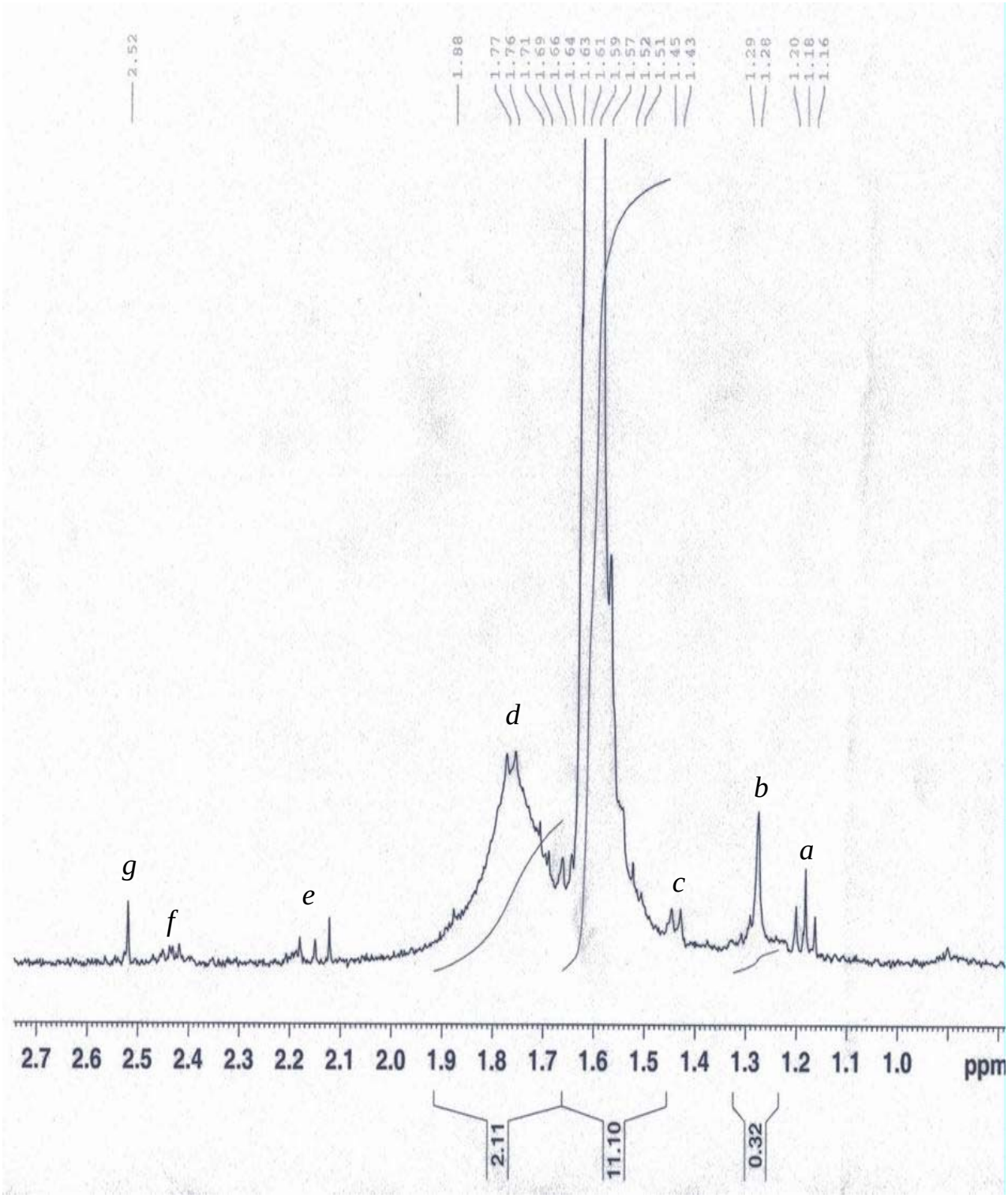

Figure 4.16 – Magnification of ^{1}H NMR of 50 Mrad irradiated PLGA from 1.0 to 2.7 ppm

Table 4.1 – Identification of the possible chemical structures of the new peaks formed on the ^{1}H NMR

δ (ppm)	Proposed structure	No. of peaks
1.18	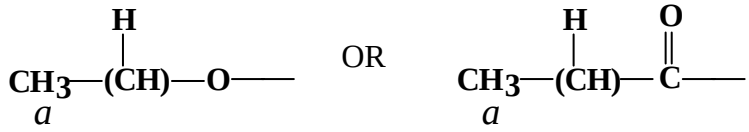	Triplets
1.28	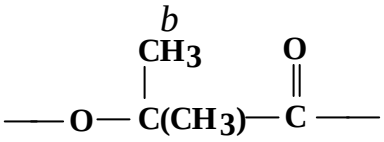	Singlet
1.45	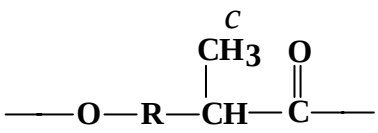 **R: CH_2 / $CH(CH_3)$ / $C(CH_3)_2$**	Doublet
1.76	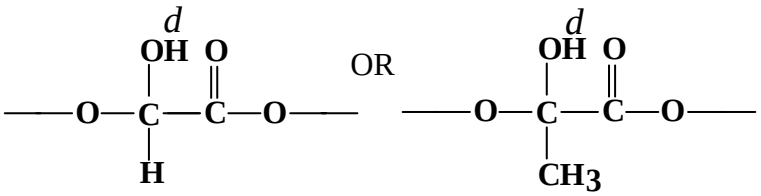 	Broad base
2.15	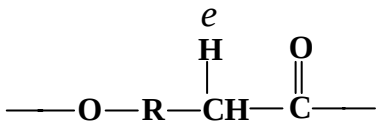 **R: CH_2 / $CH(CH_3)$ / $C(CH_3)_2$**	Multiplets
2.43	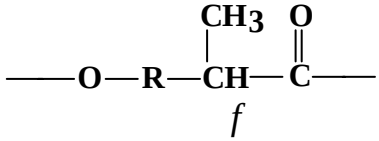 **R: CH_2 / $CH(CH_3)$ / $C(CH_3)_2$**	Multiplets
2.52	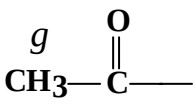	Singlet

Figure 4.17 plots the polydispersity index of PLGA and PLLA against radiation dose. The results show an increase in the polydispersity index for both polymers with increasing radiation dose. This increase results from poorer chain uniformity arising from firstly recombination of free radicals, as seen from **Table 4.1,** and secondly, a wider distribution of chain length due to random chain scission. Recombination could also result in chain branching, which would further increase the polydispersity indices of PLGA and PLLA.

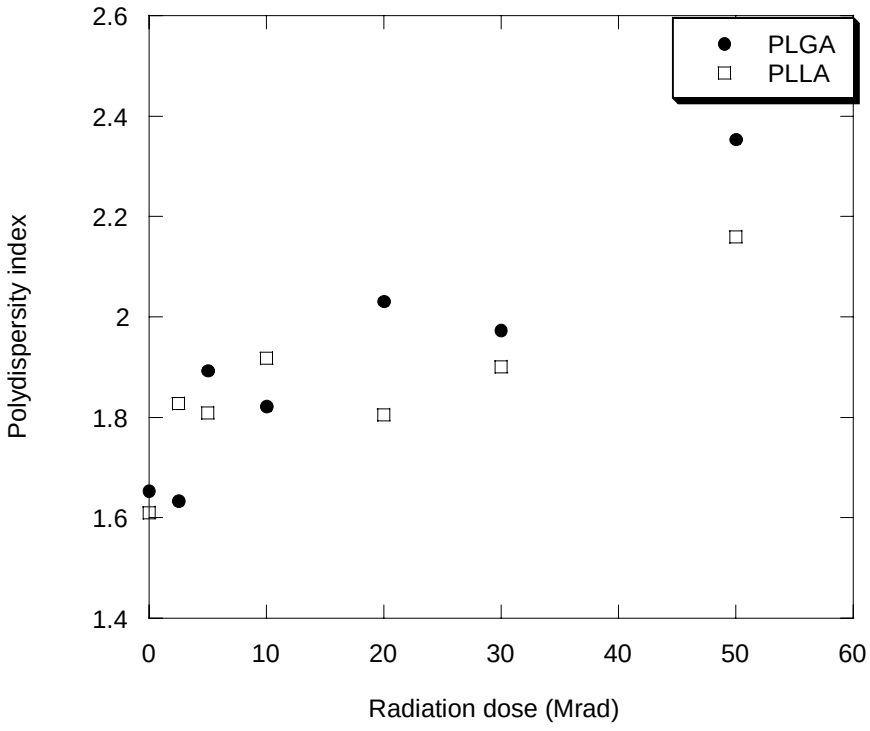

Figure 4.17 – Plot of polydispersity index of PLGA and PLLA with radiation dose

(c) Crystallinity

Another reason for the reduction in the molecular weight decrease is the formation of crystalline phases with increasing radiation dose. **Figure 4.18** plots the change in the measure of degree of crystallinity (DOC) for PLGA with radiation dose. The results show an increase in DOC of PLGA with radiation dose. Chain scission during e-beam irradiation gives rise to shorter polymer chains, which have better mobility and are able to align themselves to form a crystalline phase. The crystalline regions formed consist of chains that are more oriented and closely packed compared to the amorphous regions. The close proximity of the polymer chains in the crystalline structure encourages the trapped free radicals to recombine, through the "cage effect" [90], thus reducing the number of effective chain scission. The close-packed structure of the crystalline regions also excludes specific active radical species [30]. As a result, peroxyl free radicals are unlikely to be formed within the crystalline regions, thus reducing the number of effective chain scissions. Hence, the presence of a crystalline phase, even for semi-crystalline PLLA, as would be seen later, retards the chain scission process.

All three reasons are involved in the reduction in molecular weight decrease for PLGA and PLLA. However, the difference in radiation-induced degradation mechanism in the three stages and the increase in free radical recombination with increasing radiation dose are the most dominant reasons for this observation. The increase in degree of crystallinity in PLGA was small (**Figure 4.18**), and would have a less significant effect on the reduction in molecular weight decrease.

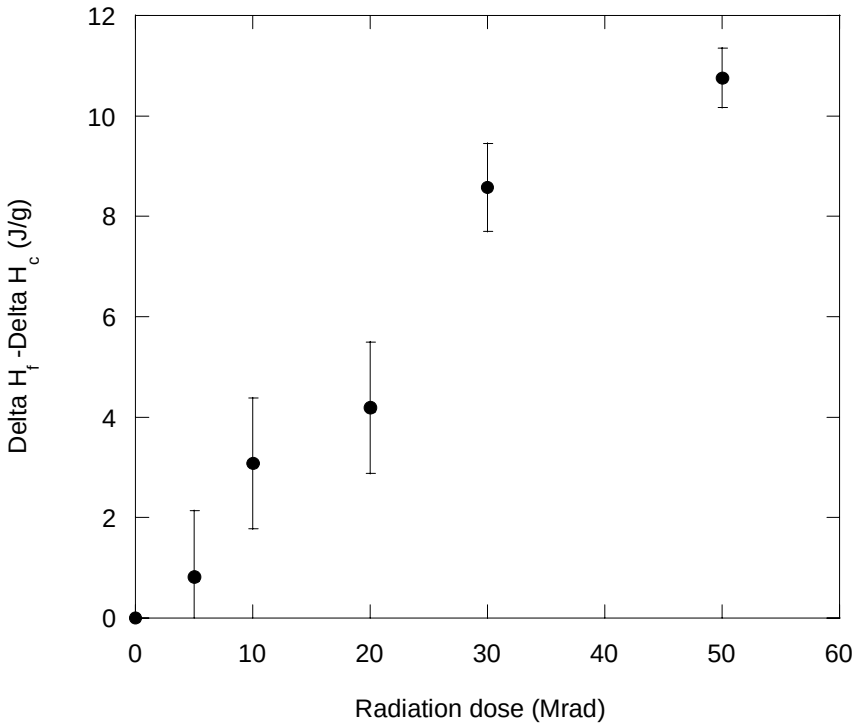

Figure 4.18 – Plot of difference of ΔH_f and ΔH_c of PLGA with radiation dose

The decrease of the molecular weight of PLGA and PLLA and the formation of hydrophilic alcohol or hydroxyl (OH) groups is therefore hypothesized to have an effect on their hydrolytic degradation rate. It is believed that these factors will increase the water uptake in these biopolymers and possibly accelerate the rate of hydrolytic degradation. This hypothesis would be examined in **Chapter 4.2**, in the hydrolytic degradation of irradiated PLGA and PLLA.

4.1.2 Relationship between molecular weight and radiation dose

From **Eq. 2.4** and **Eq. 2.5**, the dominance of chain scission and cross-linking can be quantified from the G_s and G_x values, which are the radiation chemical yields for chain scission (G_s) and cross-linking (G_x). The G_s and G_x values can therefore be obtained from the plot of the reciprocal molecular weight against radiation dose. **Figure 4.19** and **Figure 4.20** plots the reciprocal of the molecular weights against radiation dose, for PLGA and PLLA respectively. The G_s and G_x values and G_s/G_x ratio of PLGA and PLLA are tabulated in **Table 4.2**.

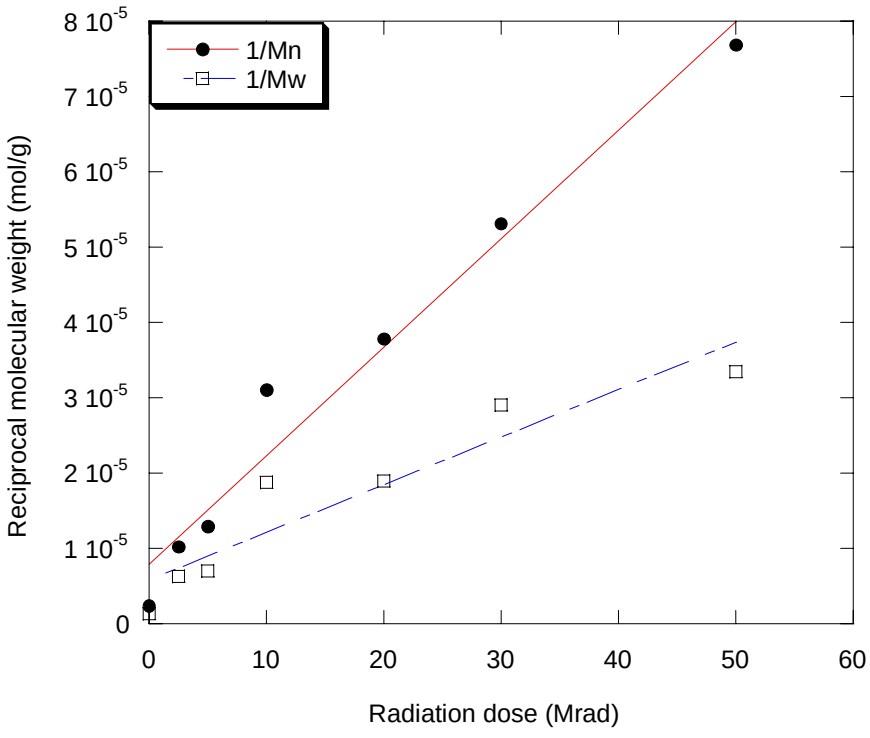

Figure 4.19 – Plot of the reciprocal of molecular weights with radiation dose for PLGA

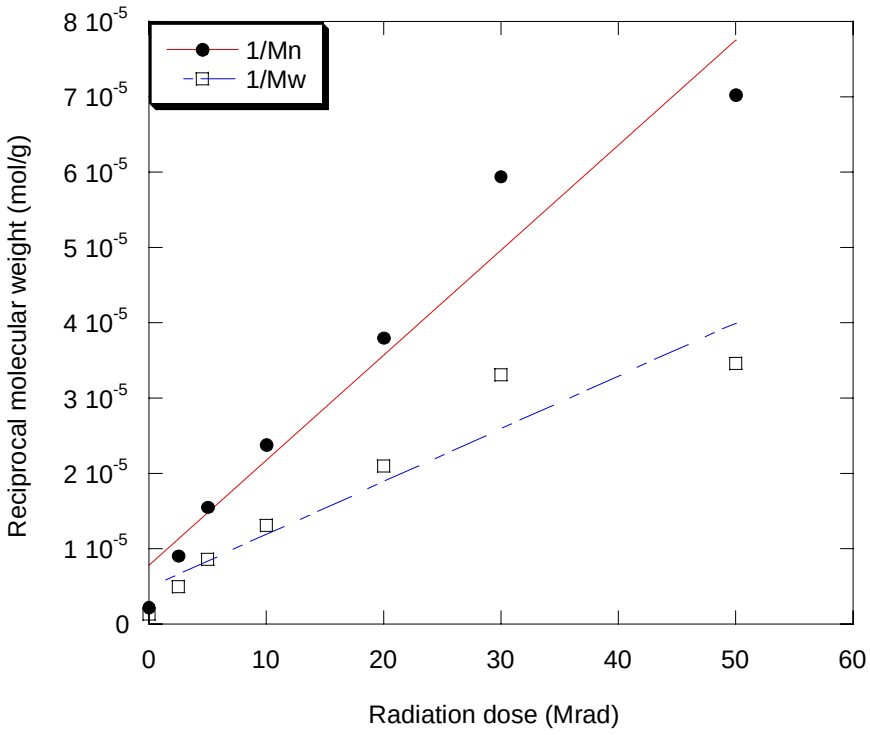

Figure 4.20 – Plot of the reciprocal of molecular weights with radiation dose for PLLA

Table 4.2 – Chain scission (G_s) and cross-link (G_x) radiation yields of PLGA and PLLA irradiated in the presence of air

Polymer	G_s	G_x	G_s/G_x
PLGA	0.133	0.006	23.1
PLLA	0.123	0.011	11.0

The plot of the reciprocal number average molecular weight with radiation in **Figure 4.19** and **Figure 4.20** show a linear plot with sample correlation coefficients [112] of 0.98 and 0.97 for PLGA and PLLA, respectively. Their respective linear

gradients are dependent on their G_s and G_x values [33], which is dependent on the polymer system, i.e. PLGA or PLLA. The linear plots could therefore be a model that relates the decrease in molecular weight of both PLGA and PLLA with radiation dose. Using the least-squares estimate to determine the estimated linear regression equation and the standard error of the estimate [112], the equation obtained for PLGA is,

$$1/M_n = 1/M_{n,0} + 1.44\times10^{-6}\times D \qquad \textbf{(Eq. 4.1)}$$

for radiation doses from 2.5 Mrad to 50 Mrad. $M_{n,0}$ is the initial number average molecular weight at 0 Mrad and D is the radiation dose, and the standard error of this estimate is $5.10\text{x}10^{-6}$ mol/g.

Similarly, the equation for PLLA is,

$$1/M_n = 1/M_{n,0} + 1.39\times10^{-6}\times D \qquad \textbf{(Eq. 4.2)}$$

for radiation doses from 2.5 Mrad to 50 Mrad, and the error of this estimate is $6.24\text{x}10^{-6}$ mol/g. It can be deduced from **Eq. 4.1** and **Eq. 4.2** that the dependence of molecular weight decrease with radiation dose is fairly close for both polymers; within their respective error of estimates. The error of estimates can be further reduced by increasing the sample population, since only a small sample population (7 radiation doses) was used for plotting of these regression lines; though it is also noted that these 2 regression lines have very good sample correlation coefficients.

Nevertheless, from these equations, it can be seen that molecular weight can be accurately controlled with the appropriate radiation dose. Since molecular weight affects the rate of hydrolytic degradation [8], **Eq. 4.1** and **Eq. 4.2** would therefore be used to model the relationship between radiation dose and the subsequent hydrolytic degradation rate of PLGA and PLLA respectively, in **Chapter 4.2**.

The ratio of G_s/G_x differs for PLGA and PLLA, as shown in **Table 4.2**. The results show that PLGA has a higher G_s/G_x ratio compared to PLLA, indicating that PLGA is more susceptible to e-beam radiation degradation than PLLA. This can be explained from the morphologies of these biopolymers, where PLGA is amorphous and PLLA has a semi-crystalline morphology. Due to the close packing of the crystalline structure in PLLA, the diffusion of oxygen into the crystalline region limits the formation of peroxyl free radicals and thus, the extent of chain scission. The "cage effect" also encourages the recombination of free radicals in the crystalline region. These factors play an important role in reducing the extent of e-beam degradation in PLLA. Another reason could be due to the stability of the skeletal backbone of PLLA in comparison to PLGA. The irregularity of the PLGA structure weakens the backbone chains and increases the statistical possibility of backbone chain scission in PLGA. This makes PLLA more resistant to e-beam radiation-induced degradation and probsbly makes PLLA implants more suitable for radiation sterilization as compared to PLGA. It is therefore hypothesized that an increase in the degree of crystallinity in PLGA, through isothermal annealing, would also retard radiation-induced degradation in PLGA. This would be studied in greater detail in the later part of this chapter.

4.1.3 Effect of chain scission on PLGA and PLLA

PLGA and PLLA undergo chain scission when irradiated with e-beam radiation. The breaking of the polymer chains causes the physiochemical properties of polymers to change, since the thermal and morphological properties of a polymer are very much affected by the changes in its molecular weight. **Figure 4.21** shows the DSC thermograms of a non-irradiated and a 50 Mrad irradiated PLGA. The non-irradiated PLGA film is an amorphous polymer, also verified with WAXD, and has a glass transition temperature (T_g) of approximately 58°C. The peak at the T_g is due to chain relaxation. Upon irradiation, the thermogram displayed a cold crystallization peak (T_c) and a melting peak (T_m). Cold crystallization is defined as the re-orientation of the amorphous chains to form crystals during the DSC heating scan. During irradiation, the chains get shorter, and are less entangled and have better mobility, thus allowing the re-orientation of the molecules when heated.

The thermograms of a non-irradiated and 50 Mrad irradiated PLLA are shown in **Figure 4.22**. PLLA is a semi-crystalline polymer with a T_g of approximately 63°C and a melting temperature (T_m) of approximately 177°C. The semi-crystalline morphology of PLLA is due to the regularity of the PLLA structure, which promotes the formation of a crystalline phase. Upon irradiation, no cold crystallization peak was observed, contrary to PLGA. The absence of a cold crystalline peak is due to the presence of the existing crystals, which allows for chain folding and continuum crystal growth, thereby eliminating the need for crystal nucleation and thus the absence of a cold crystallization peak.

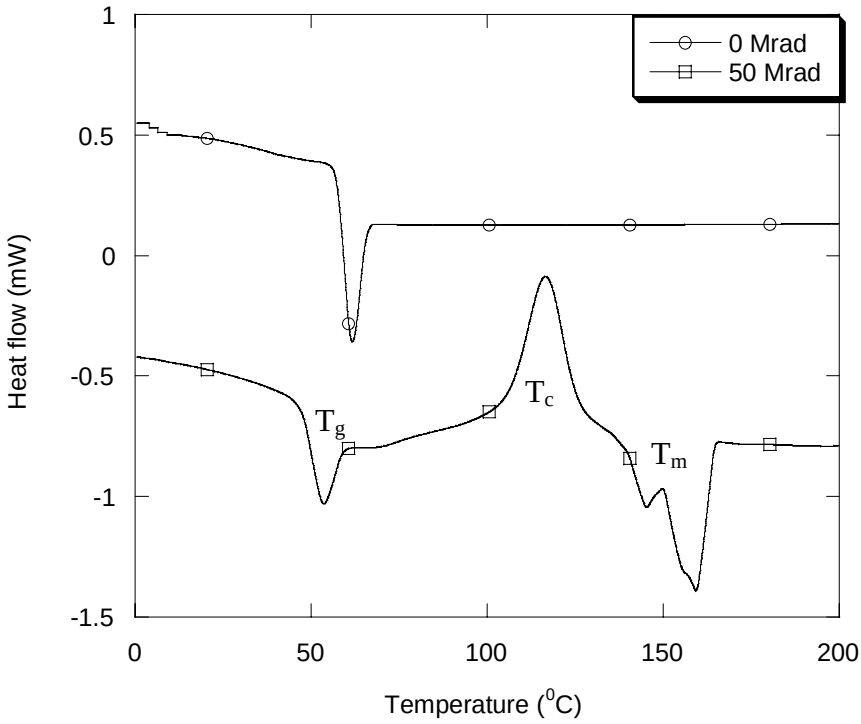

Figure 4.21 – DSC thermograms of non-irradiated and 50 Mrad irradiated PLGA heated at 5°C min^{-1}

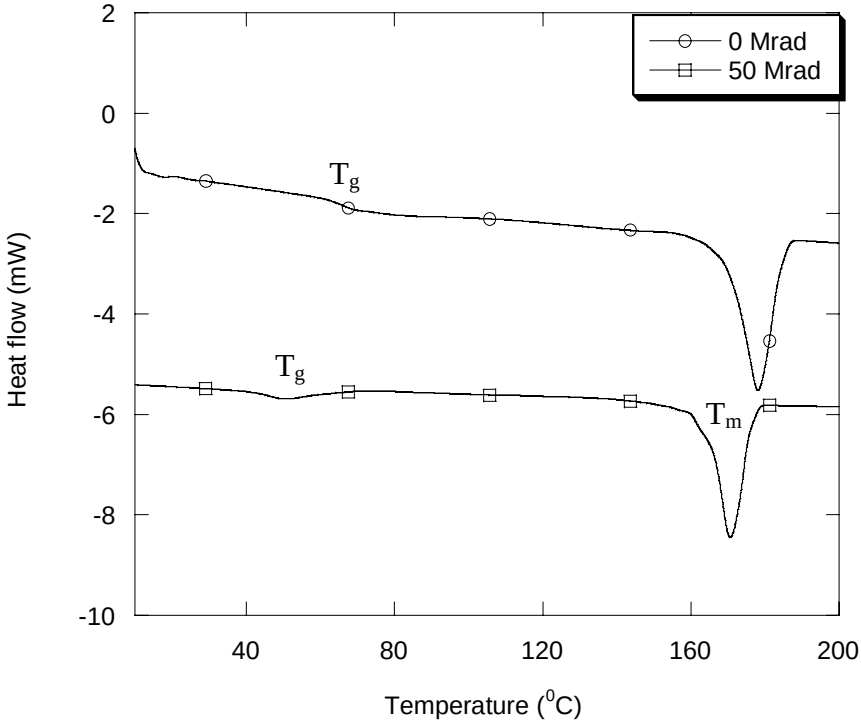

Figure 4.22 – DSC thermograms of non-irradiated and 50 Mrad irradiated PLLA heated at 5°C min^{-1}

The irradiated PLGA thermogram displayed two melting peaks (**Figure 4.21**), whereas the irradiated PLLA thermogram displayed a single melting peak (**Figure 4.22**). There are several reasons for the formation of a dual melting peak for PLGA. One possible reason is the structure of the polymer chains after irradiation. During irradiation, the recombination of free radicals can result in a linear-chained or a branch-chained polymer. The more linear and regular chains allow for closer packing, which gives rise to the higher melting temperature. The lower melting peak is a result of the more highly branched structure or more irregular chains. Another possible reason could be that some lactic units were separated from the main PLGA chain due to chain scission during irradiation. The re-crystallization of the more regular lactic units thereby gives rise to the higher melting peak, whereas the irregular PLGA chains result in the lower melting peak. The third possible reason is that the irradiation of PLGA at room temperature in the presence of oxygen produces two different peroxyl free radicals, shown in **Figure 2.9** [35]. Each of these free radicals can recombine with other PLGA chains to give chains of differing molecular structures and different packing capabilities, thus the two melting peaks. The multiple endotherms could also arise from crystals formed at the cold crystallization temperature (T_c), and the re-crystallization of the shorter amorphous chains during irradiation. Heat is evolved during irradiation [113], which would help in the re-crystallization of the shorter polymer chains. With increasing radiation dose, more chains in the amorphous regions are broken, thus further promoting crystallization. However, the heat generated from the e-beam is insufficient to encourage total re-crystallization. Hence, the crystals formed are less perfect, thus melting at a lower temperature, than those formed at the T_c.

Figure 4.23 plots the glass transition temperature (T_g) of PLGA and PLLA against radiation dose. The T_g of both biopolymers were observed to decrease with increasing radiation dose, which according to *Fox and Flory* [52], is due to the decrease in the average molecular weights of the polymers. The decrease in T_g also indicates an increase in chain mobility. Chain scission results in the removal of ester bonds, as illustrated through the formation of carbon dioxide from the FTIR in **Figure 4.3**, which subsequently increases the regularity of the backbone chains. Irradiation also causes side-chain scission, as illustrated from the schematic diagram in **Figure 4.4**, in which the methyl side group from the lactide portion may be removed. This will allow smaller free radicals, such as the hydrogen atom, to be attached as the side-group and increases the chain flexibility. The breaking of polymer chains results in shorter chains that are less entangled and have better mobility, thus decreasing the T_g in both PLGA and PLLA.

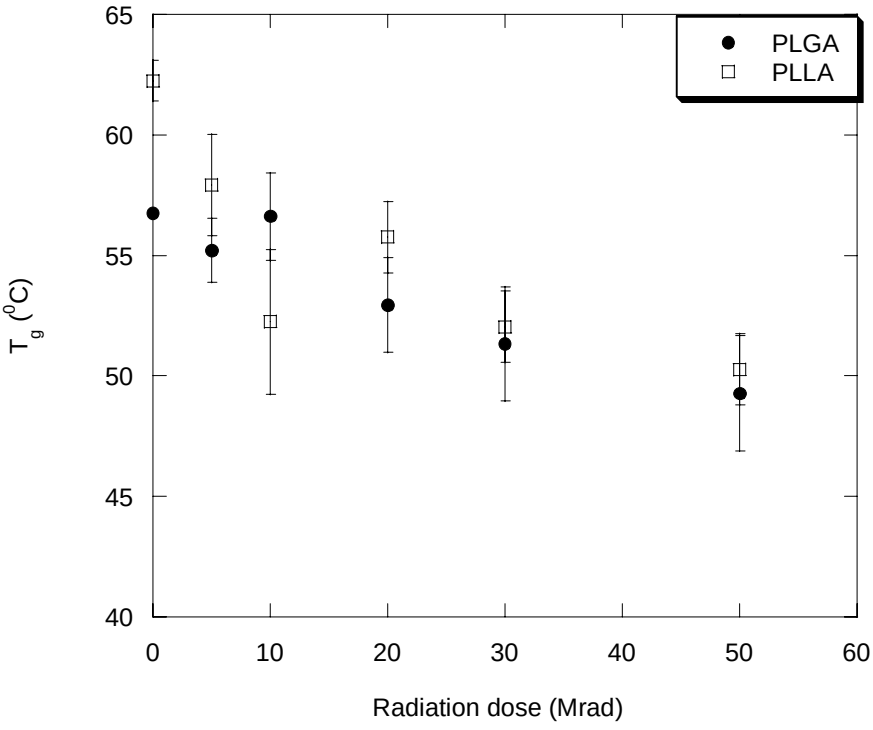

Figure 4.23 – Plot of T_g of PLGA and PLLA with radiation dose

The increase in chain mobility therefore has significant effects on the ability of PLGA to crystallize upon irradiation. **Figure 4.24** plots the cold crystallization temperatures (T_c) of PLGA against radiation dose. The results show that the T_c decreases with radiation dose. The decrease in T_c illustrates that shorter amorphous chains are better able to re-orientate and form crystals at a lower temperature. This would imply that the degree of crystallinity of PLGA could be easily increased through annealing after irradiation, and would be further discussed in **Section 4.2.2**. With better chain mobility, lower energy is therefore required to re-orientate and re-crystallize these shorter amorphous chains, thus decreasing the T_c.

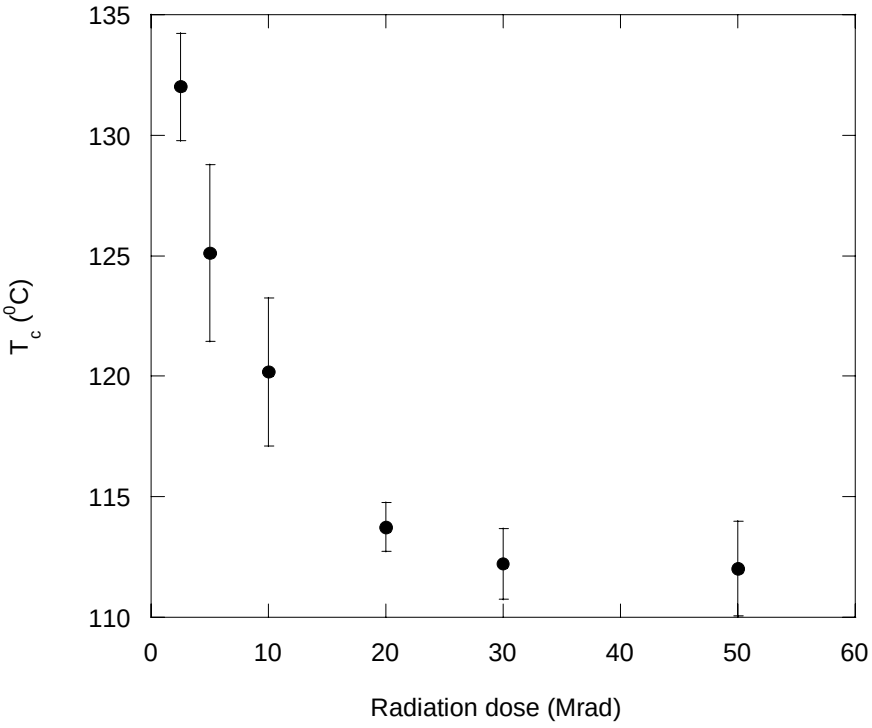

Figure 4.24 – Plot of T_c of PLGA with radiation dose

The enthalpy of fusion (ΔH_f) of PLGA was plotted against radiation dose in **Figure 4.25**. The results show an initial increase in ΔH_f that stabilizes at higher radiation dose and thus attaining a maximum degree of crystallinity. The increase in ΔH_f indicates an increase in amorphous chains that are able to crystallize due to irradiation arising from the first stage of the degradation mechanism of massive backbone chain scission. Backbone scission increases the ease of crystal formation, since the shorter amorphous chains have better mobility and are able to re-orientate. The stabilizing of the ΔH_f at higher radiation dose is due the fact that chain branching becomes more dominant at higher doses, thus reducing the possibility of amorphous chains for crystallization.

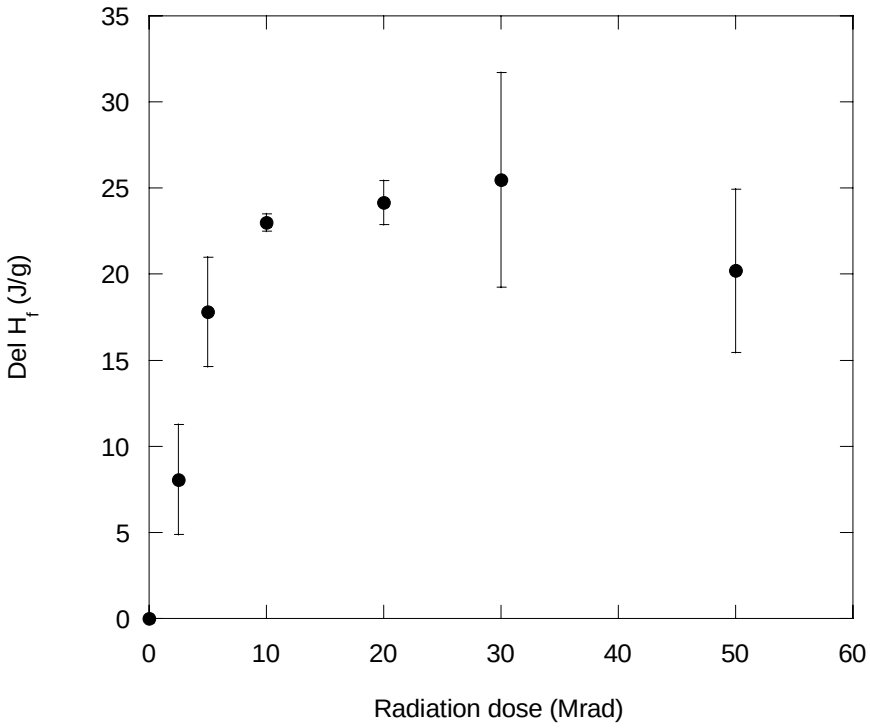

Figure 4.25 – Plot of ΔH_f of PLGA with radiation dose

The plot of the melting temperature (T_m) of PLGA against radiation dose is shown in **Figure 4.26**. The results show that the T_m (of both the melting peaks) decreases with increasing radiation dose, due to an increase in crystal defects arising from poorer chain packing capabilities, as shown in **Figure 4.17**.

The T_m of PLLA was also observed to decrease with increasing radiation dose, as shown from **Figure 4.27**, which plots the T_m of PLLA against radiation dose. The decrease in T_m for PLLA is due to crystallinity damage, as a result of the attack by peroxyl free radicals on the crystalline chains. **Figure 4.28** plots the full-width half maximum (FWHM) of the strongest crystalline peak, at 16.35°, obtained from WAXD. The results show an increase in FWHM with increasing radiation dose, which indicates that the crystal size of PLLA decreases and/or crystal defects increases with radiation dose. The recombination of these peroxyl free radicals at the crystal interface, and the recombination of alkyl free radicals within the crystalline regions, results in chains of poorer packing capability, thus disrupting the crystalline chain folding and decreasing the T_m of PLLA.

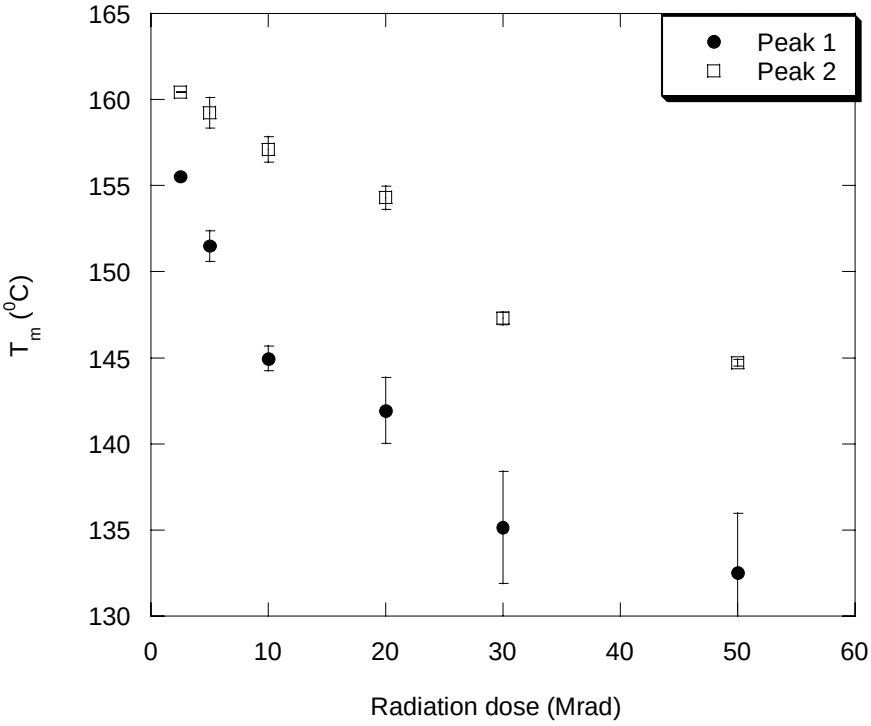

Figure 4.26 – Plot of T_m of PLGA with radiation dose

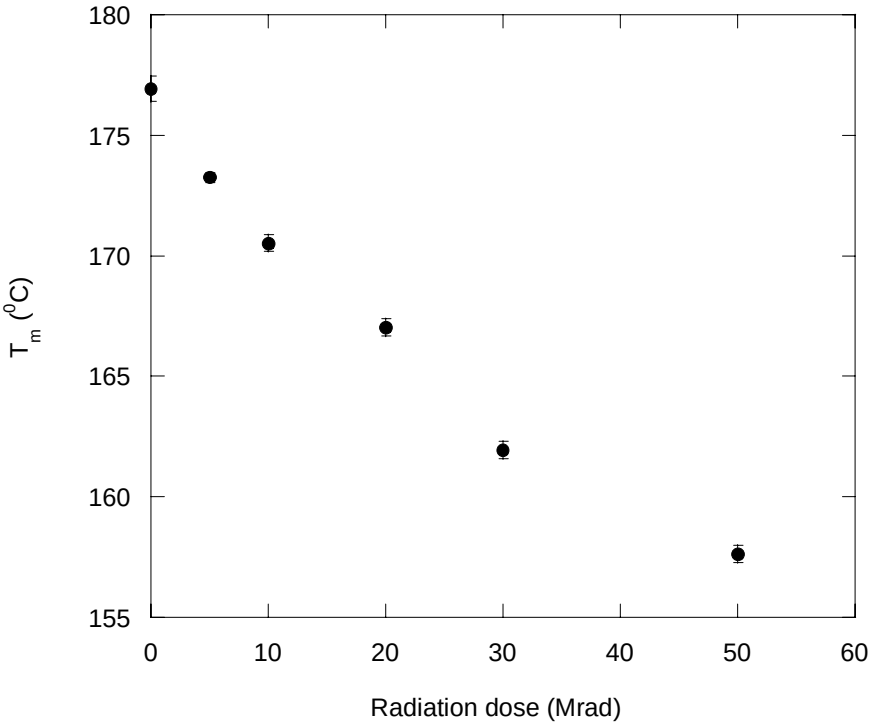

Figure 4.27 – Plot of T_m of PLLA with radiation dose

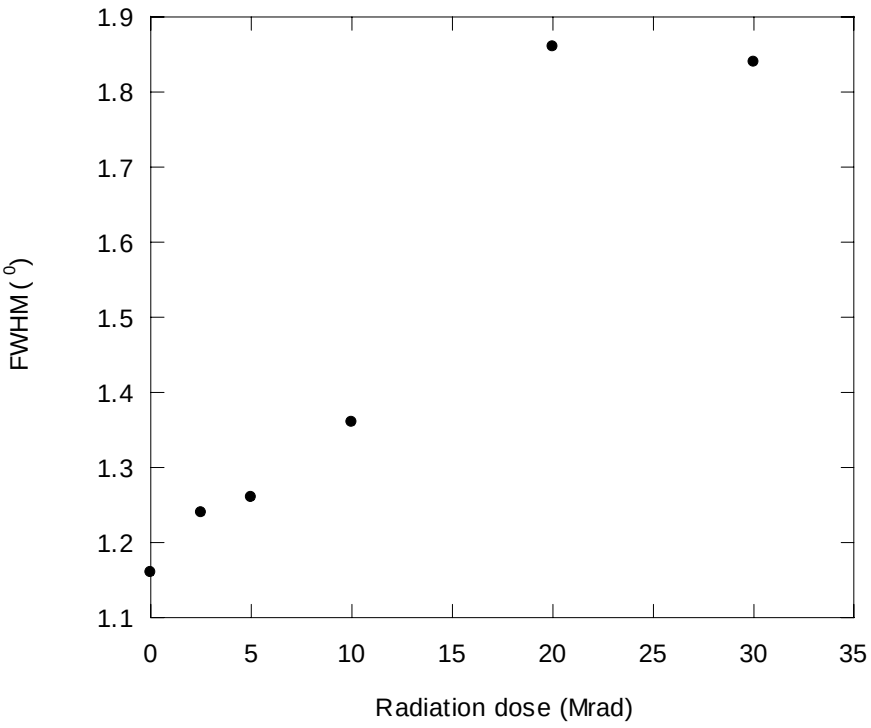

Figure 4.28 – Plot of the full-width half maximum (FWHM) of PLLA with radiation dose

The degree of crystallinity of both PLGA (**Figure 4.18**) and PLLA were also affected by e-beam radiation. The degree of crystallinity for PLLA was obtained from both the DSC and WAXD. The x-ray diffraction patterns of PLLA (non-irradiated and 50 Mrad irradiated) are shown in **Figure 4.29**

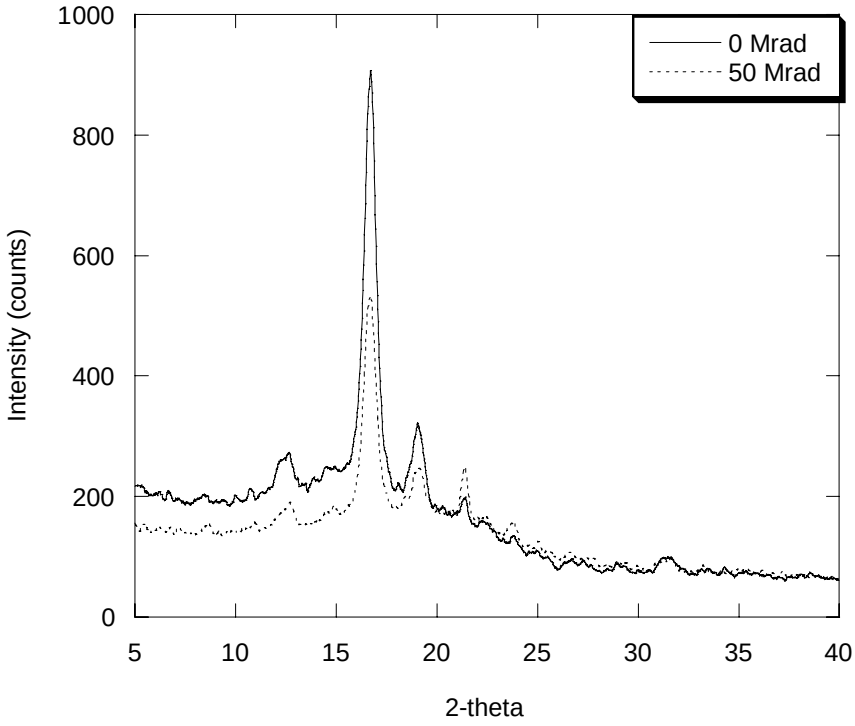

Figure 4.29 – X-ray diffraction patterns of non-irradiated and irradiated PLLA

The change in the degree of crystallinity (DOC) of PLLA with radiation dose is shown in **Figure 4.30**. The results obtained from the DSC and WAXD show similar trends, where an initial increase of DOC (up to 5 Mrad dose) and a subsequent decrease in DOC was observed. The initial increase in DOC is due to the re-orientation of the shorter amorphous chains of PLLA during irradiation; and the subsequent decrease in the DOC above 5 Mrad is due to the recombination of the free radicals within the crystalline regions, resulting in crystallinity damage. Radiation induced crystallinity damage in poly(L-lactic acid) was also reported by *Kantoglu et al.* [94]. Due to the close pack structure of crystals in PLLA, the free radicals within the crystalline regions are encouraged to undergo recombination,

resulting in highly branched and non-uniformed chains, which have poorer packing capabilities. **Figure 4.31** shows the pictures from the polarizing optical microscope (POM) showing a decrease in spherulite size of PLLA due to irradiation arising from crystallinity damage. It is believed that crystallinity damage begins from the crystal interface and subsequently moving towards the core of the crystal, since peroxyl free radicals are excluded from the crystalline regions and can only accumulate in the amorphous regions and at the crystal interface. This observation will be further elaborated, where the effect of crystallization on radiation degradation would be studied.

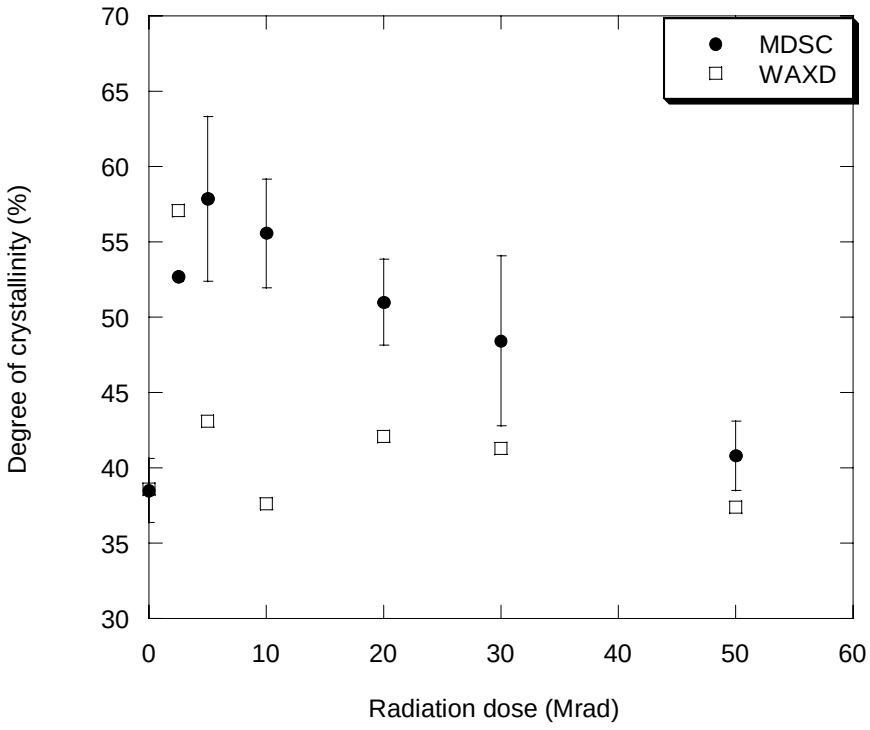

Figure 4.30 – Plot of degree of crystallinity of PLLA with radiation dose

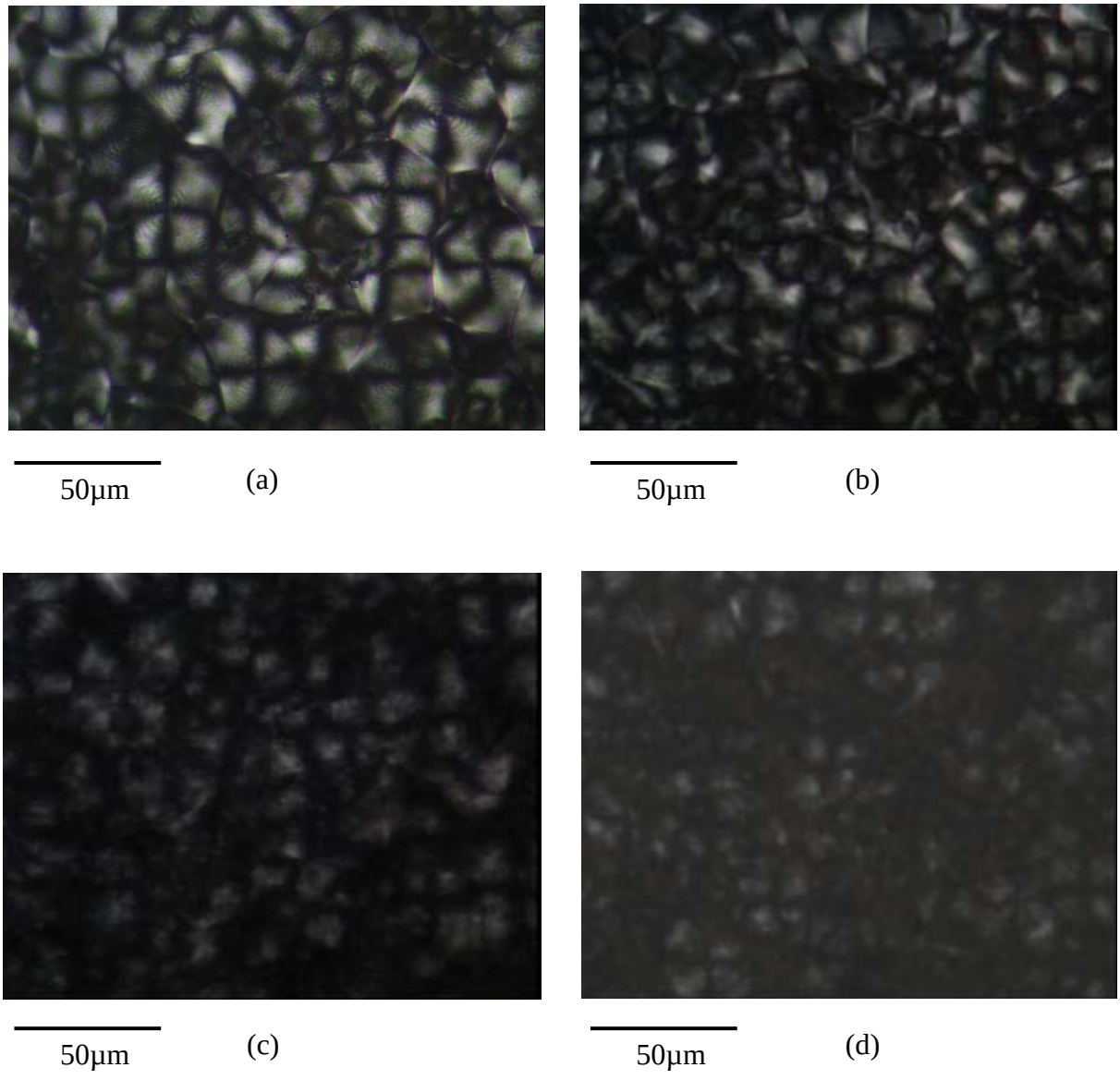

Figure 4.31 – Polarizing optical microscope pictures (x420) of irradiated PLLA crystals at (a) 0 Mrad (b) 10 Mrad (c) 20 Mrad (d) 30 Mrad

The imperfections in the polymer structure arising from changes to the polymer chains will affect its thermal stability. **Figure 4.32** plots the decomposition temperature of PLGA, obtained from the thermogravimetric analysis (TGA), with radiation dose. The results show that the thermal stability of PLGA decreases with increasing radiation dose. This decrease in decomposition temperature is due to the decrease in the molecular weight of PLGA with radiation dose [53]. E-beam irradiation also initiates degradation through the formation of weak points and defects in the PLGA structure, resulting in a decrease in its thermal stability. *Jamshidi et. al.* had also suggested that the decrease in thermal stability of lactic/glycolic acid polymers may be due to oxidative, random chain scission caused by trace amount of oxygen [50].

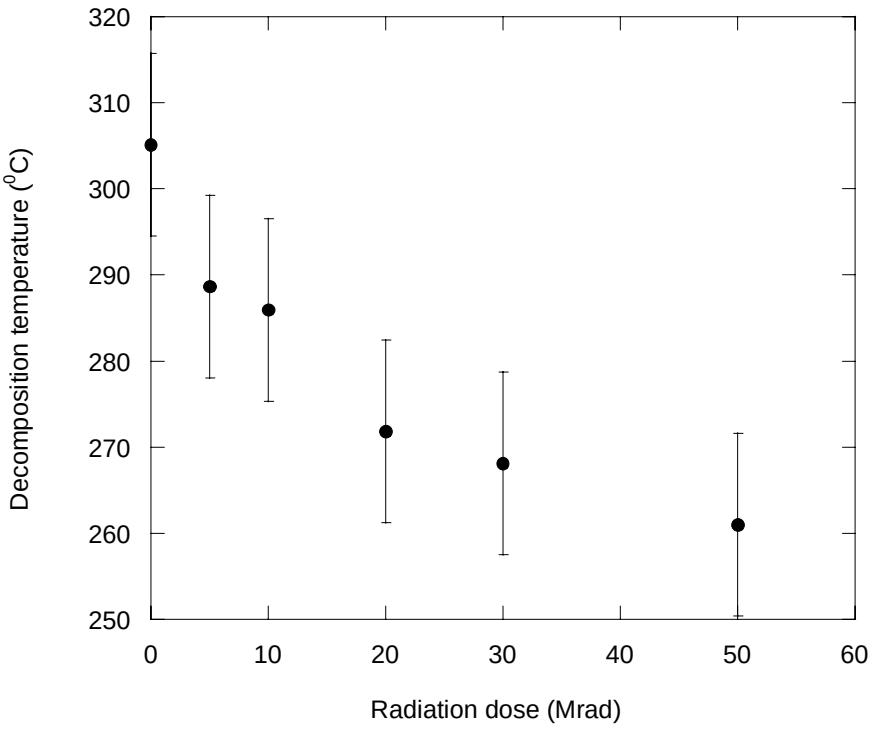

Figure 4.32 – Plot of decomposition temperature of PLGA with radiation dose

The effects of irradiation on the surface of PLGA and PLLA films were observed using the field emission scanning electron microscope (FESEM). **Figure 4.33 (a)** and **Figure 4.33 (b)** show the SEM pictures of PLGA and PLLA films respectively before and after irradiation. The SEM pictures did not show any physical damage to the films due to irradiation. Irradiation only causes damage to the polymer chains but no macro scale damage, such as cracks, was observed on the surface of the polymer films. This finding was similar to what was observed by *Chu et al.*, where surface cracks were also not observed on irradiated PGA sutures [40].

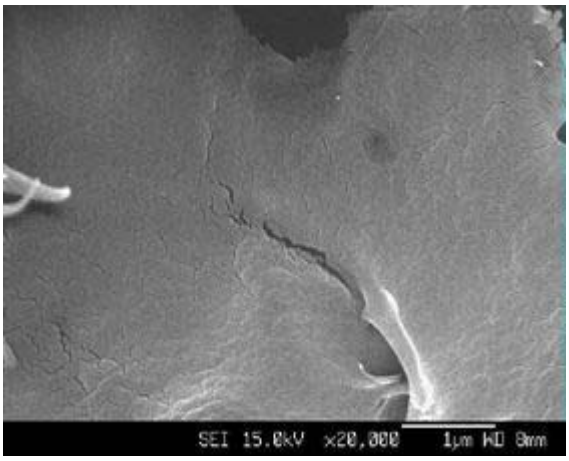

(a) PLGA at (i) 0 Mrad

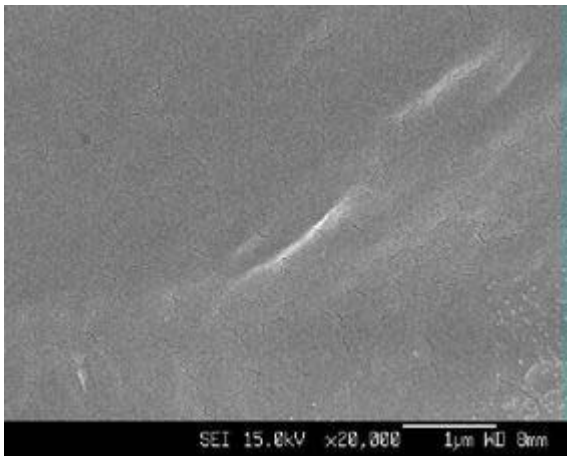

(a) PLGA at (ii) 50 Mrad

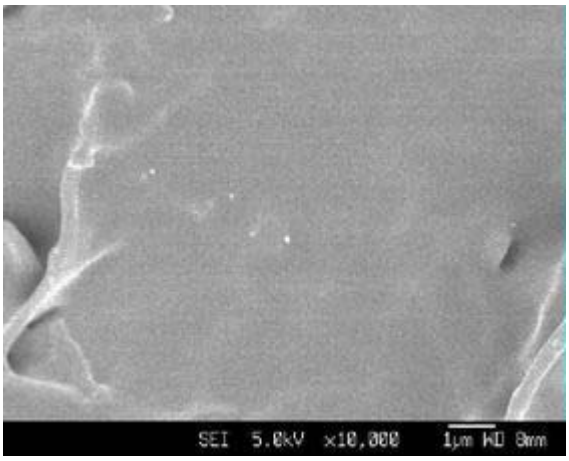

(b) PLLA at (i) 0 Mrad

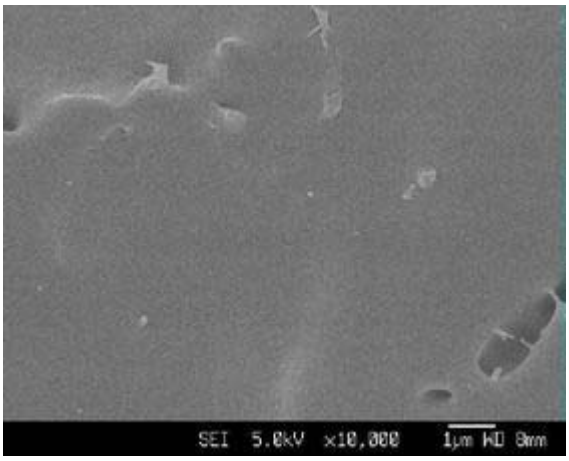

(b) PLLA at (ii) 50 Mrad

Figure 4.33 – SEM pictures of irradiated (a) PLGA and (b) PLLA films

4.1.4 Summary

PLGA and PLLA degrade through chain scission when exposed to e-beam irradiation in the presence of air, through a 3-stage degradation process, which involves a combination of backbone main chain scission and hydrogen abstraction. This causes a decrease in the average molecular weight, and thus a corresponding decrease in the physiochemical properties, such as glass-transition temperature (T_g), melting temperature (T_m) and crystallization temperature (T_c) of the biopolymers. The subsequent reduction in the extent of molecular weight decrease is attributed to the difference in degradation mechanisms in the three stages and the recombination of free radicals. Irradiation also causes the formation of a crystalline phase in PLGA but a decrease in crystallinity for PLLA. It is hypothesized, and would be proven in the next section, that the formation of crystalline regions in PLGA arrests radiation-induced degradation through the “cage effect”, by first undergoing chain scission and forming crystalline regions through chain re-orientation. The semi-crystalline nature of PLLA is therefore believed to be the key factor in its greater stability to e-beam radiation as compared to PLGA. Since e-beam radiation decreases the molecular weights of PLGA and PLLA in a predictable and fairly accurate manner, as shown from the linear relationship of the reciprocal molecular weight with radiation dose, it is therefore hypothesized that e-beam radiation can be used as a potential tool to control the hydrolytic degradation time of these biopolymers.

4.1.5 Effect of crystallization on the radiation degradation of PLGA

(a) Crystallization of PLGA through isothermal annealing

The degree of crystallinity of a polymer is one factor that may retard the extent of radiation-induced degradation, as discussed in previously, due to the "cage effect" [90]. Since this is a hypothetical statement that needs to be further verified, it would be of interest to study the effect of crystallization on the stability of PLGA under e-beam radiation. This study would not only add knowledge to existing theory of the "cage effect", but would also create an alternative route in stabilizing PLGA during irradiation.

Figure 4.34 plots the degree of crystallinity and enthalpy of fusion of PLGA with annealing times respectively. The change in the degree of crystallinity (DOC %) and enthalpy of fusion (ΔH_f) was quantified from the WAXD and DSC respectively. Similar trends were obtained from both characterization techniques, where the degree of crystallinity increased steadily to remain constant with further annealing times.

Thermal energy supplied, through annealing, enables the movement and re-orientation of the polymer chains and in the process, assists the chains in discovering the most efficient arrangement. Crystallization is firstly initiated through the creation of a stable nucleus or nucleation, brought about by the ordering of chains in parallel array, before the stabilization of long-range order or crystal

growth occurs. This results in the formation of close-packed structure of crystalline regions from an initially amorphous morphology, and increasing the degree of crystallinity of PLGA in the process. Since polymer chain diffusion is time dependent, annealing for a longer period of time allows more time for the chains to diffuse into the suitable orientations for crystalline arrangement.

The increase in the degree of crystallinity of PLGA can also be qualitatively verified from the pictures obtained from the polarizing optical microscope (POM), as shown in **Figure 4.35**. It can be seen that the annealed films of PLGA showed an increase in the white region under polarized light, indicating an increase in the number of very small PLGA crystals, during isothermal annealing at 115°C.

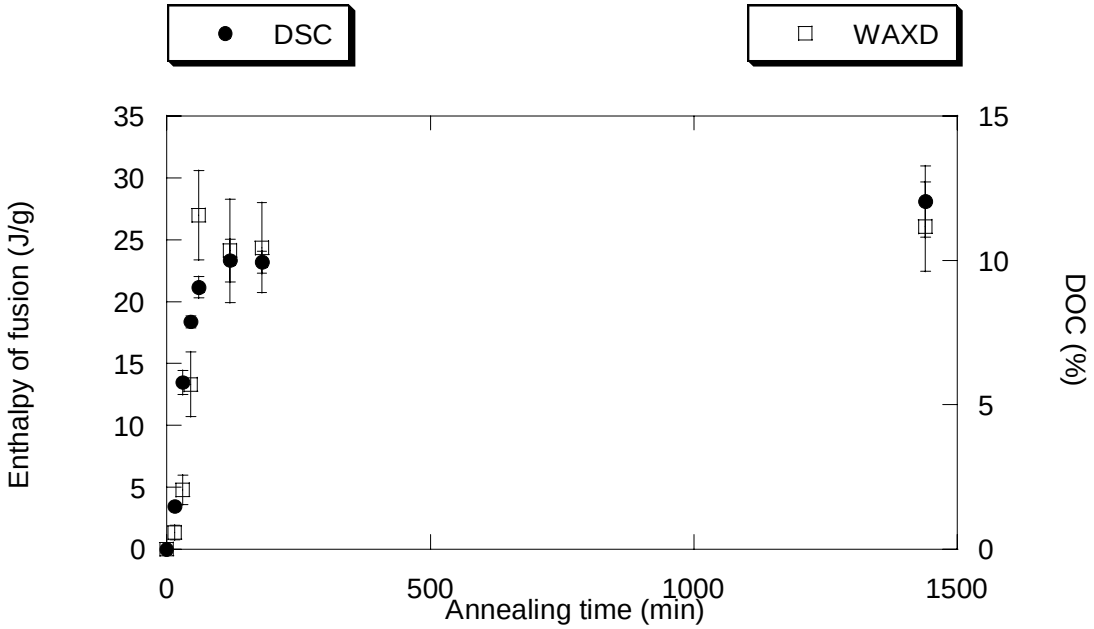

Figure 4.34 – Plot of degree of crystallinity of PLGA with annealing time

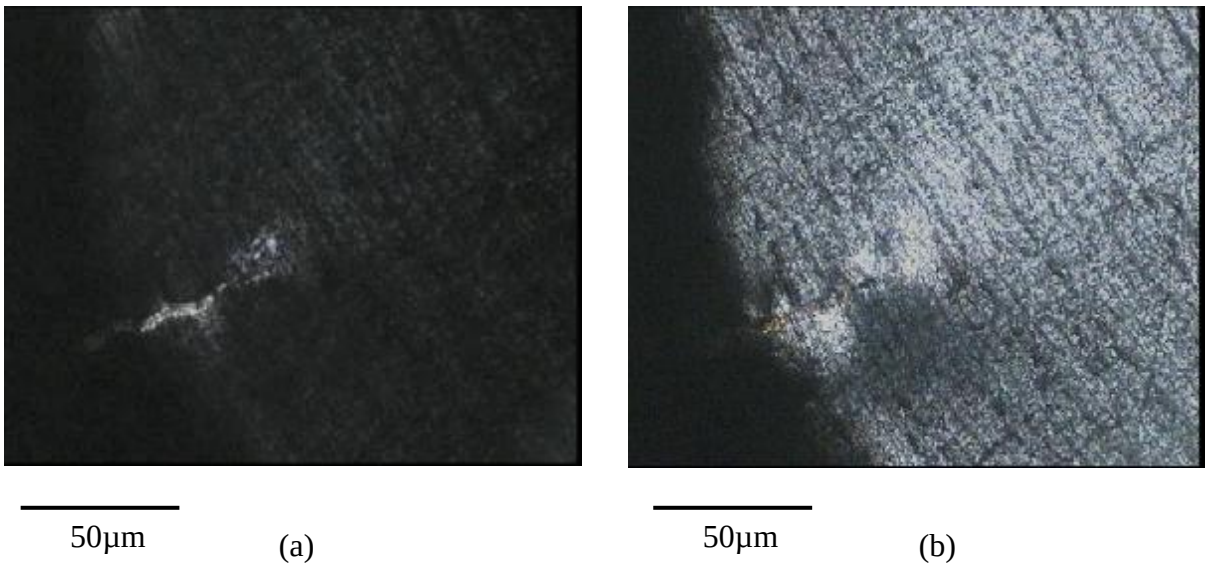

Figure 4.35 – Polarizing optical microscope pictures of PLGA crystals at annealing times of (a) 15 min and (b) 120 min

Figure 4.36 shows the x-ray diffraction patterns of the non-annealed and a 60 min annealed PLGA film, obtained from the WAXD. The x-ray diffraction pattern of the non-annealed film shows a broad amorphous peak, whereas the x-ray diffraction pattern of the annealed film shows sharp crystalline peaks at 14.85°, 16.35°, 18.95° and 22.15°; each peak corresponding to a particular crystalline orientation. The full width half maximum (FWHM) values of the x-ray diffraction peaks were obtained from the strongest x-ray diffraction peak at 16.35°. **Figure 4.37** plots the FWHM values of PLGA against annealing time. The results show a decrease in FWHM with increasing annealing time. The decrease in FWHM, according to Scherrer's equation (**Eq. 3.3)** [106], denotes an increase in the diameter of the crystallites and/or an increase in crystal perfection.

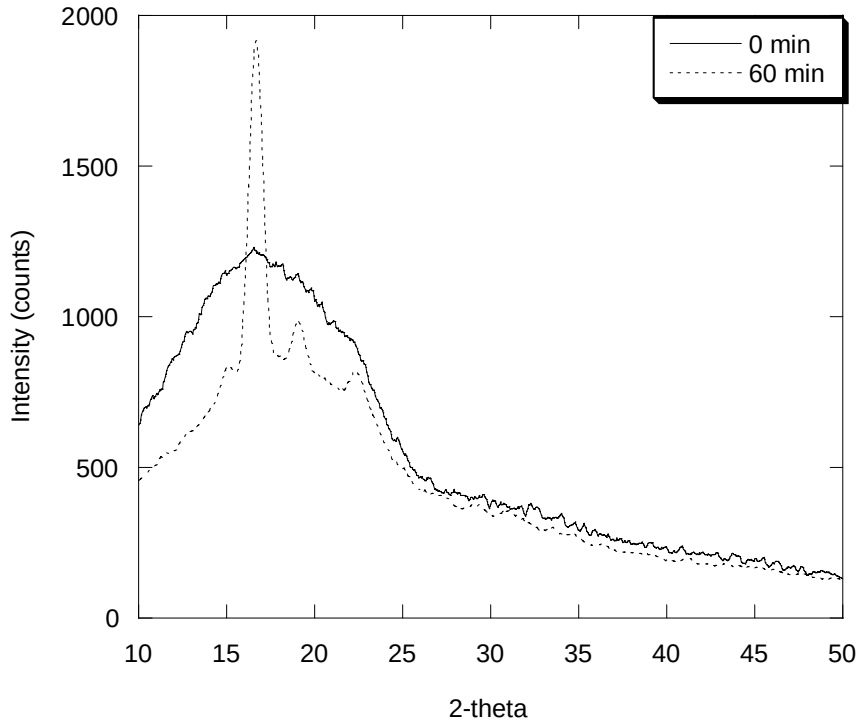

Figure 4.36 – X-ray diffraction patterns of 0 min and 60 min annealed PLGA

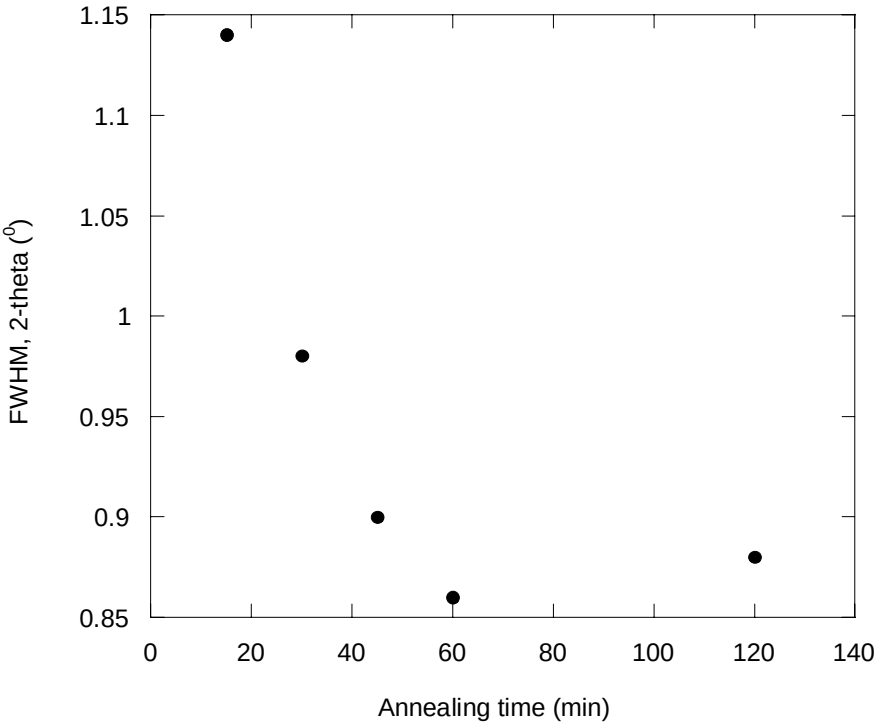

Figure 4.37 – Plot of FWHM of PLGA with annealing time

Figure 4.38 plots the glass transition temperature (T_g) of PLGA against annealing time. The results show a decrease in T_g of PLGA with annealing time. The decrease in T_g indicates an increase in chain mobility of the amorphous chains, probably arising from the formation of voids in the amorphous regions due to the loss of amorphous material [114]. The re-orientation of the amorphous PLGA chains in forming closely packed crystalline structure therefore results in a more open amorphous morphology due to the formation of voids at the crystal-amorphous interface.

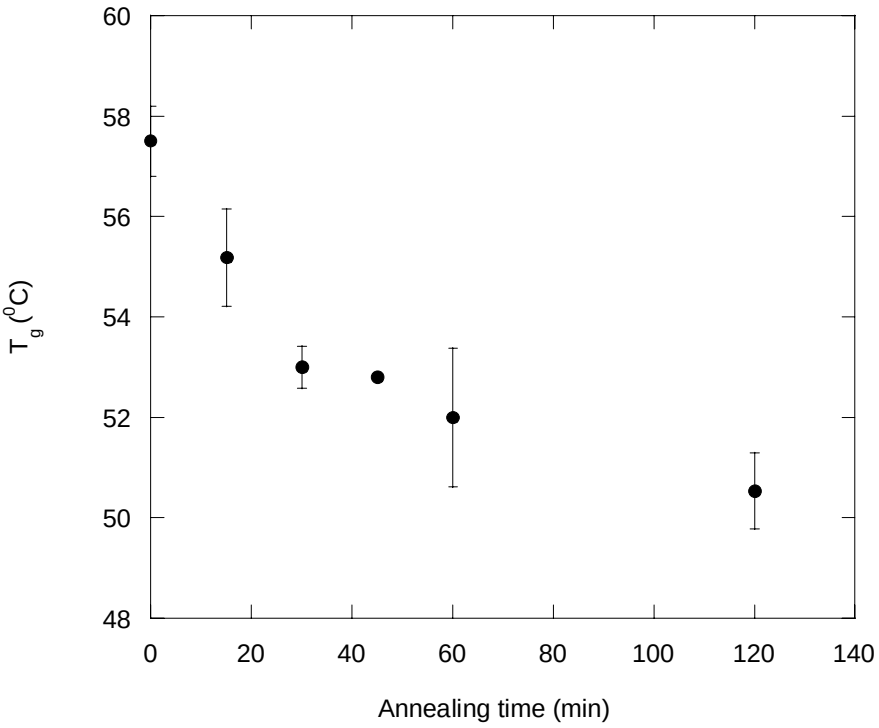

Figure 4.38 – Plot of T_g of PLGA with annealing time

Figure 4.39 plots the melting temperature (T_m) of PLGA against annealing time. The results show that the T_m remains relatively unchanged with increasing isothermal annealing time. Isothermal annealing has no effect on the packing capability of the PLGA chains.

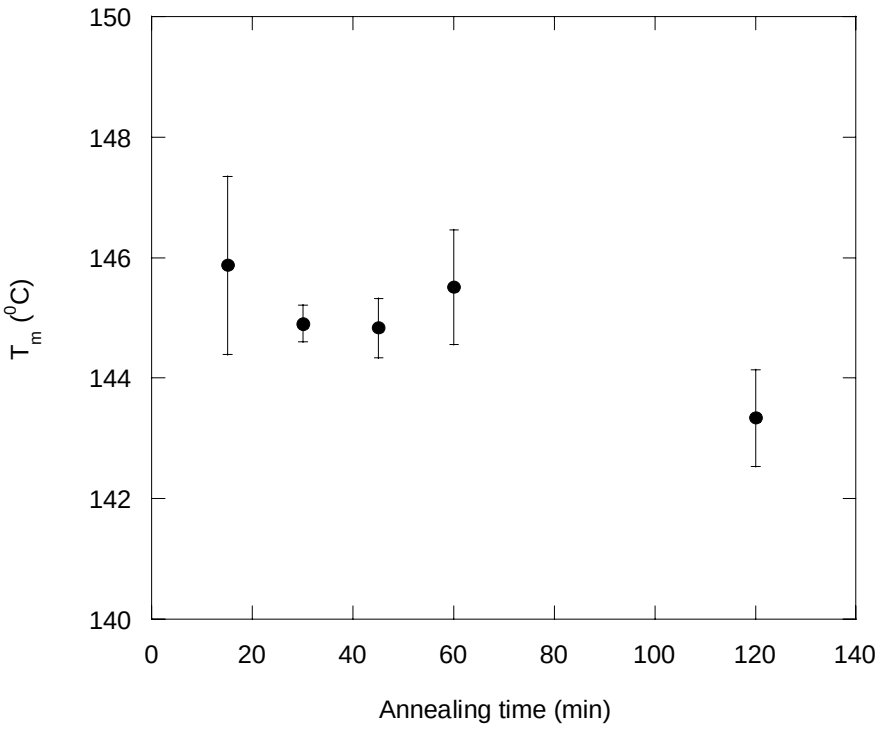

Figure 4.39 – Plot of T_m of PLGA with annealing time

(b) Effect of irradiation on annealed PLGA films

Films of PLGA were annealed for 30 min (3 %) and 120 min (12 %) and then irradiated with e-beam radiation, from 0 Mrad through 30 Mrad. The non-annealed (0 min) films were taken as control samples. **Figure 4.40** plots the weight average molecular weight (M_w) of irradiated PLGA against radiation dose. The results show a decrease in the molecular weight, indicating the occurrence of chain scission. The M_w was used because, from **Eq. 2.4**, the effect of free radical recombination is more evident from the M_w. The M_w would thus be more accurate in reflecting on the recombination process, which was postulated to be the main effect in degradation retardation due to crystals.

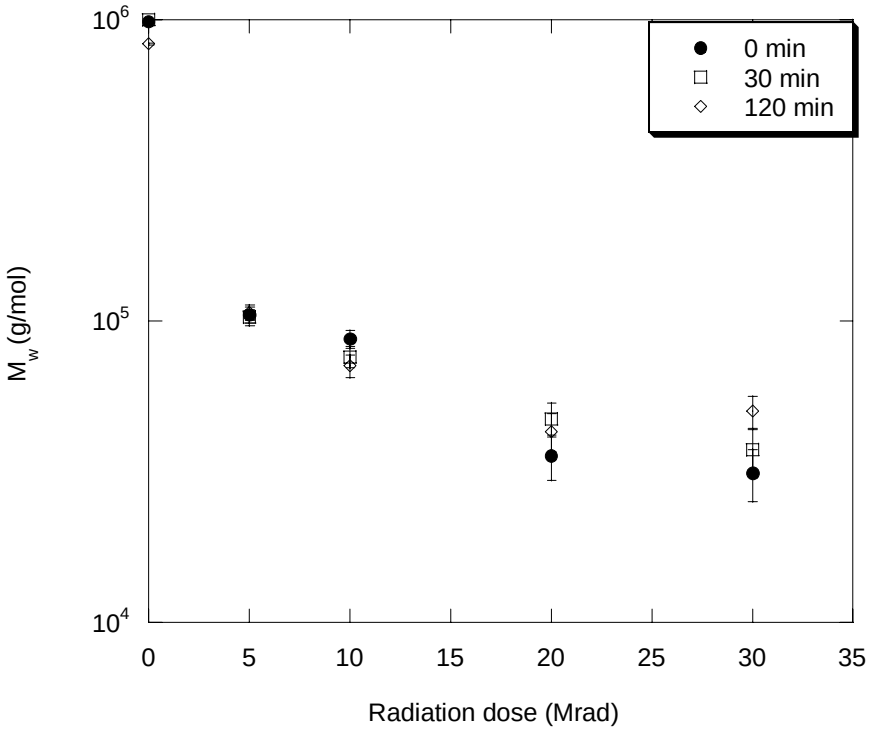

Figure 4.40 – Plot of weight average molecular weight (M_w) of PLGA (non-annealed and annealed) with radiation dose

To observe the extent of degradation, the reciprocal of the weight average molecular weight ($1/M_w$) of PLGA was plotted in **Figure 4.41**, as according to **Eq. 2.4**. The results show that the decrease in M_w was more significant for the amorphous (non-annealed) PLGA films compared to the more crystalline (annealed) PLGA films, as observed from the gradient of the graphs plotted. PLGA with a higher degree of crystallinity experienced less radiation-induced degradation.

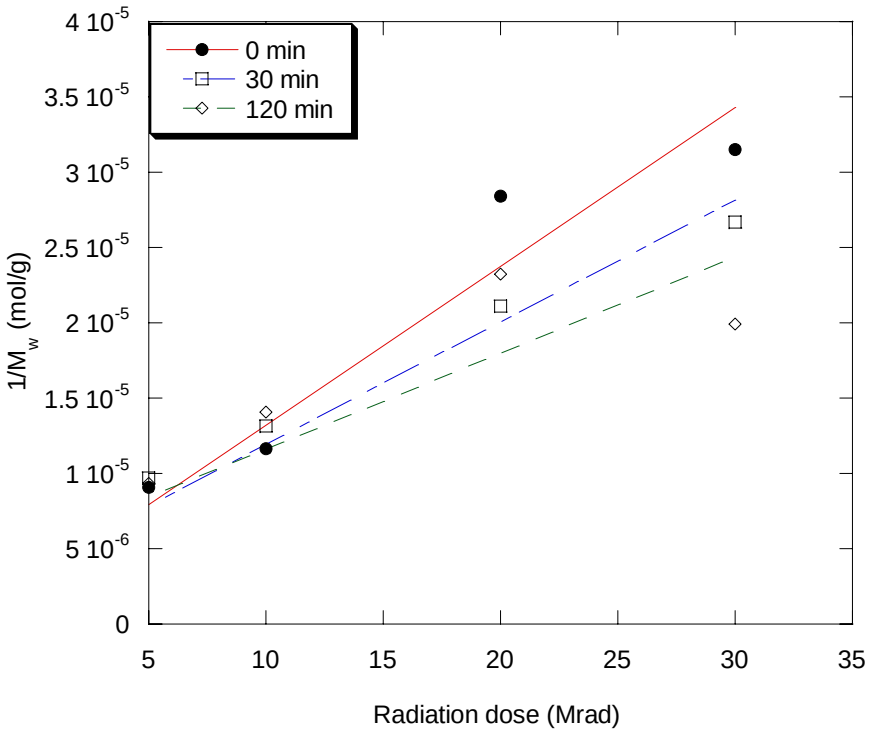

Figure 4.41 – Plot of reciprocal of weight average molecular weight ($1/M_w$) of PLGA with radiation dose

The lower extent of decrease in the molecular weight for a more highly crystalline PLGA suggests the influence crystals have on retarding e-beam radiation-induced degradation. The crystalline regions in the polymer consist of chains that are more oriented and closely packed compared to the amorphous regions. The close proximity of the polymer chains in the crystalline structure therefore reduces the number of effective chain scissions in two ways. Firstly, by restricting the diffusion of oxygen into the crystalline regions [30] and thus preventing the formation of peroxyl free radicals, which is responsible for the chain scission process; and secondly by encouraging the trapped alkyl free radicals formed to recombine, through the “cage effect” [90].

Figure 4.42 plots the polydispersity index of PLGA against radiation dose. The results show that the polydispersity index increases most significantly for the 120 min annealed PLGA. This implies that the polymer chains, for the 120 min annealed PLGA, are increasingly less uniform due to higher incidences of free radical recombination (**Table 4.1**) and a wider distribution of chain length. Higher incidences of free radical recombination occur for the more crystalline PLGA, since crystalline phases encourage recombination, which may also result in a higher degree of chain branching.

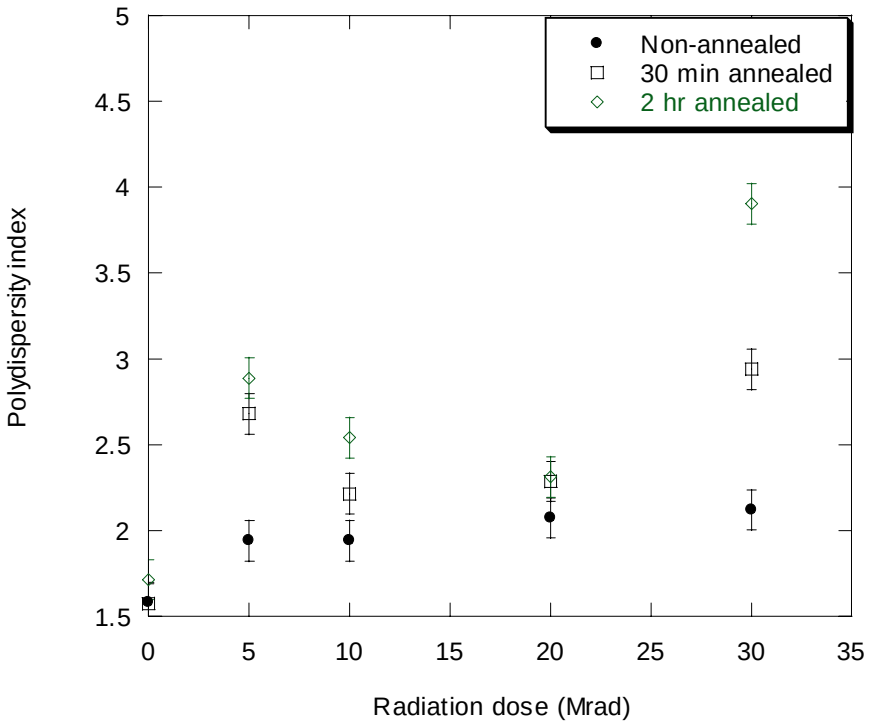

Figure 4.42 – Plot of polydispersity index of PLGA with radiation dose

Figure 4.43 plots the melting temperature (T_m) of PLGA against radiation dose. The results show an initial increase in the T_m upon irradiation, then a subsequent decrease in the T_m. The initial increase in T_m supports uniform deposition of radiation energy in both the crystalline and amorphous regions [30]. The packing capability of the crystalline chains is thus enhanced through backbone scission, through the packing of shorter chains, and hence initially increasing the T_m. Subsequently, the T_m decreases due to the recombination of the trapped free radicals in the crystalline regions, which also increases the crystal defects.

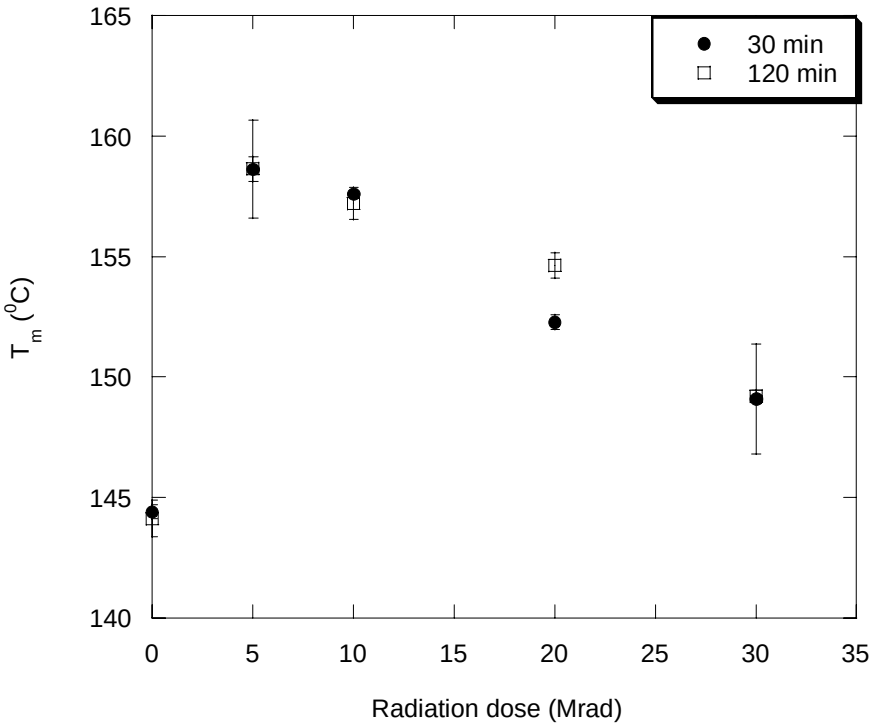

Figure 4.43 – Plot of T_m of annealed PLGA with radiation dose

The decrease in FWHM, as shown earlier in **Figure 4.37**, which reflects an increase in crystal size and/or crystal perfection with annealing time, is another factor that helps retard the degradation process. It is believed that the increase in crystal size and crystal perfection will further aid in restricting the diffusion of oxygen into the crystals and thus decreasing the extent of degradation. Therefore, annealing helps retard the extent of e-beam radiation degradation in two ways; firstly by increasing the degree of crystallinity, and secondly by increasing the crystal perfection.

Irradiation of annealed PLGA causes changes to the degree of crystallinity. The degree of crystallinity was measured using the WAXD and DSC. **Figure 4.44** and

Figure 4.45 plots the degree of crystallinity of the 30 min annealed and 120 min annealed PLGA respectively with radiation dose. The results from **Figure 4.44** show that the degree of crystallinity for the 30 min annealed PLGA initially increases, then decreases and finally increases with increasing radiation dose. A possible explanation for this observation could lie in the competition of chain re-orientation in the amorphous regions, and crystal destruction in the crystalline regions [94]. The results from **Figure 4.45** show the decrease in the degree of crystallinity for the 120 min annealed PLGA with increasing radiation dose, resulting from crystallinity damage [94].

Figure 4.46 plots the degree of crystallinity (from DSC results only) for the non-annealed (0 min), 30 min annealed and 120 min annealed PLGA. It can be observed that the degree of crystallinity increases for lowly crystalline (<5 % DOC) PLGA, but decreases for a more highly crystalline PLGA (>10 % DOC). Chain scission (lowly crystalline PLGA) encourages the formation of crystals and recombination (highly crystalline PLGA) causes the destruction of crystals. The recombination of free radicals in the crystalline regions therefore substantiates the effectiveness of crystals in retarding radiation degradation.

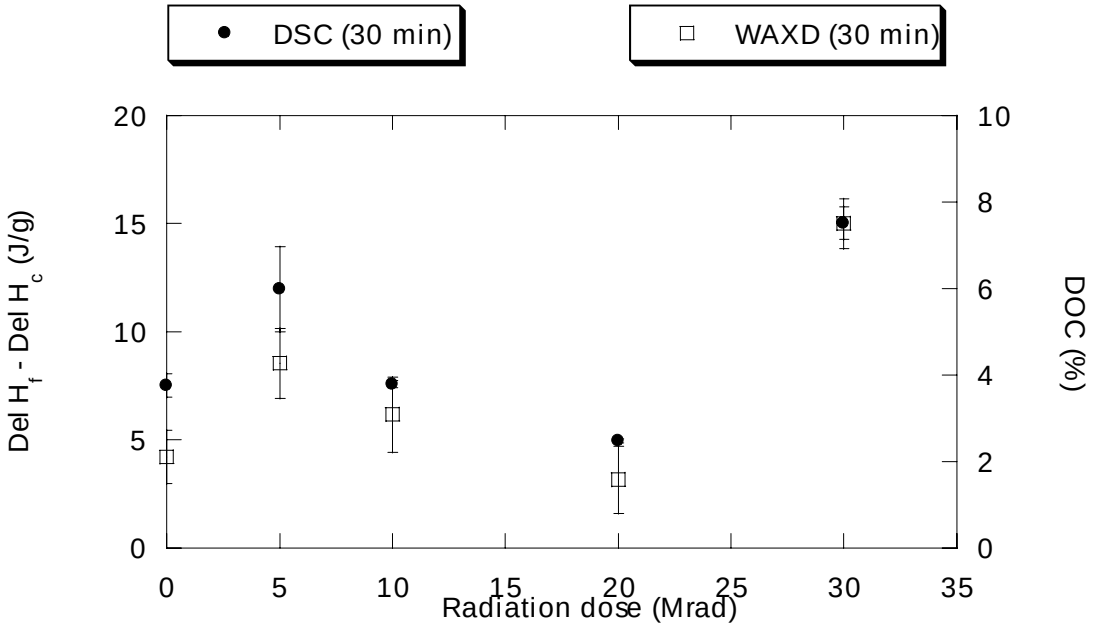

Figure 4.44 – Plot of the degree of crystallinity of 30 min annealed PLGA with radiation dose

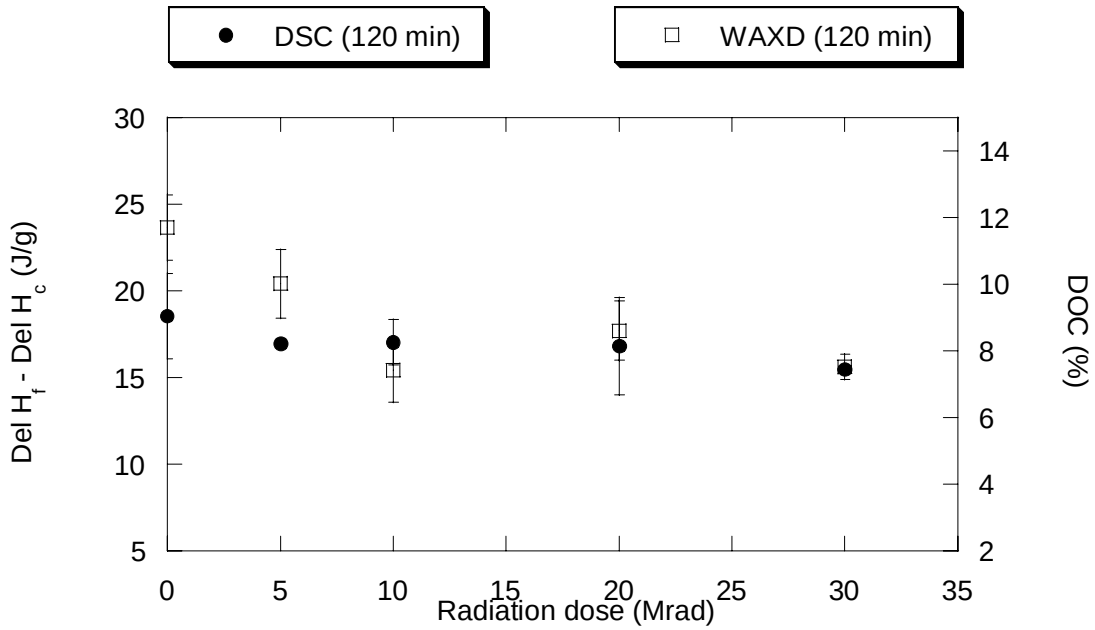

Figure 4.45 – Plot of the degree of crystallinity of 120 min annealed PLGA with radiation dose

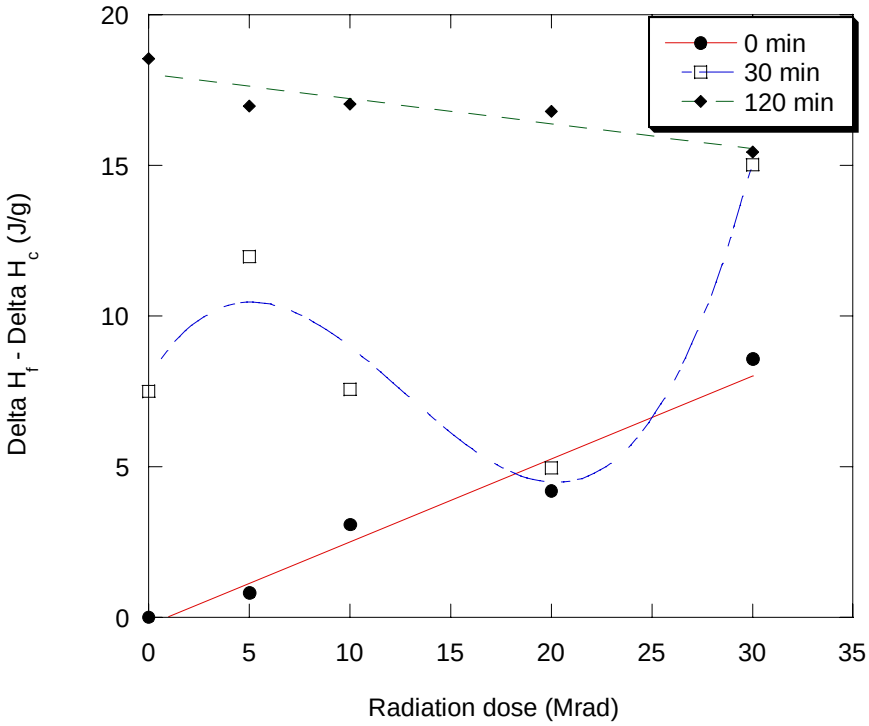

Figure 4.46 – Difference in enthalpy of fusion and enthalpy of crystallization of non-annealed (0 min), 30 min annealed and 120 min annealed PLGA

Crystallinity damage resulting in the decrease in crystal size and an increase in crystal defects can be verified from the FWHM. **Figure 4.47** plots the FWHM of the 120 min annealed PLGA against radiation dose. The results show an increase in FWHM values, which according to Scherrer's equation indicates a decrease in crystal size and/or an increase in crystal defects with radiation dose.

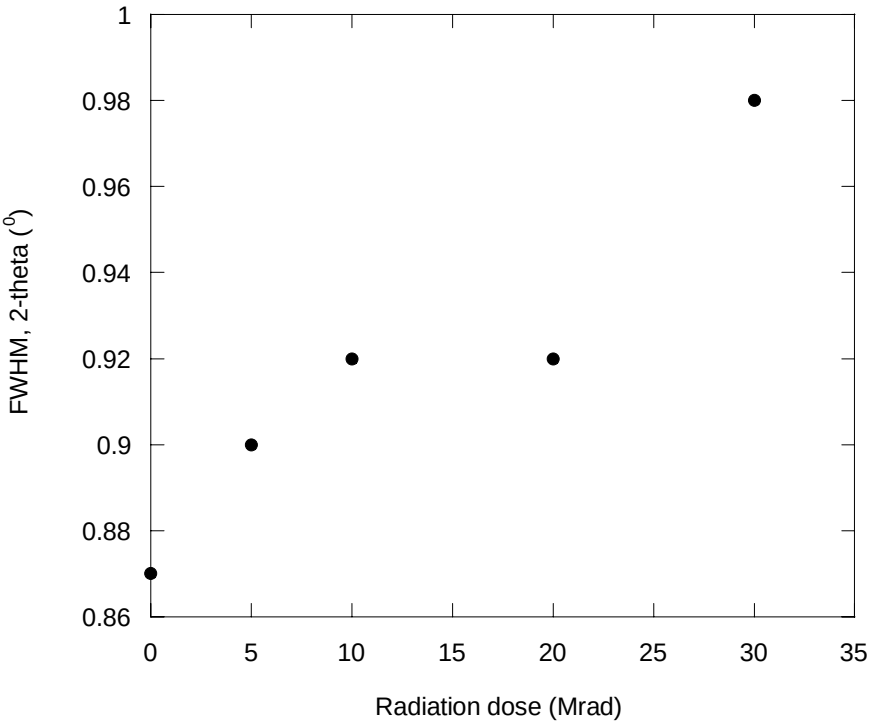

Figure 4.47 – Plot of FWHM of 120 min annealed PLGA with radiation dose

(c) Summary

The isothermal annealing of PLGA films at 115°C encourages the formation of crystals. The degree of crystallinity increases with annealing time; achieving maximum crystallinity of approximately 12 %, after 120 min of annealing time. E-beam irradiation, in the presence of air, causes polymer degradation through chain scission. However, the existence of crystals in annealed PLGA was able to retard radiation degradation. This was attributed to the exclusion of oxygen in the crystalline regions and the 'cage effect', where more recombination of free radicals would occur within the crystalline regions. The degree of crystallinity was observed to change with radiation dose. At maximum degree of crystallinity (~12 %), radiation reduces the degree of crystallinity, whereas at zero or lower degree of crystallinity (<5 %), crystallinity increases with radiation dose. The degree of crystallinity increases due to chain scission but decreases due to the recombination of free radicals.

4.2 Hydrolytic degradation of e-beam irradiated PLGA and PLLA

Compared to the wealth of information dealing with the hydrolytic degradation behaviour of PLGA and PLLA, there is hardly any journals that relate the effects of irradiation to the hydrolytic degradation of PLGA and PLLA, which makes this study a novel contribution in this thesis. This chapter reports on the investigation into the influence of e-beam radiation on the hydrolytic degradation behaviour of PLGA and PLLA, and establishes a relationship between radiation dose and the hydrolytic degradation times of these biopolymers, through in vitro hydrolytic degradation studies.

Films of PLGA and PLLA irradiated at doses of 5 Mrad, 10 Mrad and 20 Mrad were used for the in vitro degradation study. The non-irradiated (0 Mrad) films were used as control samples. The number-average molecular weight ($M_{n,D}$), T_g and degree of crystallinity (DOC) of PLGA and PLLA films after irradiation are tabulated in **Table 4.3** and **Table 4.4** respectively. ΔH (calculated from $\Delta H_f - \Delta H_c$) is taken as the degree of crystallinity for PLGA.

Table 4.3 – Number-average molecular weight ($M_{n,D}$), T_g and ΔH of PLGA films after electron beam irradiation

Radiation dose	$M_{n,D}$ (g/mol)	T_g (°C)	ΔH (J/g)
0 Mrad	4.40×10^5	56.7	0
5 Mrad	5.75×10^4	55.2	2.7
10 Mrad	3.47×10^4	53.5	2.5
20 Mrad	1.95×10^4	52.9	3.2

Table 4.4 – Number-average molecular weight ($M_{n,D}$), T_g and DOC % of PLLA films after electron beam irradiation

Radiation dose	$M_{n,D}$ (g/mol)	T_g (°C)	DOC (%)
0 Mrad	4.06×10^5	66.3	36.6
5 Mrad	6.47×10^4	60.8	50.5
10 Mrad	4.32×10^4	57.2	50.8
20 Mrad	2.31×10^4	53.4	47.8

It is assumed in the hydrolytic degradation of irradiated PLGA and PLLA that the changes to the DOC of these polymers due to irradiation would have no significant effect on the rate of hydrolytic degradation. This assumption would be proven in a latter part of this chapter where the hydrolytic degradation of varying DOC of PLGA would be studied in greater detail.

4.2.1 Hydrolytic degradation of irradiated PLGA and PLLA

Visual examination of the hydrolytically degraded irradiated and non-irradiated PLGA and PLLA samples was conducted, when they were removed from the PBS solution. The degraded PLGA films were initially transparent, in agreement with the amorphous and lowly crystalline polymer structure. After 5 weeks, the 20 Mrad irradiated films became opaque white, while the non-irradiated (0 Mrad) and 5 Mrad irradiated films still remained relatively transparent.

Figure 4.48 plots the change in mass loss as a function of hydrolytic degradation time in days for PLGA. The results show that mass loss was most significant for the 20 Mrad irradiated PLGA films and least significant for the non-irradiated (0 Mrad) films. Mass loss commenced at an early stage of the in vitro study for the more highly irradiated films (i.e. 20 Mrad and 10 Mrad). The initial mean loss in mass for the 20 Mrad films was about 15 % (in the first 5 weeks), and the loss in mass increased rapidly up to 80 % after 12 weeks of degradation. For the 10 Mrad films, 50 % loss in mass was observed after 12 weeks. This rapid loss in mass corresponds to the second stage of the degradation process where soluble oligomeric fragments and monomer products are formed, as according to *Raghuvanshi et al.* [12]. Mass loss occurs from the release of these water-soluble oligomers into the degrading medium. On the other hand, the 0 Mrad and 5 Mrad films had the lowest mass loss of only 2 % and 7 % respectively after 12 weeks of degradation. These samples were still within the first stage of degradation, in which no or minimal soluble products were formed.

Figure 4.49 plots the change in mass loss for PLLA with hydrolytic degradation time. The results show that mass loss increases with degradation time. However, the mass loss was most significant for the 20 Mrad irradiated films at 60 % after 26 weeks of degradation study, but was insignificant for the 0 Mrad (3 %), 5 Mrad (3 %) and 10 Mrad (9 %) films. From the results, it can be observed that PLGA experienced more significant mass loss than PLLA for the same degradation period, indicating that PLGA hydrolytically degrades faster than PLLA. The difference in hydrolytic rate lies in the water uptake, in which PLLA is more hydrophobic than PLGA. This is because lactic acid units are more hydrophobic than glycolic acid units, as they provide steric hindrance to attack by water molecules, due to the presence of the methyl side group [8, 45].

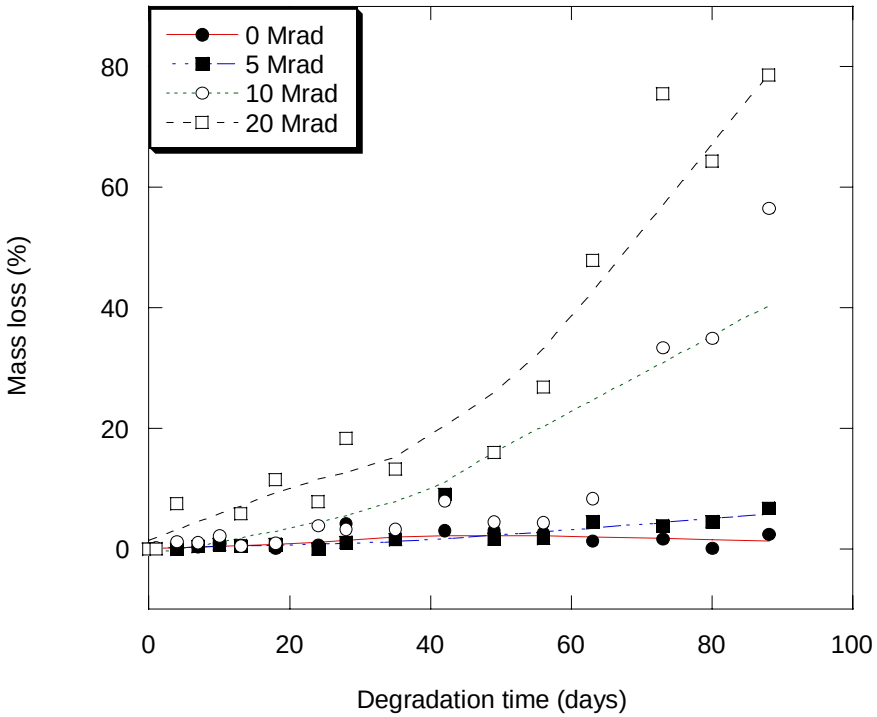

Figure 4.48 – Plot of change in mass loss of PLGA with hydrolytic degradation time

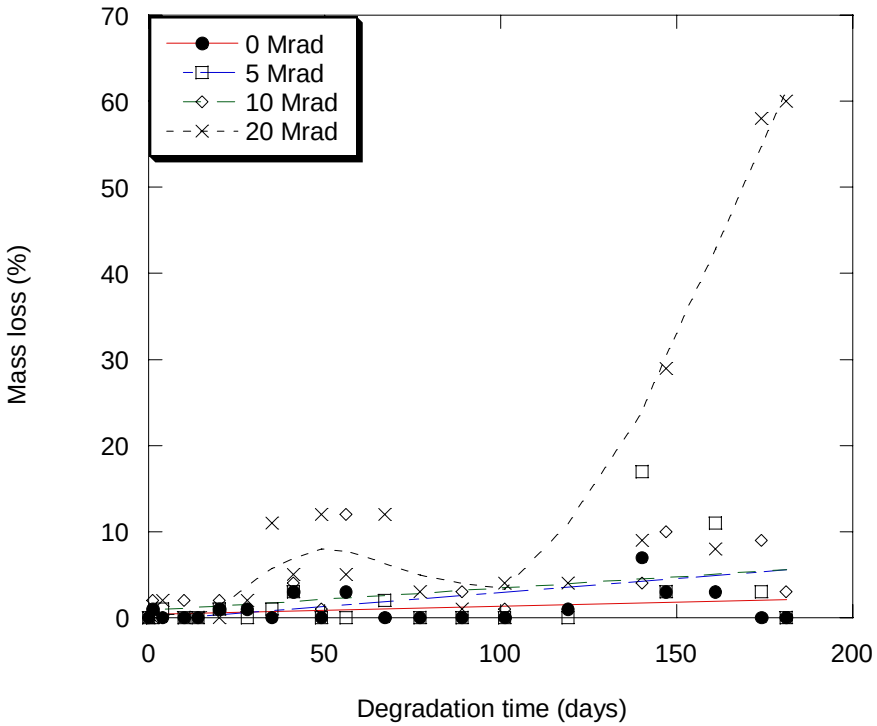

Figure 4.49 – Plot of change in mass loss of PLLA with hydrolytic degradation time

The water uptake (%) of PLGA and PLLA was plotted as a function of hydrolytic degradation time as shown in **Figure 4.50** and **Figure 4.51** respectively. Measurements for water uptake were taken until 20 % of mass loss occurred, beyond which the measurement of water uptake was difficult and inaccurate. The results show that water uptake for both PLGA and PLLA were higher for the more highly irradiated films. This suggests that the equilibrium water uptake may be dependent on the molecular weight, where a lower molecular weight resulted in a higher water uptake, supporting the results reported by *Chu et al.* [95] and *Schliecker et al.* [66]. This is contrary to the results reported by *Birkinshaw et al.*, who observed a lower water uptake for irradiated samples of poly-D-L-lactide [36]. The conclusion by *Birkinshaw et al.* lacks sufficient evidence for the observation made, since *Birkinshaw et al.* only conducted the study at one radiation dose of 2.5 Mrad.

The higher water uptake for lower molecular weight polymers was due to the presence of more hydrophilic end groups, such as carboxyl or hydroxyl end groups, in these polymers. Irradiation also results in the formation of hydrophilic hydroxyl (OH) groups, as seen from **Chapter 4.1**, which also explains for the increase in water uptake with radiation dose.

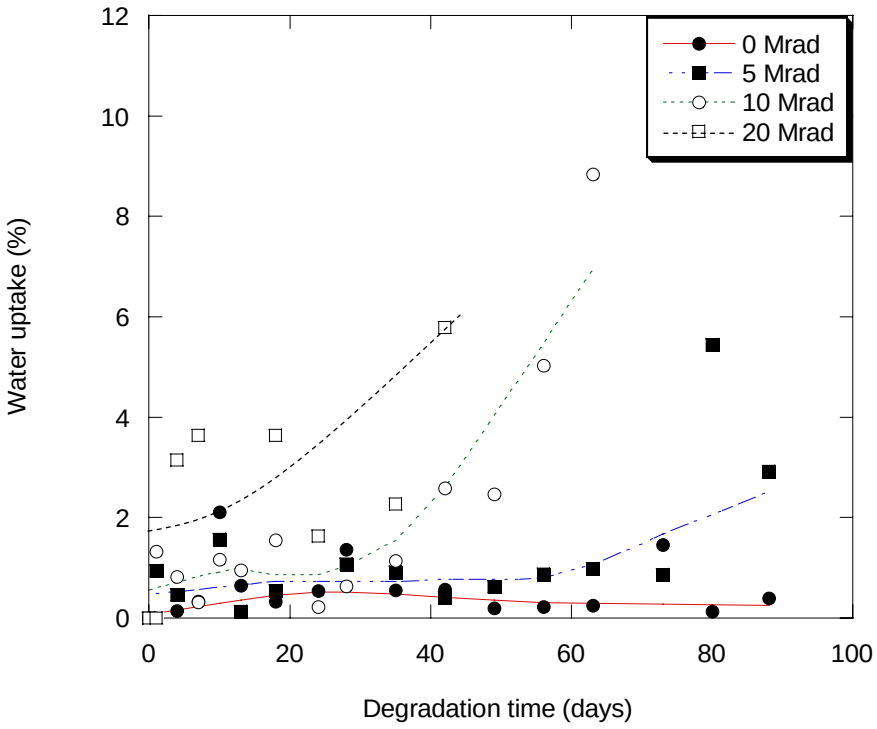

Figure 4.50 – Plot of water uptake for PLGA with hydrolytic degradation time

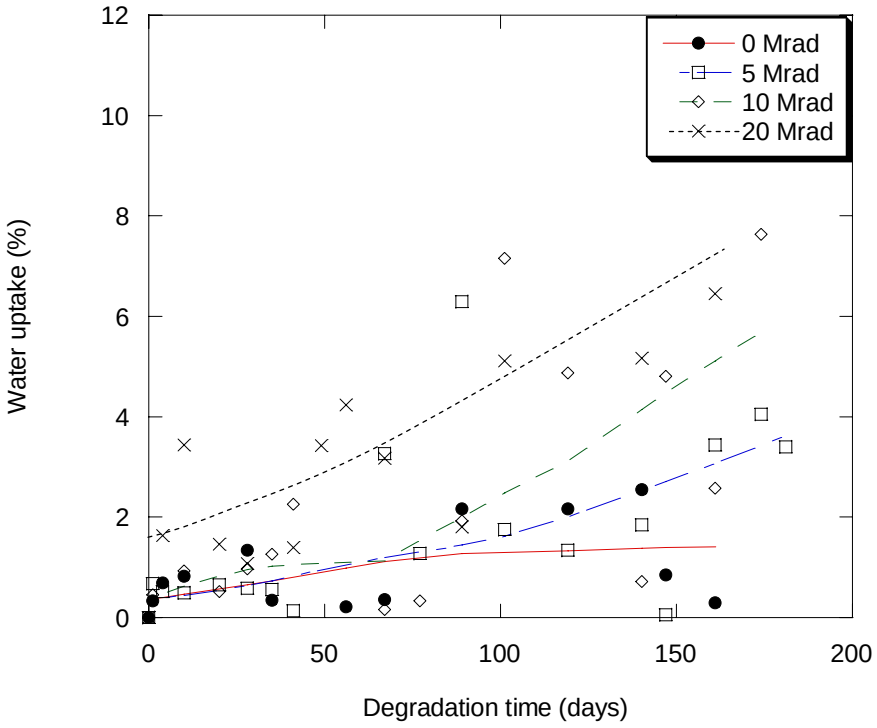

Figure 4.51 – Plot of water uptake for PLLA with hydrolytic degradation time

The results obtained illustrates that a lower molecular weight (higher irradiated) PLGA and PLLA sample experienced an earlier commencement of mass loss and higher water uptake during hydrolytic degradation. The higher percentage of hydrophilic end groups (both hydroxyl and carboxyl) in the irradiated samples increased their hydrophilicity and allow for more influx of water molecules into the polymer matrix. The decrease in the T_g with radiation dose resulting in an increase in chain mobility, as shown in **Table 4.3** and **Table 4.4**, would also facilitate water uptake into these films.

The influx of water molecules will then cause a build up of osmotic pressure within the polymer matrix, which will result in osmotic cracking [72]. This build up of osmotic pressure is due to poor diffusivity of the oligomers and the strong water affinity for these hydrophilic oligomer solutes, initiating crack propagation and the formation of microcavities. Microcavitation occurs due to the leaching of polymeric material into the surrounding medium, resulting in mass loss. The initial increase in the water uptake for the 20 Mrad irradiated PLGA sample resulted in osmotic cracking and the formation of microcavities after 7 days of in vitro degradation. The formation of more microcavities after 5 weeks of degradation can be seen from **Figure 4.52 (b)**. The formation of microcavities was also observed for 10 Mrad irradiated PLGA samples, but only after 6 weeks of degradation. Signs of microcavitation were however absent for the remaining PLGA and PLLA samples until the end of their respective hydrolytic degradation studies, which verifies that mass loss had not occurred for these samples, as illustrated in **Figure 4.48** and **Figure 4.49** for PLGA and PLLA respectively.

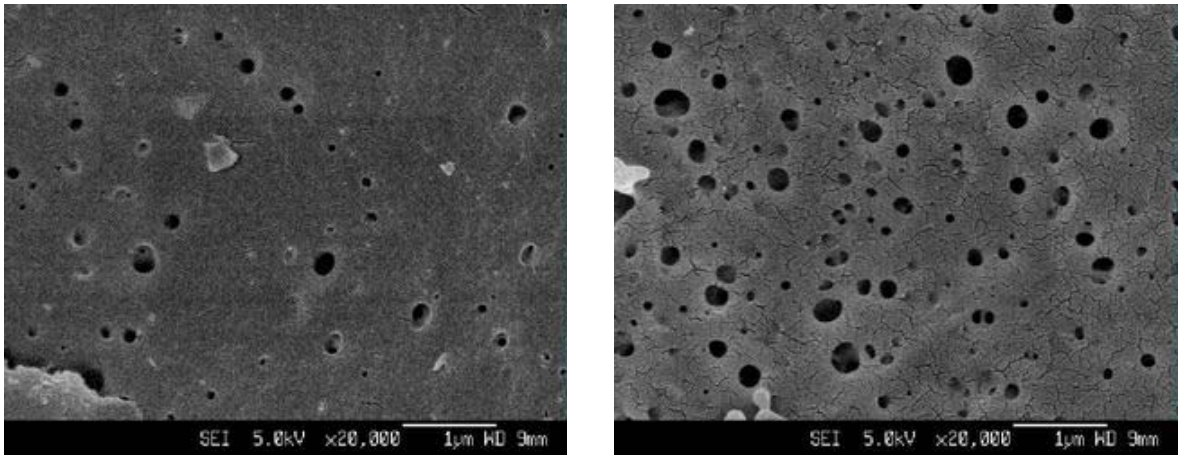

(a) **(b)**

Figure 4.52 – SEM pictures of 20 Mrad irradiated PLGA at (a) 7 days, (b) 5 weeks of hydrolytic degradation

(a) Relationship between molecular weight and degradation rate constant

The increase in water uptake in the highly irradiated PLGA and PLLA would affect their rate of hydrolytic degradation. **Figure 4.53** and **Figure 4.54** plots the natural logarithmic number-average molecular weight (ln $M_{n,D}$) of PLGA and PLLA respectively as a function of hydrolytic degradation time. Only molecular weights before 20 % mass loss occurred, which corresponded to the first stage of the degradation mechanism [12], were taken. This was because beyond 20 % mass loss, medical applications of PLGA and PLLA that requires good mechanical strength, such as temporary implants, would be rendered useless for any practical use. From the graphs, linear plots showing a strong statistical linear correlation ($R^2 > 0.9$) were obtained. The results show that the molecular weight of both PLGA and PLLA decreases with hydrolytic degradation time.

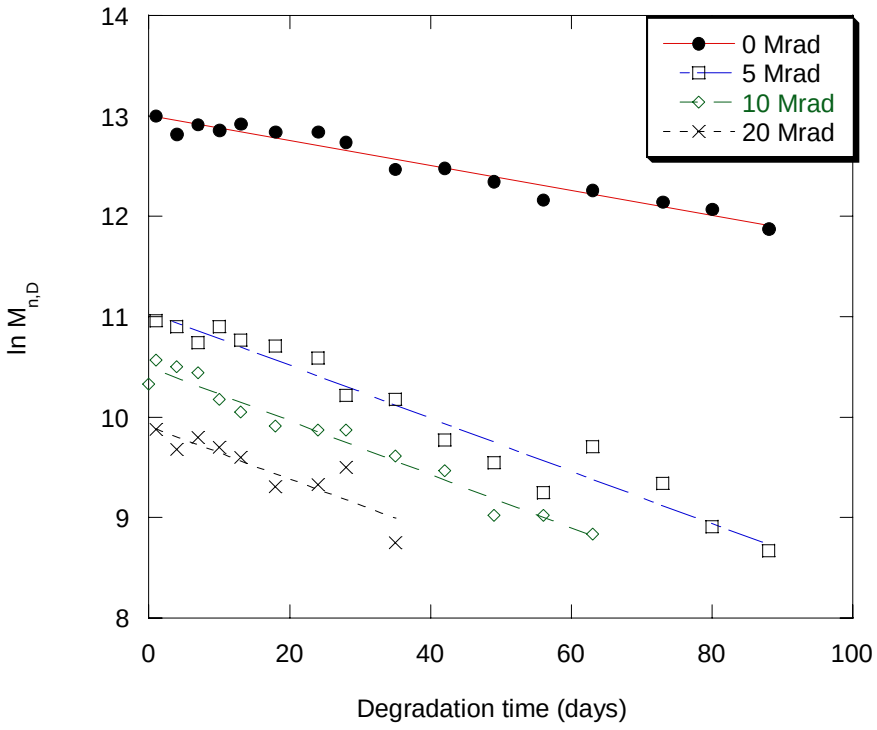

Figure 4.53 – Plot of ln $M_{n,D}$ of PLGA with hydrolytic degradation time

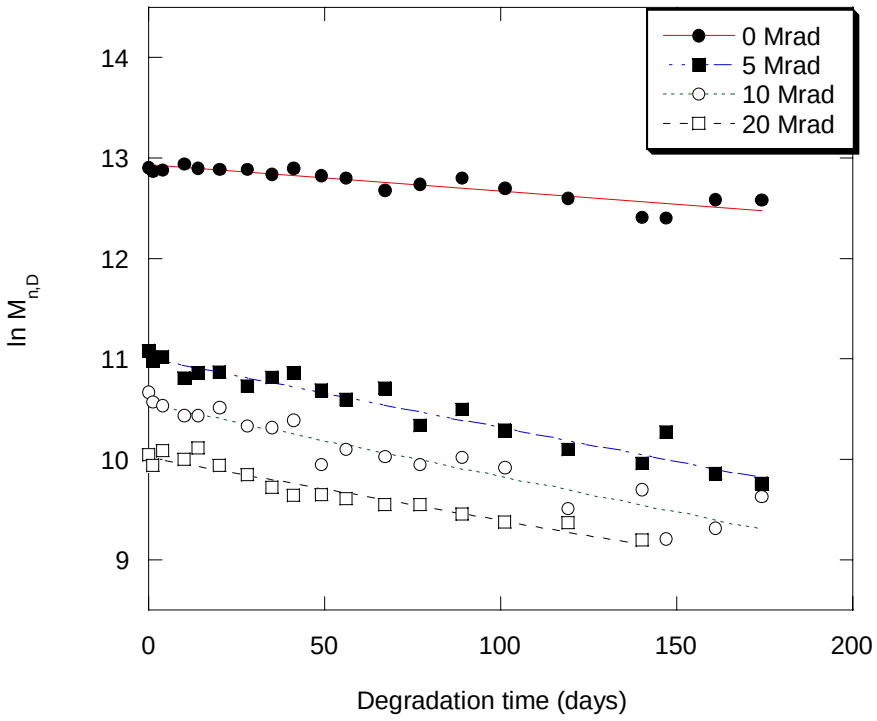

Figure 4.54 – Plot of ln $M_{n,D}$ of PLLA with hydrolytic degradation time

The degradation rate constants (k), taken as the gradient of the linear plots, and the initial number-average molecular weight of the irradiated polymers ($M_{n,D}$) of PLGA and PLLA are summarized in **Table 4.5** and **Table 4.6** respectively.

Table 4.5 – Degradation rate constants (k) and initial number-average molecular weight ($M_{n,D}$) of irradiated PLGA films

Radiation dose	Rate constant, k ($g/mol.day^{-1}$)	$M_{n,D}$ (g/mol)
Non-irradiated (0 Mrad)	0.0124	4.40×10^5
5 Mrad	0.0263	5.75×10^4
10 Mrad	0.0267	3.07×10^4
20 Mrad	0.0264	1.95×10^4

Table 4.6 – Degradation rate constants (k) and initial number-average molecular weight ($M_{n,D}$) of irradiated PLLA films

Radiation dose	Rate constant, k ($g/mol.day^{-1}$)	$M_{n,D}$ (g/mol)
Non-irradiated (0 Mrad)	0.0026	4.06×10^5
5 Mrad	0.0068	6.47×10^4
10 Mrad	0.0070	4.32×10^4
20 Mrad	0.0062	2.31×10^4

From **Table 4.5** and **Table 4.6**, the results show that, firstly, the k values of the irradiated PLGA samples are about four times larger than the k values for irradiated PLLA. Secondly, irradiation increases the degradation rate constants in both PLGA and PLLA, where the k values were observed to be higher for irradiated samples compared to non-irradiated samples. Thirdly, the k values for irradiated PLGA are approximately twice that of non-irradiated PLGA, whereas the k values for irradiated PLLA are more than two-and-half times that of the non-irradiated PLLA.

The two key reasons for the difference in the rates of degradation between the non-irradiated and irradiated samples are the lower molecular weight and the changes to the chemical structure during irradiation. Irradiated lactic/glycolic acid polymers have a higher percentage of hydrophilic hydroxyl and carboxyl end groups, which allows for higher influx of water molecules into the polymer matrix (**Figure 4.50** and **Figure 4.51**). Subsequently, the formation of more hydroxyl and carboxyl end groups, as the end products of hydrolytic degradation, further increases the rate of hydrolytic degradation, resulting in an autocatalytic effect. This can be observed from **Figure 4.55** and **Figure 4.56** respectively, which shows the FTIR spectra of the 10 Mrad irradiated PLGA samples at 0 day, 6 weeks and 12 weeks of degradation. **Figure 4.55** shows the FTIR spectra of O–H stretching of alcohols and carboxyl groups (~3300 cm^{-1}) and overtones of O–H bends and C–O stretch in carboxyl groups (2605 cm^{-1}), which increases relative to other peaks with increasing degradation times. **Figure 4.56** shows the FTIR spectra of C–O stretching of alcohols (1130cm^{-1}) and carboxyl groups (1215cm^{-1}), which similarly increases relative to other peaks with increasing degradation times.

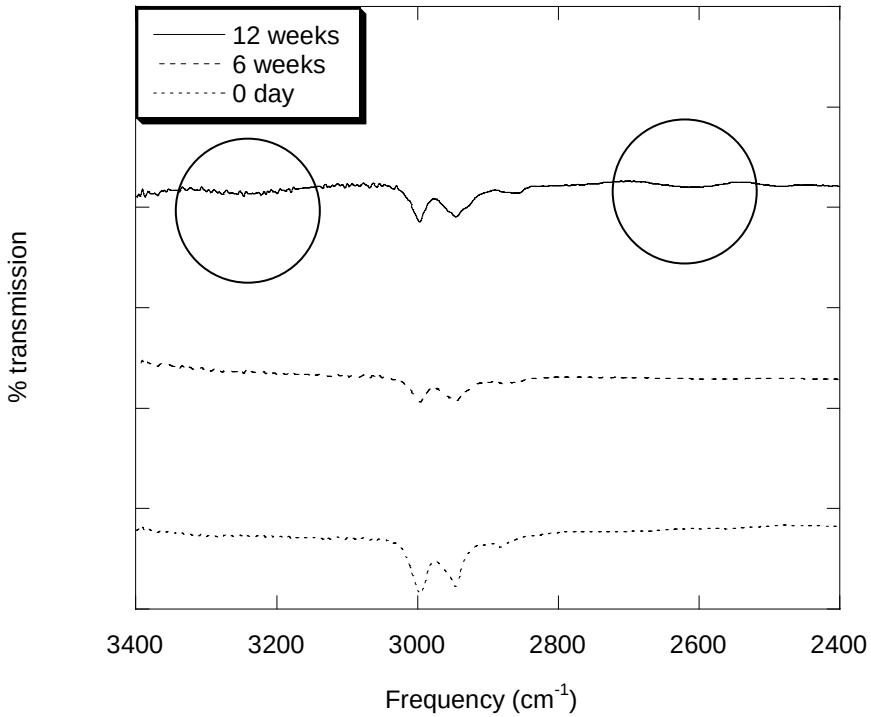

Figure 4.55 – FTIR spectra showing O–H stretching of alcohols and carboxyl groups with overtones of O–H bends and C–O stretch in carboxyl groups

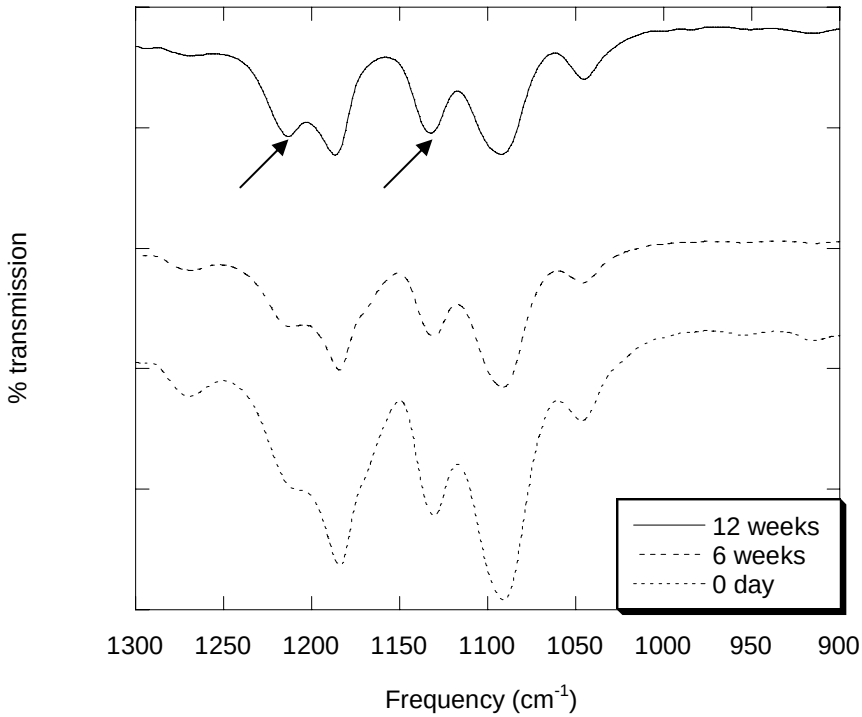

Figure 4.56 – FTIR spectra showing C–O stretching of alcohols (1130cm^{-1}) and carboxyl groups (1215cm^{-1}) with hydrolysis (Arrows indicate peaks with changes)

The fourth observation made from the degradation rate constants, from **Table 4.5** and **Table 4.6**, was that the k values were found to be similar among the irradiated PLGA samples, and, likewise, among the irradiated PLLA samples. The average k value for the irradiated PLGA samples was about 0.0265 g/mol.day^{-1}, and for PLLA was about 0.0067 g/mol.day^{-1}. This implies that e-beam radiation could be used to accelerate the rate of hydrolytic degradation, but will not result in any distinctive difference in degradation rates between samples of varying radiation doses. Irradiation causes the recombination of skeletal backbones (**Table 4.1**), as shown from the schematic diagram in **Figure 4.4**. The irradiated polymer chains are therefore shorter, with a higher concentration of methyl side groups, and having a more regular backbone chain and fewer ester bonds, as observed from the various structures in **Table 4.1**. The reduction in the number of ester bonds, through irradiation, help to decrease the incidents of chain scission through hydrolysis and thus decrease the hydrolytic degradation rate for highly irradiated (20 Mrad) PLGA and PLLA films. This "backbone-recombination effect" is therefore responsible for the relatively similar degradation rate constants of the irradiated films, by encouraging the recombination of polymer backbone during irradiation, resulting in a backbone chain with a lower percentage of ester bonds.

The hydrolytic degradation behaviour of e-beam irradiated PLGA and PLLA can thereby be expressed accordingly in **Eq. 4.3** and **Eq. 4.4** respectively,

$$\ln M_n = \ln M_{n,D} - 0.0265 \times t \qquad \textbf{(Eq. 4.3)}$$

$$\ln M_n = \ln M_{n,D} - 0.0067 \times t \qquad \textbf{(Eq. 4.4)}$$

where M_n is the number-average molecular weight at degradation time, t, in days, and k is the degradation rate constant. The hydrolytic life span (t) of PLGA and PLLA can therefore be taken as the time required to hydrolytically degrade these biodegradable polyesters. The hydrolytic in vitro life span of irradiated PLGA and PLLA can thus be modeled with the radiation dosage.

The hydrolytic life span of PLGA (t_{PLGA}) and PLLA (t_{PLLA}) can be calculated by combining **Eq. 4.1** and **Eq. 4.3** for PLGA and **Eq. 4.2** and **Eq. 4.4** for PLLA respectively. The number of days required to hydrolytically degrade PLGA and PLLA, after irradiation, can then be expressed as,

$$t_{PLGA} = 38 \times \ln \frac{M_{n,0}}{M_n (1 + 1.44 \times 10^{-6} \times D \times M_{n,0})} \qquad \textbf{(Eq. 4.5)}$$

$$t_{PLLA} = 149 \times \ln \frac{M_{n,0}}{M_n (1 + 1.39 \times 10^{-6} \times D \times M_{n,0})} \qquad \textbf{(Eq. 4.6)}$$

where $M_{n,0}$ is the initial number-average molecular weight before irradiation, and D is the radiation dose in Mrad. M_n can be taken as the number-average molecular weight at 20 % mass loss of approximately 6.0 x 10^3 g/mol for both PLGA and PLLA. Thus, from the in vitro hydrolytic degradation studies, it has been shown

that the life span of PLGA and PLLA can thus be controlled using **Eq. 4.5** and **Eq. 4.6** respectively, with the appropriate e-beam radiation dose.

(b) Physiochemical properties of hydrolytically degraded PLGA and PLLA

The DSC thermograms of PLGA for a non-irradiated (0 Mrad) sample and irradiated (10 Mrad) sample after 7 weeks of degradation are shown in **Figure 4.57**. The irradiated sample reveals a cold crystallization peak (T_c), which is absent in the non-irradiated sample. This cold crystallization peak is due to the re-orientation of the less entangled shorter chains (a product of irradiation chain scission) in forming regularly ordered crystalline regions, as observed for all irradiated PLGA samples shown in **Figure 4.21**. The thermograms of the irradiated samples revealed two melting peaks, whereas the non-irradiated samples revealed only a single weak melting peak. The single melting peak of the non-irradiated samples was due to the re-orientation of the hydrolytically degraded shorter chains during hydrolysis in forming hydrolysis-induced crystals. For the irradiated samples, the lower melting peak (Peak 1) was due to the existence of hydrolysis-induced and radiation-induced crystals [102], and the larger and higher T_m peak (Peak 2) was due to the cold crystallization crystals from the T_c. It can also be observed that there is a double T_g for the 10 Mrad irradiated PLGA after hydrolytic degradation, contrary to the single T_g that was observed for the irradiated non-degraded PLGA sample, as shown from **Figure 4.21**. The DSC thermograms of PLLA for a non-irradiated (0 Mrad) and irradiated (10 Mrad) sample after 20 weeks of degradation are shown in **Figure 4.58**. The thermograms did not show a cold crystallization peak, unlike in PLGA.

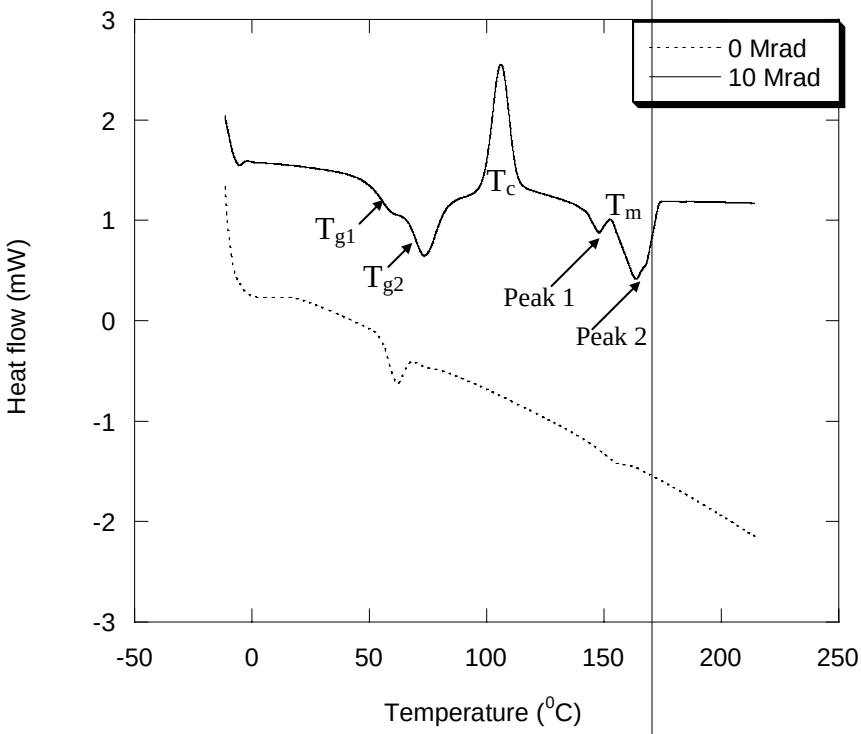

Figure 4.57 – DSC thermograms of 0 Mrad and 10 Mrad PLGA samples after 7 weeks of hydrolytic degradation

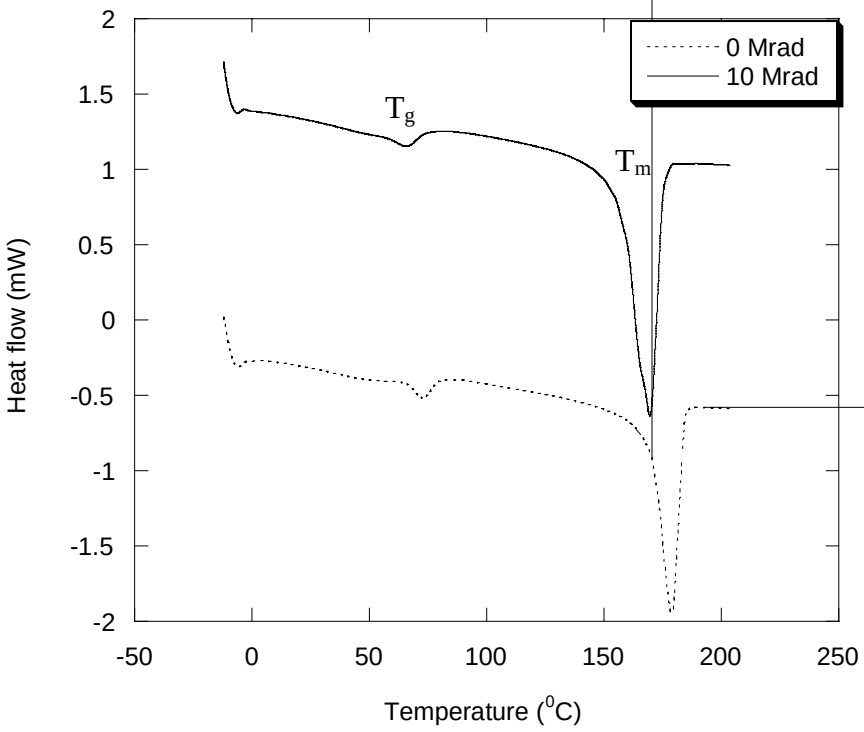

Figure 4.58 – DSC thermograms of 0 Mrad and 10 Mrad PLLA samples after 20 weeks of hydrolytic degradation

Figure 4.59 plots the T_c of the irradiated PLGA films against degradation time. A decrease in T_c was observed with degradation time. The T_c is representative of the amorphous chains, which underwent chain scission during irradiation and during hydrolysis. The decrease in the T_c illustrates that less energy is required to re-orientate the shorter amorphous chains, because of chain scission during hydrolysis. This affirms that hydrolysis is taking place in the amorphous regions, due to the water uptake of the more open amorphous regions, as proposed by *Chu et al.* [40]. The higher irradiated films had a lower T_c, due to shorter chains resulting from more radiation-induced chain scission occurring at higher radiation dose.

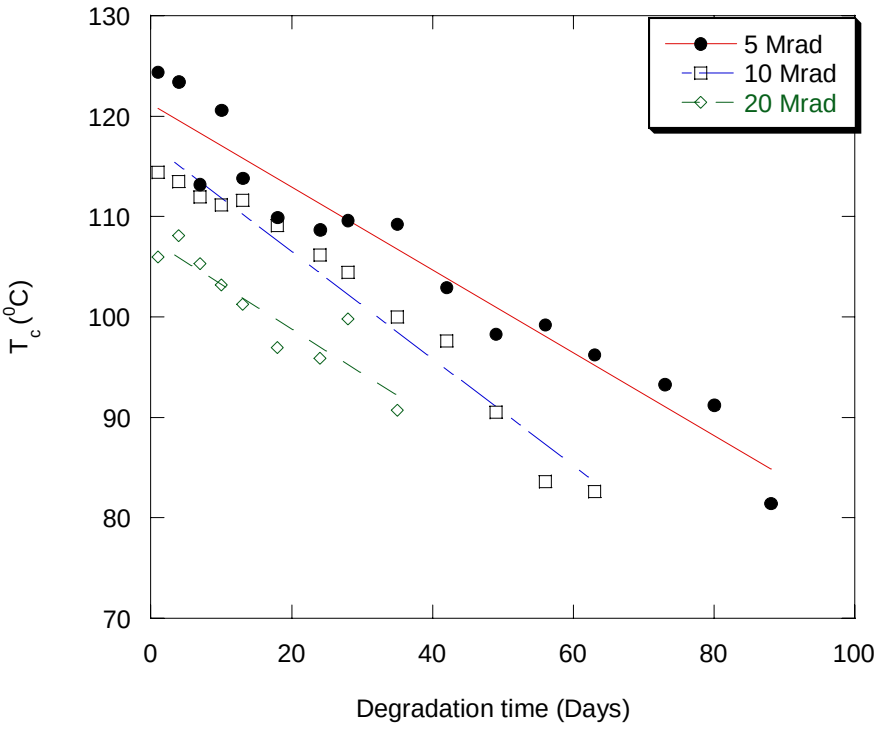

Figure 4.59 – Plot of T_c of PLGA with hydrolytic degradation time

Figure 4.60 plots the T_m (Peak 1) of the PLGA films against degradation time. The T_m increases with degradation time for the non-irradiated films, which is attributed to an increase in crystal perfection, arising from the loss of defects by the removal of amorphous material and reordering of the degradation products. The decrease in T_m of the irradiated films is due to the decrease in chain uniformity arising from the irradiation process [102], which during hydrolysis gives rise to even less perfect crystals [115]. The decrease in T_m for PLGA could also arise from the decrease in molecular weight [50], especially so for the irradiated PLGA samples, which had lower molecular weights in comparison to the non-irradiated PLGA sample and faster degradation rates.

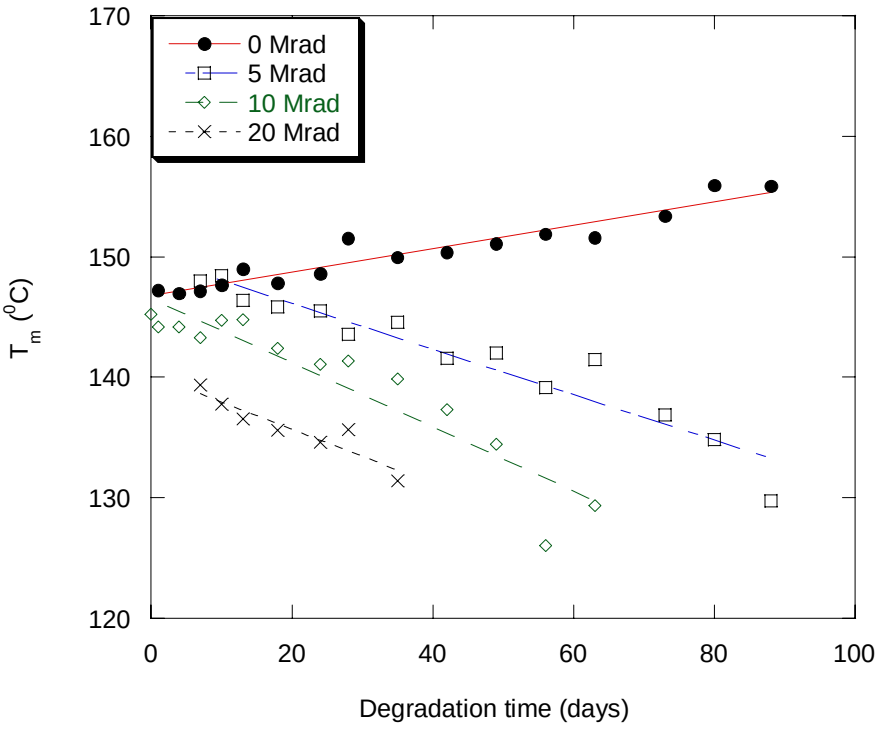

Figure 4.60 – Plot of T_m (Peak 1) of PLGA with degradation time

The plot of the T_m of PLLA with hydrolytic degradation time is plotted in **Figure 4.61**. The results show similar trend as that for PLGA (**Figure 4.60**), where the T_m of the non- irradiated PLLA increases, whereas the T_m of the irradiated PLLA decreases with degradation time. Similarly, the increase in T_m for PLLA is due to an increase in the crystal perfection for the non-irradiated samples. The decrease in T_m for the irradiated PLLA samples is due to the decrease in molecular weight during hydrolysis [50]. *Jamshidi et al.* [50] reported a decrease in T_m with molecular weight for PLLA, when its molecular weight is below $5x10^4$ g/mol. The decreasing low molecular weights and faster degradation rate constants (**Table 4.6**) for the irradiated PLLA samples therefore explains for the decrease in their T_m.

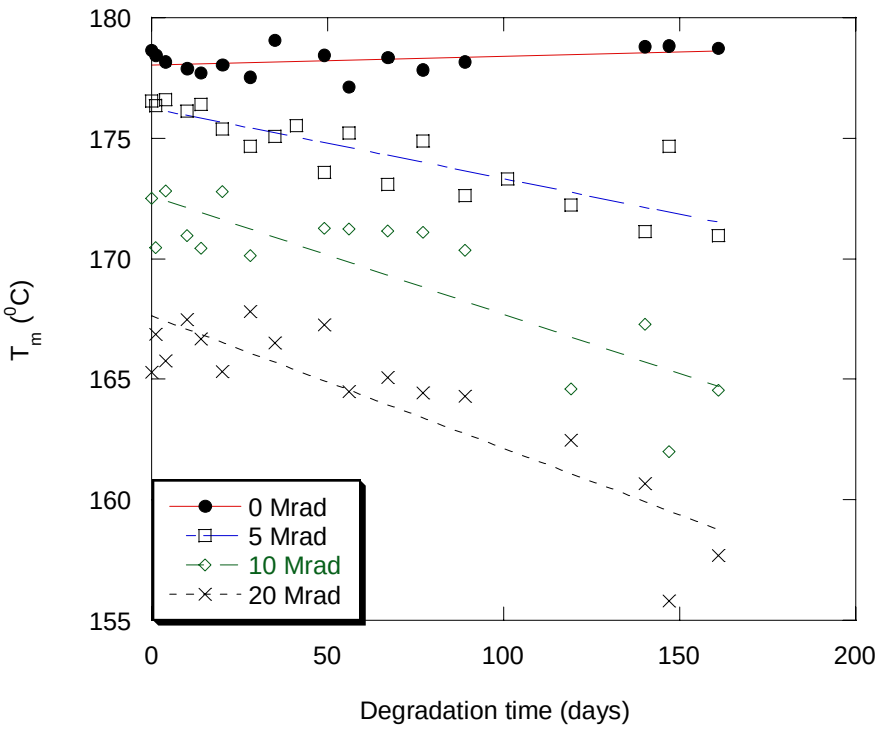

Figure 4.61 – Plot of T_m of PLLA with degradation time

The degree of crystallinity for all the degraded samples remained low (< 8 J/g), as shown from **Figure 4.62**. From the measurement of the degree of crystallinity (ΔH), no significant change was observed immediately after hydrolytic degradation, except for the non-annealed PLGA, which saw a small increase in degree of crystallinity with degradation time. The randomness of the degree of crystallinity for the annealed PLGA is due to the large error margin (approximately 1.3 J/g) of the DSC. From the results obtained, it can be implied that without sufficient heat energy, the amorphous chains could not re-orientate much during hydrolysis. The amorphous chains therefore remain rigid and relatively immobile. The irregular structure of the PLGA also inhibits the movement and packing of the chains in forming crystals.

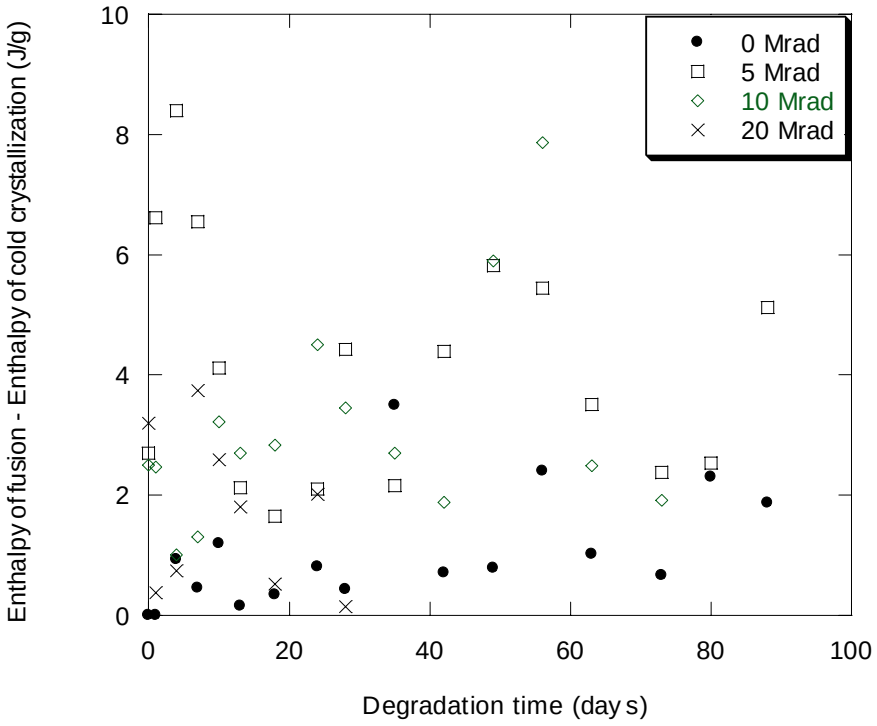

Figure 4.62 – Difference in enthalpy of fusion and enthalpy of crystallization for irradiated PLGA after hydrolysis

Figure 4.63 plots the normalized degree of crystallinity of PLLA with degradation time. The results show that, contrary to PLGA, the degree of crystallinity for PLLA increases significantly with degradation time. This was similar to the studies conducted by *Schliecker et al.* [66] and *Eldaster et al.* [67], who also observed an increase in crystallinity with degradation time. This observation indicates the ease of crystal formation in PLLA in comparison to PLGA. The ability of the hydrolyzed PLLA chains to re-orientate is due to the increased regularity of the shorter PLLA chains. The presence of existing crystals also allows for chain folding and continuum crystal growth, which increases the degree of crystallinity. The semi-crystalline morphology of PLLA and its higher hydrophobicity in comparison to PLGA therefore explains the difference in k values for PLLA (0.0026 g/mol.day^{-1}) and PLGA (0.0124 g/mol.day^{-1}), as observed from **Table 4.5** and **Table 4.6**.

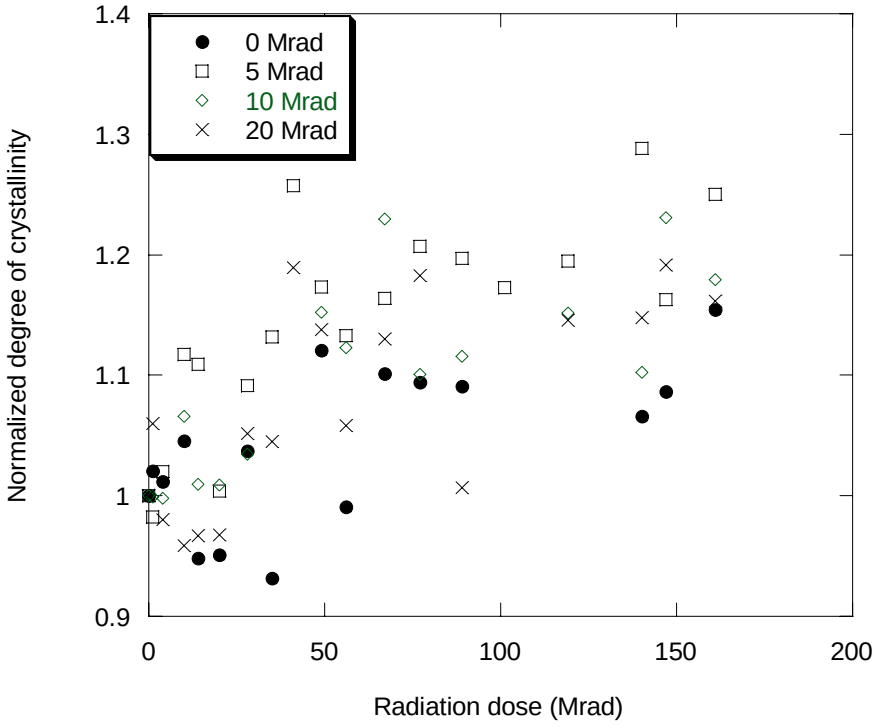

Figure 4.63 – Plot of normalized degree of crystallinity of PLLA with degradation time

It can be observed from **Figure 4.57** that the hydrolysis of irradiated PLGA results in the splitting of the T_g into two separate peaks with degradation time. **Table 4.7** gives a summary of the T_g of the split peaks and its occurrence time. The splitting of the T_g peaks probably indicates the scissioning of the PLA (poly-lactic acid) chains from PLGA. The lower T_g, plotted in **Figure 4.64**, corresponds to the T_g of the PLGA matrix, whereas the higher T_g corresponds to the T_g of PLA (T_g of PLA ≈ 72°C) [8]. The remaining degradation product at the splitting of the T_g is therefore a blend of PLGA co-polymer and PLA homo-polymer. The splitting of the T_g is, however, not evident for the degraded PLLA samples, since PLLA is a homo-polymer. The T_g of irradiated PLLA was also found to decrease with degradation time, shown from the plot of T_g of PLLA with degradation time in **Figure 4.65**. The decrease in T_g of the degraded PLGA and PLLA samples therefore indicates the increase in chain mobility with increasing degradation time.

Table 4.7 – Splitting of T_g peaks for hydrolytically degraded PLGA films

Radiation dose	$T_{g,1}$ (°C)	$T_{g,2}$ (°C)	Time observed
0 Mrad	No splitting of peak, T_g constant ~ 55.6°C		
5 Mrad	48.9	61.5	42 days
10 Mrad	54.4	65.9	18 days
20 Mrad	53.2	66.0	7 days

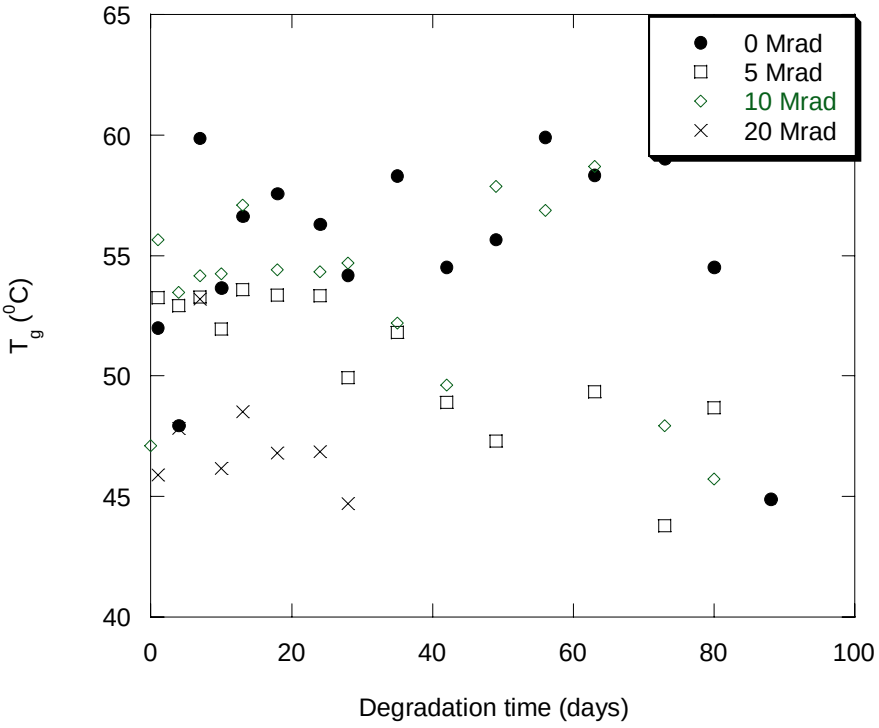

Figure 4.64 – Plot of T_g (Peak 1) of PLGA with degradation time

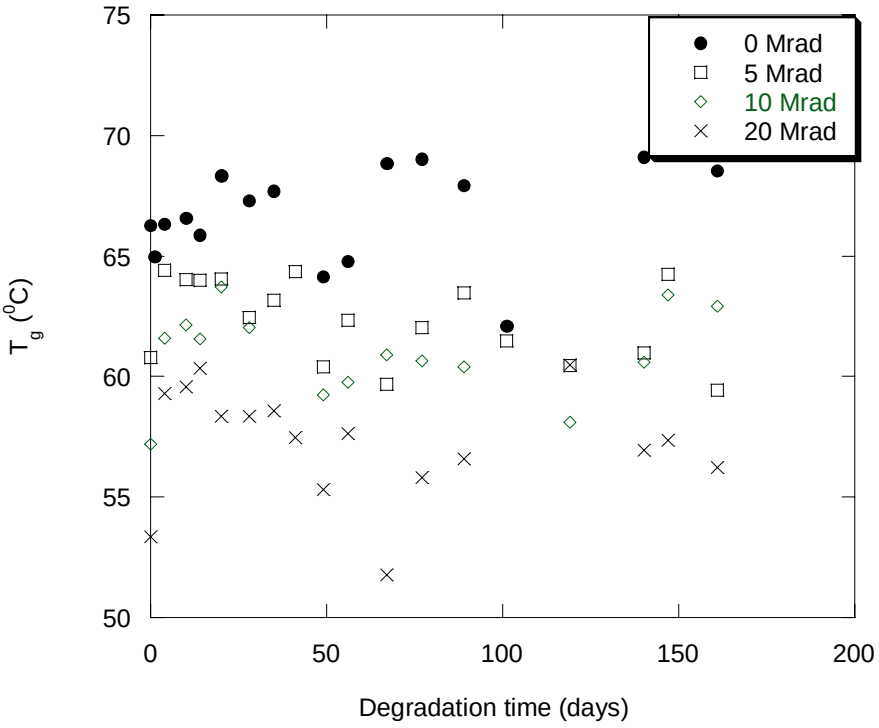

Figure 4.65 – Plot of T_g of PLLA with degradation time

(c) Summary

Irradiated samples of PLGA and PLLA, when placed in PBS solution, were found to degrade faster than the non-irradiated samples, by at least twice the hydrolytic degradation rate. This was because of higher water uptake for the irradiated samples, which had lower T_g and lower molecular weights. The presence of more hydrophilic hydroxyl groups, a by-product of irradiation, was also responsible for the increase in the influx of water molecules into the polymer matrix. This led to an increase in osmotic pressure and subsequently an increase in mass loss due to microcavitation and osmotic cracking. The thermal properties of hydrolytically degraded PLGA and PLLA samples also changed with degradation times. The T_m increases for the non-irradiated samples, but decreases for the irradiated samples. The decrease in T_m was due to the decrease in molecular weight of the polymers with hydrolysis. However, it was noted that the hydrolytic degradation rate constants remained relatively unchanged irrespective of radiation dose, due to the "backbone-recombination effect". A relationship between radiation dose and the hydrolytic degradation time, through their molecular weights, was thus established. This relationship allows for a more accurate and precise control of the hydrolytic degradation times of PLGA and PLLA through the use of e-beam radiation. Hence, the hydrolytic in vitro life span of irradiated PLGA and PLLA polyesters can be determined and controlled using e-beam radiation.

4.2.2 Effect of isothermal annealing on the hydrolytic degradation of PLGA

Crystallinity is an important property in the characterization of lactic/glycolic acid polymers. The percentage or degree of crystallinity not only affects the mechanical strength of the polymer, but also their swelling behaviour, and consequently, its rate of hydrolytic degradation [8, 17-18]. Although it is widely accepted that the degree of crystallinity affects the rate of hydrolytic degradation of polyesters, the significance of this effect on the rate of hydrolytic degradation is uncertain. There is also a lack of data relating the degree of crystallinity of PLGA to its hydrolytic degradation rate; in which this thesis aims to contribute. This section studies the effects of crystallization on the hydrolytic degradation behaviour of PLGA through isothermal annealing of non-irradiated and irradiated PLGA. It would be determined if the changes in degree of crystallinity would have a significant effect on the rate of hydrolytic degradation in PLGA.

(a) Hydrolytic degradation of annealed PLGA (non-irradiated)

In vitro hydrolytic degradation studies were conducted on non-irradiated PLGA films, annealed for 15 min, 30 min, 45 min and 60 min over a length of 150 days in phosphate buffer saline (PBS) solution (pH 7.4) at 37.0°C. The non-annealed films (0 min) were used as the control sample. The degree of crystallinity (obtained from the WAXD in %) and enthalpy of fusion (obtained from the DSC in J/g), taken as an indirect measurement of the degree of crystallinity, for these films are tabulated

in **Table 4.8**. The results, from the WAXD (DOC %) and DSC (J/g), show an increase in the amount of crystallinity with annealing time.

Table 4.8 – Degree of crystallinity (WAXD) and enthalpy of fusion (DSC) for annealed PLGA films

Annealing time	0 min	15 min	30 min	45 min	60 min
DOC (%)	0	3.87	9.34	19.34	29.62
DSC (J/g)	0	1.17	4.60	13.58	21.22

The average water uptake of the annealed PLGA samples, after 150 days of in vitro hydrolytic degradation, is plotted in **Figure 4.66**. It can be observed that the non-annealed film (0 min) has the highest average water uptake. The average water uptake decreases with annealing time, up to 30 min, and then increases for the 45 min and 60 min samples. The average water uptake was highest for the non-annealed film because of its amorphous morphology. Amorphous regions are more open as compared to the closely packed crystalline regions, thus allowing more water molecules to penetrate into the amorphous region. The formation of crystalline regions, on the other hand, inhibits the penetration of water molecules, thus reducing the overall average water uptake. However, the increase in the average water uptake, for the 45 min and 60 min annealed films can be explained from the advance loss of amorphous material and the formation of voids within the

amorphous region and at the crystal interface. The formation of voids can be observed from the decrease in the T_g with annealing time as shown in **Figure 4.38**. Overall, the increase in degree of crystallinity does not cause drastic changes to its water uptake (< 1%).

There was no significant mass loss (less than 2.5 %) in the non-annealed and annealed films, even after 150 days of degradation. This implies that no or little soluble products and oligomers are formed after 150 days of degradation.

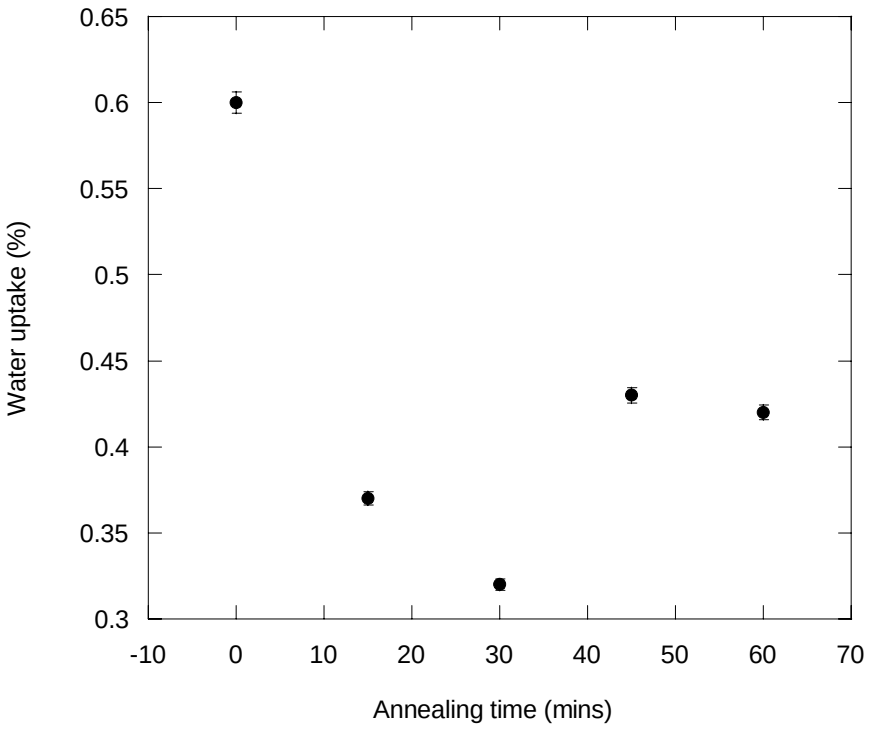

Figure 4.66 – Plot of average water uptake after 150 days of degradation for samples of different annealing times

The natural logarithmic of the number-average molecular weight (ln M_n) of PLGA was plotted against degradation time in **Figure 4.67**. The plots show that the natural logarithmic molecular weight (ln M_n) of PLGA decreases linearly ($R^2 > 0.9$) with degradation time, indicating chain scission, due to the hydrolysis of the ester bonds. The degradation rate constants (k), for the films, as obtained from **Eq. 2.3** and **Figure 4.67,** are plotted in **Figure 4.68** against annealing time.

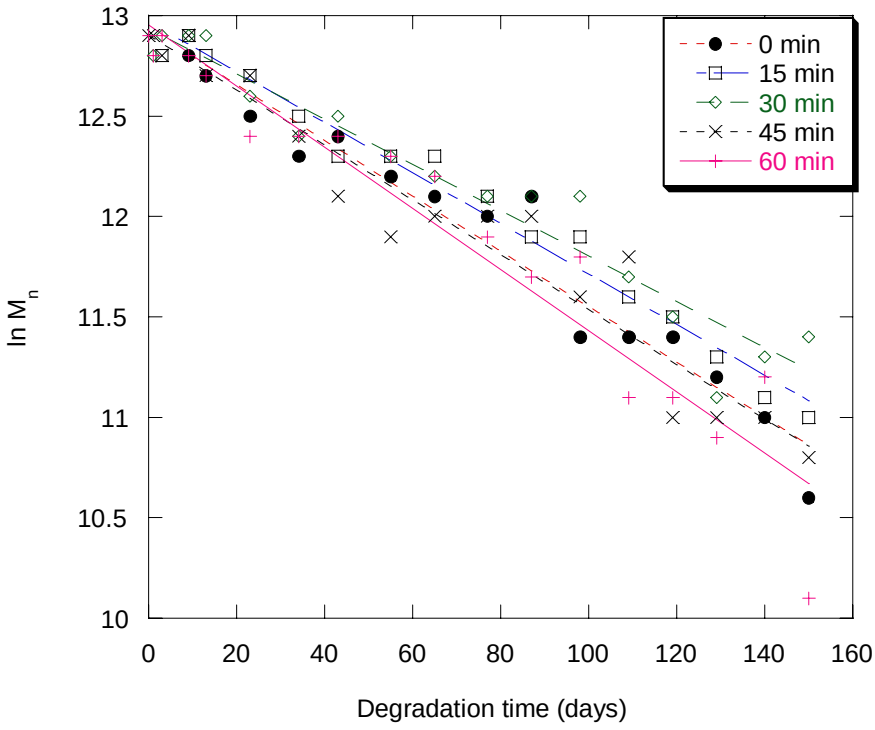

Figure 4.67 – Plot of ln M_n of annealed PLGA with hydrolytic degradation time

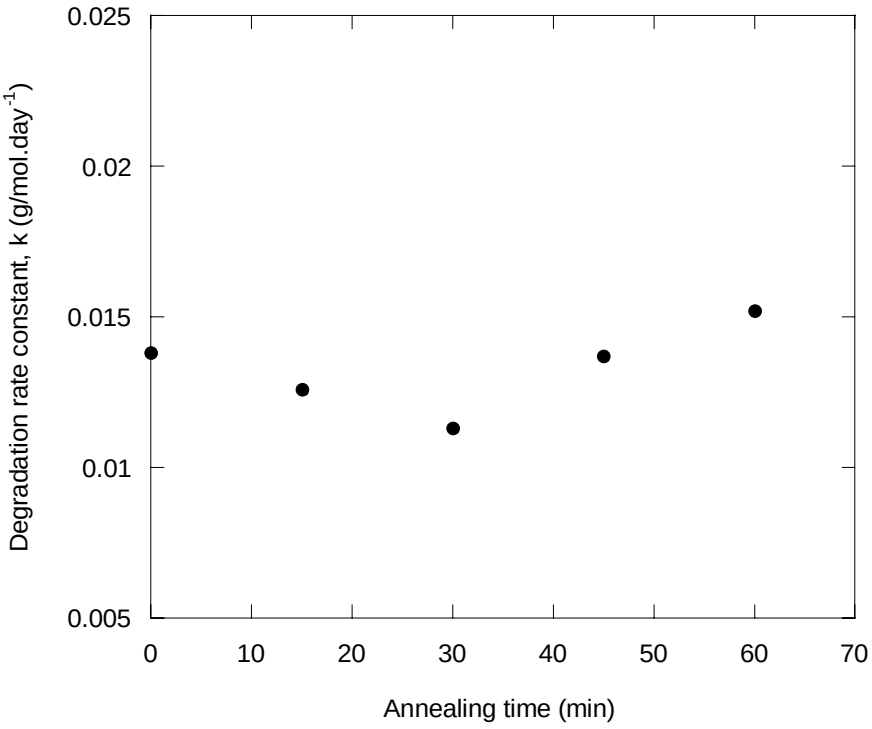

Figure 4.68 – Plot of degradation rate constants (k) of PLGA with annealing time

From the k values of **Figure 4.68**, it would be tested using a student's t-statistics to observe if there is any significant difference in the k values of the annealed samples to the non-annealed samples at 95 % confidence level, and at n-2 degrees of freedom. A 95 % confidence interval for the non-annealed k value can be calculated as [112]:

$$\hat{\beta}_1 \pm t_{.025}\left(\frac{s}{\sqrt{SS_{xx}}}\right) \qquad \textbf{(Eq. 4.7)}$$

where $\hat{\beta}_1$ is the unbiased estimator of the true k value for the non-annealed sample, $t_{.025}$ is 2.16, and $\frac{s}{\sqrt{SS_{xx}}}$ is the standard error of $\hat{\beta}_1$. From this, the 95 % confidence interval for the k value should therefore lie between 0.0138 g/mol.day^{-1} ± 0.0019 or (0.0118, 0.0157) g/mol.day^{-1}, which effectively includes the k values of all the annealed samples within this range. This proves that an increase in the degree of crystallinity has no significant effect on the rate of hydrolytic degradation.

The DSC thermograms of the hydrolytically degraded films (non-annealed and annealed) displayed a cold crystallization peak (ΔH_c) and two melting peaks (ΔH_f), as shown in **Figure 4.69**. The formation of the cold crystallization peak was due to the re-orientation of the shorter amorphous chains, formed through chain scission, during the DSC heating scan. These shorter chains are better able to re-orientate to form crystals when thermal energy is supplied during the heating scan. Two melting peaks were observed from the DSC thermograms, in which one of the melting peaks (Peak 1) is due to the crystals present immediately after hydrolytic degradation (through annealing and the product of hydrolysis chain scission) and the other melting peak (Peak 2) is due to the crystals formed through cold crystallization, from the cold crystallization peak.

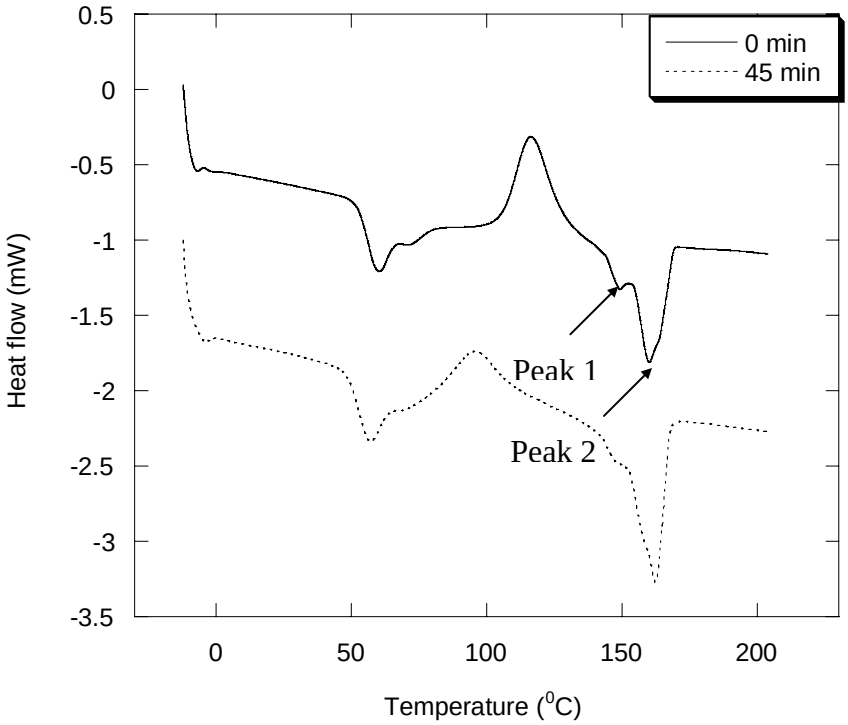

Figure 4.69 – DSC thermograms of non-annealed and annealed PLGA after 150 days hydrolytic degradation

Figure 4.70 plots the melting temperature of Peak 1 against hydrolytic degradation time. The T_m from Peak 1 is a representation of the crystals formed during annealing that has undergone hydrolytic degradation. The results show an initial increase in the T_m during the first fifteen days of hydrolytic degradation, and the T_m remained unchanged with further degradation. The initial increase in the T_m is due to the increase in lamellae thickness. Chain relaxation in the crystalline structure as water is absorbed into the polymer was probably responsible for this.

The crystal perfection can be observed from the plots of the change in the FWHM of the most intense diffraction peak at 16.35° with degradation time, as shown in **Figure 4.71**. The increase in lamellae thickness may have resulted in the decrease in crystal perfection of the crystal unit cell [114]. The decrease in crystal perfection could have resulted from the water uptake of the amorphous regions, and possibly selective degradation of the amorphous regions [67], between lamellae, which disrupts the folding of the crystalline chains, thus increasing the overall crystal defect.

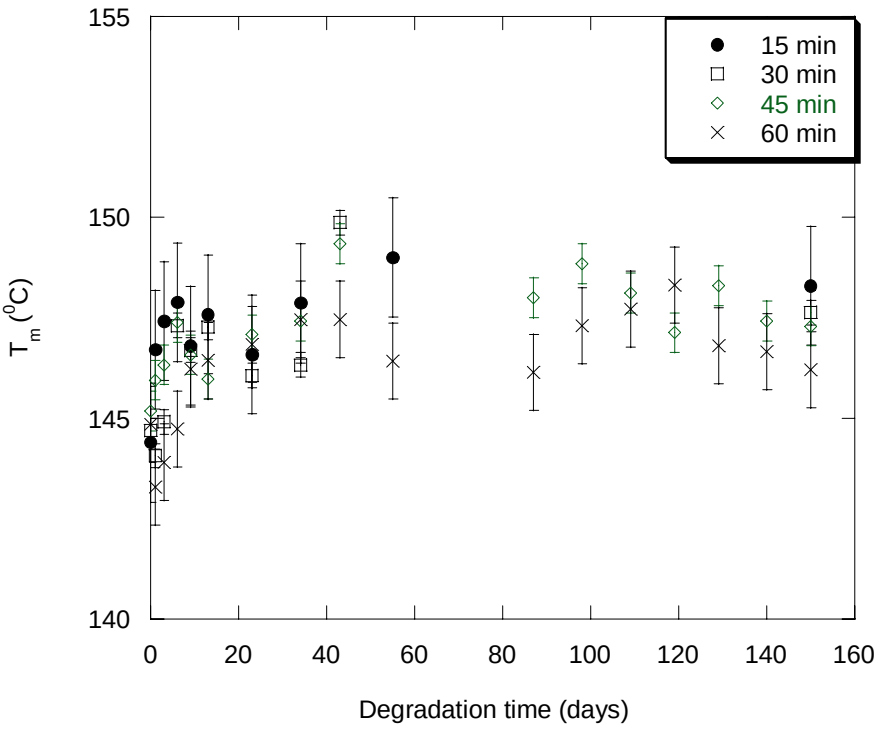

Figure 4.70 – Plot of T_m (Peak 1) of annealed PLGA with hydrolytic degradation time

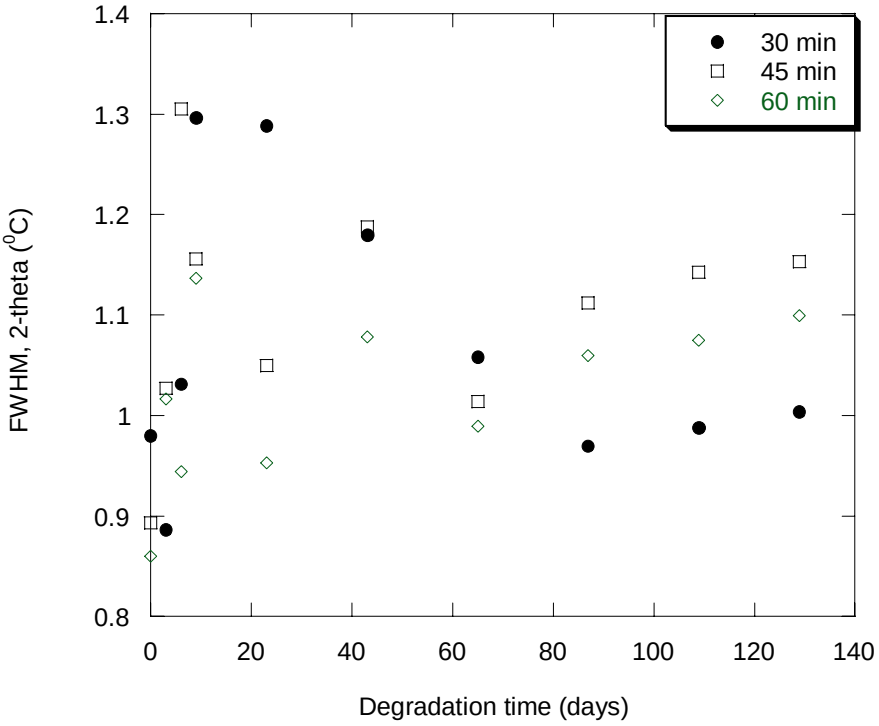

Figure 4.71 – Plot of FWHM of annealed PLGA with degradation time

Figure 4.72 shows the plot of the melting temperature of Peak 2 against hydrolytic degradation time. The T_m from Peak 2 is a representation of the crystals arising from the cold crystallization peak. The results show that the T_m increases with increasing degradation time. The amorphous chains undergo chain scission during hydrolysis, which result in better packing capabilities.

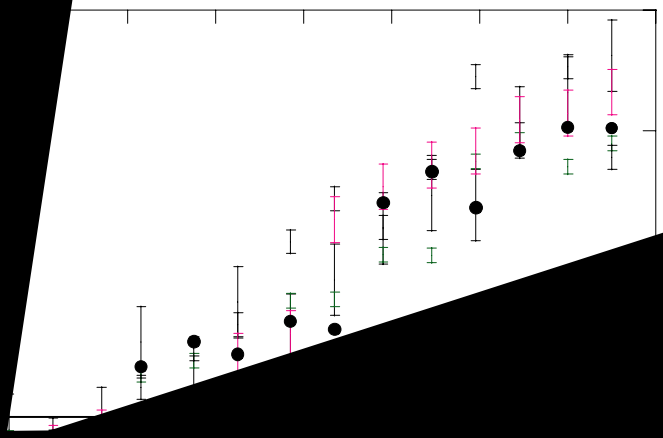

i i

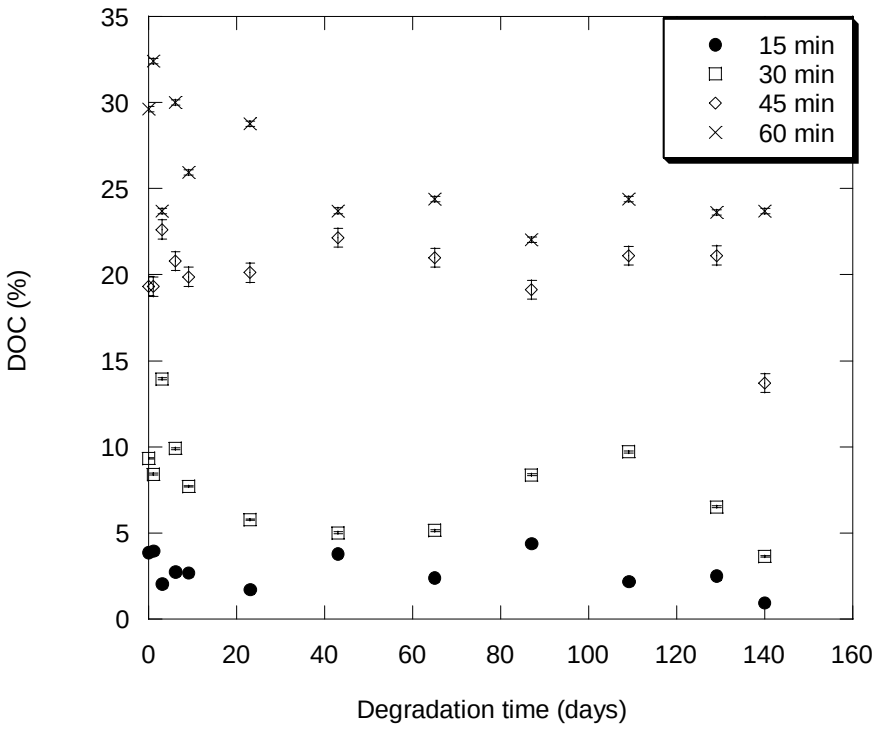

Figure 4.73 – Plot of degree of crystallinity of annealed PLGA with hydrolytic degradation time

The increase in degree of crystallinity, through isothermal annealing, does not significantly affect, at 95 % confidence level, the rate of hydrolytic degradation. The study conducted by *Chu et. al.* on the hydrolytic degradation of poly(glycolic acid) [40], observed the initial degradation of the amorphous regions for this highly crystalline polymer using the SEM. This observation could not be use to conclude that the decreased rate of degradation for a more crystalline polymer, since it is also noted that some re-orientation of the degraded amorphous chains could have increase the degree of crystallinity during hydrolysis [8]. It was also observed that the crystals formed through annealing had little effect on the water uptake. It was observed, from **Figure 4.66**, that the water uptake for the non-annealed, amorphous

films were low. The low water uptake for thin films, as also observed by *Venkatraman et al.* [116], can be attributed to the smaller mass of the thin films as compared to the study of larger devices, such as circular plates [71] and matrices [72]. The small difference in water uptake between the annealed and non-annealed films, thus result in an insignificant difference in their rate of hydrolytic degradation. The possibility of the effect of irradiation on the hydrolytic degradation rate, due to the changes of the degree of crystallinity, can therefore be safely ignored. The changes of the molecular weight with radiation therefore have a more significant impact on the degradation rate constant of the polymers, than degree of crystallinity.

(b) Hydrolytic degradation of annealed PLGA after irradiation

It had been observed that irradiated PLGA undergoes re-crystallization when heated, as shown from the DSC thermogram in **Figure 4.21**. This re-crystallization is due the re-orientation of the shorter amorphous chains, as a result of chain scission during irradiation. These chains are therefore less entangled and have better mobility. The re-orientation of these molecules thereby forms a crystalline phase when given sufficient heat energy for the re-orientation of the amorphous chains.

Previously, it was discussed that an increase in DOC for a non-irradiated PLGA would have an insignificant effect on the rate of hydrolytic degradation. However, it was unknown if an increase in DOC for an irradiated PLGA would have a

significant effect on its rate of hydrolytic degradation. This would therefore be studied through the hydrolytic degradation of isothermally annealed PLGA after irradiation.

From **Figure 4.25**, the enthalpy of fusion (ΔH_f) of irradiated PLGA was observed to increase and subsequently stabilize with increasing radiation dose. In this study, 5 Mrad and 20 Mrad irradiated PLGA were annealed to study the effect of crystals, formed through post-irradiation annealing, in retarding hydrolytic degradation. Annealing was conducted at their respective crystallization temperatures, as obtained from **Figure 4.24**, of approximately 125°C (5 Mrad) and 114°C (20 Mrad), and the degree of crystallinity (DOC) obtained was approximately 17 J/g and 23 J/g respectively. These samples were then hydrolytically degraded in PBS solution and the non-annealed 5 Mrad (DOC = 1.5 J/g) and 20 Mrad (DOC = 4 J/g) irradiated PLGA samples. For identification purposes, the non-annealed samples will be identified by their respective radiation doses (‘5 Mrad’ or ‘20 Mrad’), and the annealed samples will be identified as ‘5 Mrad Ann’ and ‘20 Mrad Ann’.

The weight loss for the 5 Mrad Ann and 20 Mrad Ann PLGA samples were plotted against degradation time as shown in **Figure 4.74**. The results show that weight loss commences at an early stage of the degradation study for the 20 Mrad Ann samples, and 20 % of mass loss was observed after 8 weeks of degradation.

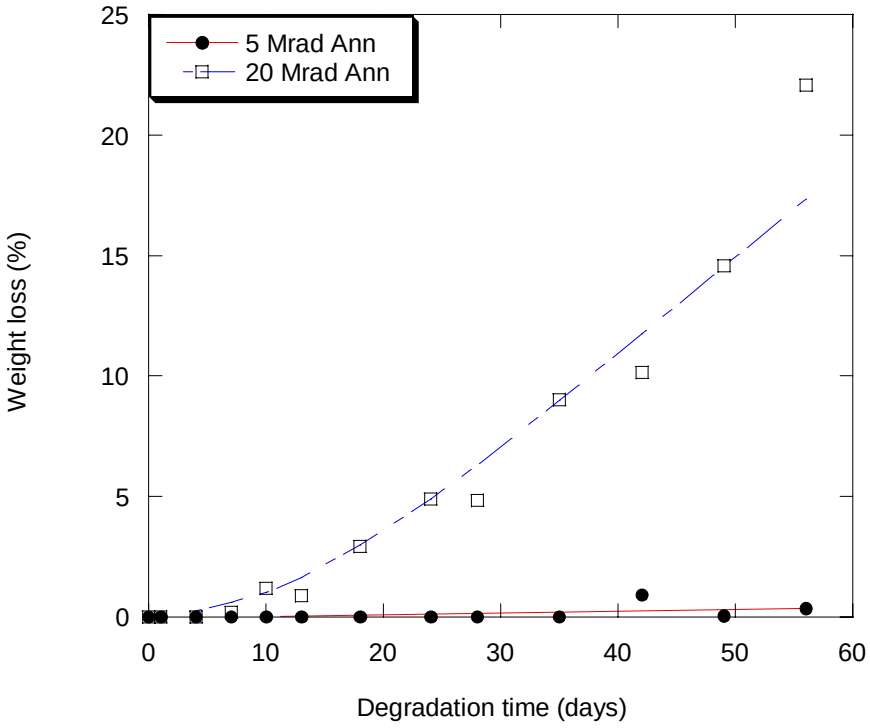

Figure 4.74 – Plot of weight loss of 5 Mrad Ann and 20 Mrad Ann PLGA with degradation time

The water uptake for the irradiated PLGA samples after 7 weeks of degradation is summarized in **Table 4.9**. The results show that the water uptake for the 20 Mrad Ann samples was higher than the 5 Mrad Ann samples. This was due to the lower in molecular weight and the formation of the more hydrophilic hydroxyl groups at higher radiation dose. The higher water uptake for the more highly irradiated PLGA was therefore responsible for the higher mass loss as observed in **Figure 4.74**. In comparison between the non-annealed and annealed PLGA samples, there is no significant difference in their water uptake, irrespective of the radiation dose. This indicates that the increase in the degree of crystallinity had little effect in the water uptake for the annealed PLGA films.

Table 4.9 – Water uptake for irradiated PLGA (non-annealed and annealed) samples after 7 weeks of degradation

Sample	5 Mrad	5 Mrad Ann	20 Mrad	20 Mrad Ann
Water uptake	1.0 %	0.7 %	5.8 %	5.2 %

The plot of the natural logarithmic number-average molecular weight (ln M_n) of the irradiated-annealed samples is shown in **Figure 4.75**. The results show that the molecular weight decrease with degradation time, indicating the hydrolysis of the ester bonds through random chain scission.

From the linear plot obtained from **Figure 4.75**, the degradation rate constant (k), as derived from **Eq. 2.3**, can thus be calculated. The k values are summarized in **Table 4.10**. From **Table 4.10**, it is seemingly observed that for the samples irradiated at 5 Mrad, the annealed samples had a lower k value than the non-annealed sample; and for the PLGA samples irradiated at 20 Mrad, the k value was higher for the annealed sample. A student's t-statistics test (**Eq. 4.7**) was therefore conducted to observe if annealing results in any significant difference in the k values at 95 % confidence level, and at n-2 degrees of freedom. For the 5 Mrad non-annealed samples, the 95 % confidence interval is 0.0263 g/mol.day^{-1} ± 0.00338, in which the k value of the annealed sample falls within this range. Similarly, for the 20 Mrad non-annealed samples, the 95 % confidence interval is 0.0264 g/mol.day^{-1} ± 0.00294. Therefore, there is no significant difference in the k values of annealed and non-annealed samples.

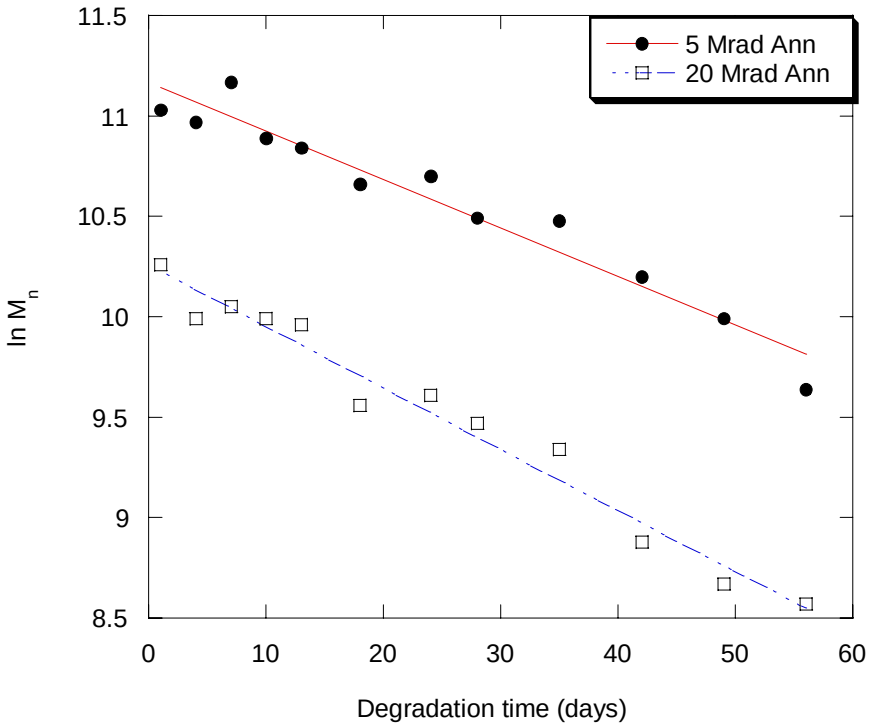

Figure 4.75 – Plot of ln M_n of annealed PLGA (5 Mrad and 20 Mrad) with degradation time

Table 4.10 – Degradation rate constants (k) of irradiated-annealed PLGA films

Sample	5 Mrad	5 Mrad Ann	20 Mrad	20 Mrad Ann
Rate constant ($g/mol.day^{-1}$)	0.0263	0.0241	0.0264	0.0281

The results show that an increase in crystallinity of PLGA, through annealing (for non-irradiated or post-irradiated), had no significant effect on the hydrolytic rate constants. Annealing, though increases the degree of crystallinity, resulted only in

small differences in water uptake of the films. This can be explained from the already low water uptake (< 1%) of the non-annealed films, thus making the existence of crystals seemingly ineffective. The low water uptake of the non-annealed films can be attributed to the small mass of the thin films used in this study, as also observed by *Venkatraman et al.* [116]. The results therefore show that the use of thin films give rise to low water uptake, and the existence of crystals thus had little effect on the degradation rate constants.

(c) Summary

It was reported by several papers, that the degree of crystallinity for PLGA is one of the factors that may affect the rate of hydrolytic degradation, since degree of crystallinity affects the water uptake. However, it was found from this study that the increase in the degree of crystallinity for irradiated and non-irradiated PLGA samples was found to be insignificant in reducing the rate of hydrolytic degradation, due to the low water uptake of thin films. This proves that the changes to the DOC during irradiation will not significantly affect the water uptake and thus the hydrolytic degradation rate of irradiated thin films. The changes in DOC of the irradiated samples may thus be ignored.

Chapter 5 Conclusions

The study of the effects of electron beam (e-beam) radiation on the degradation of PLGA and PLLA was reported in this thesis. The first part of the objective was therefore to examine the radiation-induced degradation of PLGA and PLLA, using e-beam radiation. The results obtained show conclusive evidence that PLGA and PLLA degrade through chain scission when exposed to e-beam irradiation in the presence of air, with minimal cross-linking. Chain scission causes a decrease in the average molecular weights, and thus a corresponding decrease in the glass-transition temperature (T_g), melting temperature (T_m) and crystallization temperature (T_c) of the biodegradable polyesters. The e-beam radiation-induced degradation occurs through backbone main chain scission and hydrogen abstraction. The degradation was observed to follow a 3-stage radiation-induced degradation mechanism. The first stage involves backbone main chain scission as the dominant mechanism. The second stage involves a combination of backbone chain scission and hydrogen abstraction. The third stage involves dominantly hydrogen abstraction. It was also observed that the recombination of free radicals increases with increasing radiation dose. Recombination of free radicals is the result of excessive alkyl free radicals present during irradiation and also due to the “cage effect”, if crystalline phases are present. The difference in degradation mechanism at the three stages and the recombination of free radicals are reasons for the reduction in molecular weight decrease with increasing radiation dose.

Irradiation causes the formation of more hydrophilic hydroxyl groups in PLGA and PLLA due to hydrogen abstraction. The irradiation process also results in the removal of ester bonds from the polyester backbone, in forming carbon dioxide. As a result, a phenomenon, known as the “backbone recombination effect” was observed. Irradiation therefore results in a biodegradable polyester that has higher percentage of lactic acid units along the backbone and hydroxyl groups along the polymer chain.

E-beam irradiation causes the formation of a crystalline phase in the amorphous PLGA but a decrease in degree of crystallinity for the semi-crystalline PLLA. It has been proven that the formation of crystalline regions arrests radiation-induced degradation. This was done by investigating the effect of crystallization on the radiation-induced degradation of PLGA. The isothermal annealing of PLGA films at 115°C encourages the formation of crystals and its degree of crystallinity increases with annealing time. Maximum crystallinity of approximately 12 % was achieved after 120 min of annealing. In spite of the presence of crystals in PLGA, e-beam irradiation still causes polymer degradation through chain scission. Similarly, chain scission results in the decrease of molecular weights and thermal properties of PLGA with radiation dose. However, semi-crystalline PLGA, and PLGA samples of higher degree of crystallinity (~12 %) were better able to retard radiation-induced degradation. This was attributed to the exclusion of oxygen in the crystalline regions and the ‘cage effect’, where more recombination of free radicals would occur within the crystalline regions. However, the recombination of free radicals would result in crystallinity damage and a subsequent decrease in the degree of

crystallinity. In spite of this, the retardation of radiation-induced degradation by crystalline regions was indeed conclusive. The semi-crystalline nature of PLLA is therefore believed to be the key factor in its greater stability to e-beam radiation as compared to PLGA.

The decrease in molecular weight was then observed to follow a linear relationship with radiation dose, when the reciprocal molecular weight was plotted against radiation dose. Equations relating the molecular weight with radiation dose, for both PLGA and PLLA, were thus modeled. These equations were subsequently used to model the relationship between radiation dose and the subsequent hydrolytic degradation times of these biopolymers.

The second part of the main objective was therefore to study the hydrolytic degradation of irradiated PLGA and PLLA. Here, two hypotheses were investigated. Firstly, it is hypothesized that irradiation will accelerate the hydrolytic degradation of PLGA and PLLA. Secondly, it is hypothesized that irradiation at higher radiation doses will result in a faster rate of hydrolysis.

Irradiated samples of PLGA and PLLA, when placed in PBS solution, were found to degrade faster than the non-irradiated samples, by more than twice the hydrolytic degradation rates for both polymers. This was because the irradiated samples had a higher water uptake. This was attributed to the lower T_g, lower molecular weight and more hydroxyl groups for the irradiated polyesters, thus making them more hydrophilic. An increase in hydrophilicity was therefore responsible for the increase

in the influx of water molecules into the polymer matrix, leading to an increase in osmotic pressure and subsequently an increase in mass loss due to microcavitation and osmotic cracking. The hypothesis that radiation increases the rate of hydrolytic degradation was thus proven true for both PLGA and PLLA.

However, the hydrolytic degradation rate constants, for both PLGA and PLLA, remained relatively unchanged irrespective of radiation dose. This was due to the "backbone-recombination effect" where irradiation causes the recombination of skeletal backbones, resulting in the removal of the ester groups in forming carbon dioxide. The irradiated polymer chains therefore have a higher concentration of lactic acid units and fewer ester bonds. This reduction in ester bonds helps to decrease the incidents of chain scission through hydrolysis and thus stabilizing the hydrolytic degradation rates for the highly irradiated polyesters. The hypothesis that higher radiation dose would have a faster rate of hydrolysis was thus appropriately rejected.

The thermal properties of hydrolytically degraded PLGA and PLLA samples also changed with degradation times. The T_m increases for the non-irradiated samples, but decreases for the irradiated samples, due to an increase in crystal defects arising from the re-orientation of the irradiated non-uniform amorphous chains. The splitting of the T_g peaks was observed only for the PLGA samples, indicating the scissioning of the PLA (poly-lactic acid) chains from PLGA. The T_g of the degraded PLGA and PLLA samples thereby decreases with degradation time, which indicates a decrease in chain mobility.

E-beam radiation not only causes a reduction in molecular weight, but also changes the degree of crystallinity for PLGA and PLLA. It was proven that the changes to the degree of crystallinity due to irradiation have an insignificant contribution to the degradation rate constants. This was done by studying the hydrolytic degradation rate of isothermally annealed, non-irradiated and irradiated, PLGA of varying degree of crystallinity. It can therefore be assumed that changes to the degree of crystallinity with irradiation have no significant effect on the degradation rate constant. With this, the molecular weight of irradiated PLGA and PLLA was then appropriately modeled to the radiation dose.

A relationship between radiation dose and the hydrolytic degradation time, through the molecular weights, was thus established for both PLGA and PLLA, and the third part of the thesis objective was met. This relationship allows for a more accurate and precise control of the hydrolytic degradation times of PLGA and PLLA through the use of e-beam radiation, as shown from the equations, **Eq. 4.5** and **Eq. 4.6** respectively. It is thereby concluded that e-beam radiation can be used to accurately control the hydrolytic degradation times of PLGA and PLLA.

Chapter 6 Future Work

Based on existing knowledge of the effects of e-beam radiation degradation on biopolymers, it will help set directions for the future work that can be conducted. The following work could therefore be done in the near future to further substantiate the research work that has been reported in this thesis. These studies will give a greater and deeper understanding on the effects of e-beam on biopolymers.

1. E-beam irradiation of PLGA and PLLA microspheres

Films were used in this thesis for studying the effects of e-beam radiation on the degradation of PLGA and PLLA. However, for drug delivery purposes, where microspheres may be used, the understanding of how microspheres degrade through irradiation and subsequently through hydrolytic degradation would be a more effective study. This would provide a better understanding on the effectiveness of using e-beam radiation in controlling the rate of hydrolytic degradation of PLGA and PLLA microspheres.

Microspheres can be prepared through various techniques, such as the oil-in-water emulsion technique. The study of how the microspheres sizes would affect radiation and hydrolytic degradation could also be studied.

2. Comparison of degradation rates and behaviour of a non-irradiated PLLA and irradiated PLLA of similar molecular weights

It was found that the molecular weight of PLLA (a homo-polymer) decreases with radiation dose, and the rate of hydrolytic degradation increases upon irradiation. It would thus be of interest to study the hydrolytic degradation rate and behaviour of a non-irradiated PLLA, of similar molecular weights. This would give a better understanding on how radiation affects the rate of hydrolytic degradation of PLLA, and the use of radiation to control the rate of degradation and be further justified.

3. In vivo degradation of irradiated PLGA and PLLA

In vitro hydrolytic degradation studies were reported in this thesis. However, it would be of greater interest to understand the in vivo degradation rates and behaviour of these polymers. A study on the in vivo degradation of irradiated PLGA and PLLA, used as temporary implants, would give a more complete insight into the degradation behaviour of these polymers after irradiation.

4. Effects of e-beam radiation on drug release

Biopolymers, such as PLGA and PLLA, are often used for drug release purposes. These polymers can be encapsulated or coated with various drugs, such as Ganciclovir (GCV), and then released at the targeted site over time. Since irradiation was found to decrease the molecular weight of PLGA and PLLA, no

information was found concerning the drug release profiles of these biopolymers after irradiation. It would certainly be of interest to study and understand how radiation can affect the rate of drug release of these drug-incorporated polymers over time.

5. Effects of e-beam radiation on mechanical properties of PLGA and PLLA

E-beam radiation is known to cause a decrease in molecular weight and subsequently degradation in mechanical properties. It would be of interests to study the decrease in mechanical properties and understand the effects radiation dose has on the degradation of mechanical strength.

6. Effects of e-beam radiation on the degradation of other biodegradable polymers

The study of irradiation could also be extent to other biodegradable polymers, such as poly(ethylene glycol) (PEG). The irradiation of other polyesters with an aromatic group would also be an interesting study. This is because the presence of the aromatic group would decrease the water uptake. The ability to retard the rate of hydrolytic degradation would then allow these polymers to be used in situations where a longer degradation time is required. The irradiation and subsequent hydrolytic degradation of these polymers could then be investigated.

Chapter 7 References

[1] Park JB, Lakes RS. Biomaterials: An introduction. New York: Plenum Press, 1979. p.1-6

[2] Wang HT, Schmitt E, Flanagan DR, Linhardt RJ. Influence of formulation methods on the in vitro controlled release of protein from poly(ester) microspheres. J of Controlled Release 1991; (17): 23-32

[3] Linhardt RJ, Flanagan DR, Schmitt E, Wang HT. Quantitative analysis of the monomer products formed on the hydrolysis of poly(esters) and poly(anhydrides). Polymer Prepr 1989; (30): 464-465

[4] Linhardt RJ, Flanagan DR, Schmitt E, Wang HT. Biodegradable poly(esters) and the delivery of bioactive agents. Polymer Prepr 1990; (30): 249-250

[5] Dahlmann J, Rafler G, Fechner K, Mehlis B. Synthesis and properties of biodegradable aliphatic polyesters. British Polym J 1990; (23): 235-240

[6] Pitt CG, Gratzl MM, Kimmel GL, Surles J, Schindler A. Aliphatic polyester II. The degradation of poly (DL-lactide), poly (ε-caprolactone) and their copolymers in vivo. Biomaterials 1981; (2): 215-220

[7] Peppas NA, Huang Y, Torres-Lugo M, Ward JH, Zhang J. Physicochemical foundations and structural design of hydrogels in medicine and biology. Annual Review of Biomedical Engineering 2000; (2): 9-27

[8] Wu XS. Synthesis and properties of biodegradable lactic/glycolic acid polymers. Encyclopedic handbook of biomaterials and bioengineering. New York: Marcel Dekker, 1995. p. 1015-1054

[9] Jain RA. The manufacturing techniques of various drug loaded biodegradable poly(lactide-co-glycolide) (PLGA) devices. Biomaterials 2000; (21): 2475-2490

[10] Arshady R. Preparation of biodegradable microspheres and microcapsules: 2. Polylactides and related polyesters. J of Controlled Release 1991; (17): 1-22

[11] Barrows TH. Degradable implant materials: A review of synthetic absorbable polymers and their applications. Clin Mater 1986; (1): 233-257

[12] Raghuvanshi RS, Singh M, Talwar GP. Biodegradable delivery system for single step immunization with tetanus toxoid. Int. J. Pharm. 1993; (93): R1-5

[13] Freed LE, Gordana VN, Langer R. Biodegradable polymer scaffolds for tissue engineering. Bio-Technology 1994; (12): 689-693

[14]Griffith LG. Polymeric biomaterials. Acta Materialia 2000; (48): 263-277

[15] Tice TR, Tabibi ES. Parenteral drug delivery: injectables. Treatise on controlled drug delivery: fundamentals optimization, applications. New York: Marcel Dekker, 1991. p. 315-339

[16] Kitchell JP, Wise DL. Poly(lactic/glycolic acid) biodegradable drug-polymer matrix systems. Methods Enzymol 1985; (112): 436-448

[17] Lewis DH, in: Chasin M, Langer RS, editors. Controlled release of bioactive agents from lactide/glycolide polymers. Biodegradable polymers as drug delivery systems. New York: Marcel Dekker, 1990. p. 1-41

[18] Cohen S, Alonso MJ, Langer R. Novel approaches to controlled-release antigen delivery. Int. J. Technol Assessment Health Care 1994; (10): 121-130

[19] Chapiro A. Radiation chemistry of polymeric systems. London: Interscience, 1962. p. 353

[20] Charlesby A. Radiation chemistry principles and applications, New York: VCH, 1987. p. 451

[21] Ichikawa T. Mechanism of radiation-induced degradation of poly(methyl methacrylate) - temperature effect. Nuclear Instruments and Methods in Physics Research Section B 1995; (105): 150-153

[22] Charlesby A. Atomic radiation and polymers. England, Oxford: Pergamon, 1960

[23] D'Alelio GF, Haberli R and Pezdirtz GF. Effect of ionizing radiation on a series of saturated polyesters. J. Macromol. Sci. Chem. 1968; (A2-3): 501-588

[24] Gillen KT, Clough RL, in: Clegg DW, Collyer AA, editors. Irradiation effects on polymers. London: Elsevier, 1991. p. 157

[25] Carlsson DJ, in: Scott G, editor. Atmospheric oxidation and antioxidants. Amsterdam: Elsevier, 1993. p. 495

[26] Pionteck J, Hu J, Pompe G, Albrecht V, Schulze U, Borsig E. Characterization of radiation behaviour of polyethylene/polymethacrylates interpenetrating polymer networks. Polymer 2000; (41): 7915-7923

[27] Goldman M, Gronsky R, Ranganathan R, Pruitt L. The effects of gamma radiation sterilization and ageing on the structure and morphology of medical grade ultra high molecular weight polyethylene. Polymer 1996; (37): 2909-2913

[28] Krupa I, Luyt AS. Thermal properties of isotactic polypropylene degraded with gamma irradiation. Polymer Degradation and Stability 2001; (72): 505-508

[29] Tidjani A, Watanabe Y. Study of the effect of γ-dose rate on the oxidation of polypropylene. J. Appl. Polym. Sci. 1996; (60): 1839-1845

[30] Williams JL. Stability of polypropylene to gamma irradiation. In: Clough RL, Shalaby SW, editors. Radiation effects on polymers. ACS symposium Series 475, 1990. p. 554-568

[31] Ramani R, Ranganathaiah C. Degradation of acrylonitrile-butadiene-styrene and polycarbonate by UV irradiation. Polymer Degradation and Stability 2000; (69): 347-354

[32] Park K, Chin EY. Effect of diamond-like carbon thin film deposition on the resistance of polycarbonate to radiation-induce degradation. Polymer Degradation and Stability 2000; (68): 93-96

[33] Sen M, Uzun C, Kantoglu O, Erdogan SM, Deniz V, Guven O. Effect of gamma irradiation conditions on the radiation-induced degradation of isobutylene-isoprene rubber. Nucl. Instr. & Meth. in Phys. Res B 2003; (208): 480-484

[34] Gupta MC, Deshmukh VG. Radiation effects on poly(lactic acid). Polymer 1983; (24): 827-830

[35] Montanari L, Cilurzo F, Valvo L, Faucitano A, Buttafava A, Groppo A, Genta I, Conti B. Gamma irradiation effects on stability of poly(lactide-co-glycolide) microspheres containing clonazepam. J of Controlled Release 2001; (75): 317-330

[36] Birkinshaw C, Buggy M, Henn GG, Jones E. Irradiation of poly-D,L-lactide. Polymer degradation and stability 1992; (38): 249-253

[37] Dieck EL, Holl P. Experiences with inert-gas-free electron beam curing of coatings on formed parts, Radcure-Society of Manufacturing Engineers 1985: FC85-445

[38] Moore DW, Electron bombardment in thin film microcircuitry production. Electron beam technology: Fourth Symposium. Massachusetts, 1962. Cambridge, Mass.: Alloyed Electronics, 1962, p. 324-339

[39] Lancker MV, Herer A, Cleland MR, Jongen Y, Abs M. The IBA Rhodotron: an industrial high-voltage high-powered electron beam accelerator for polymers radiation processing. Nuclear Instruments and Methods in Physics Research Section B: Beam Interactions with Materials and Atoms 1999; (151): 242-246

[40] Chu CC, Campbell ND. Scanning electron microscopic study of the hydrolytic degradation of poly(glycolic acid) suture. J. Biomed. Mat. Res. 1982; (16): 417-430

[41] Gilding DK, Reed AM. Biodegradable polymers for use in surgery – Polyglycolic /polylactic acid homo- and copolymers. Polymer 1979; (20): 1459-1464

[42] Jalil R, Nixon JR. Biodegradable poly(lactic acid) and poly(lactide-co-glycolide) microcapsules: problems associated with preparative techniques and release properties. J Microencapsulation 1990; (7): 297-325

[43] Benicewicz BC, Hopper PK. Polymers for absorbable surgical suture. Part II. J. Bioact Compatib Polym 1991; (6): 64-94

[44] Belbella A, Vauthier C, Fessi H, Devissaguet JP, Puisieux F. In vitro degradation of nanospheres from poly(D,L-lactides) of different molecular weights and polydispersities. Intl. J. of Pharmceut. 1996; (129): 95-102

[45] Zhu X, Lu L, Currier BL, Windebank AJ, Yaszemski MJ. Controlled release of NFκappaB decoy oligonucleotides from biodegradable polymer microparticles. Biomaterials 2002; (23): 2683-2692

[46] Sperling LH. Molecular weights and sizes. Introduction to physical polymer science. Canada: John Wiley & Sons, 1986, p. 56-94

[47] Sperling LH. Introduction to polymer science. Introduction to physical polymer science. Canada: John Wiley & Sons, 1986, p. 1-21

[48] Cohn D, Younes H, Marom G. Amorphous and crystalline morphologies in glycolic acid and lactic acid polymers. Polymer 1987; (28): 18-22

[49] Holland SJ, Tighe BJ, in: Ganderton D, Jones TJ, editors. Biodegradable polymers. Advances in pharmaceutical sciences. London: Academic Press, 1992. Vol. 6, p. 101-164

[50] Jamshidi K, Hyon SH, Ikada Y. Thermal characterization of polylactides. Polymer 1988; (29): 2229-2234

[51] Pitt CG, Schindler A, in: Hafez ESE, van Os WAA, editors. The design of controlled drug delivery systems based on biodegradable polymers. In progress in contraceptive delivery systems, Vol. 1, Biodegradables and delivery systems for contraception. Lancaster, England: MTP Press, 1980, p. 17-46

[52] Fox TG, Flory PJ. J. Appl Phys 1950; (21): 581

[53] Conti B, Pavanetto F, Genta I. Use of polylactic acid for the preparation of microparticulate drug delivery systems. J. Microencapsulation 1992; (9): 153-166

[54] Linhardt RJ, in: Rosoff M, editor. Biodegradable polymers for controlled release of drugs. Controlled release of drugs: Polymers and aggregate systems. New York: VCH Publishers, 1989, p. 53-95

[55] Tice TR, Cowsar DR. Biodegradable controlled-release parenteral systems. Pharm Technol 1994; (11): 26-35

[56] Hollinger JO, Battistone GC. Biodegradable bone repair materials: Synthetic polymers and ceramics. Clin Orthop Related Res 1986; (207): 290-305

[57] Li SM, Garreau H, Vert M. Structure-property relationships in the case of the degradation of massive aliphatic poly-(α-hydroxy acids) in aqueous media. Part I: Poly(D,L-lactic acid). J. Mater Sci: Mater Med 1990; (1): 123-130

[58] Thies C, Bissery MC, in: Lim F, editor. Biodegradable microspheres for parenteral administration, Biomedical Applications of Microencapsulation. Boca Raton, FL: CRC Press, 1984, p. 53-74

[59] Anderson JM. Perspectives on the in vivo responses of biodegradable polymers. In: Hollinger JO, editor. Biomedical applications of synthetic biodegradable polymers. Boca Raton, FL: CRC Press, 1995. p. 223-233

[60] Li S, Vert M. Biodegradation of aliphatic polyesters. In: Scott G, Gilead D, editors. Degradable polymers – principles and applications. London: Chapman and Hall, 1995. p. 43-87

[61] Chu C. Degradation and biocompatibility of synthetic absorbable suture materials: general biodegradation phenomena and some factors affecting biodegradation. In: Hollinger JO, editor. Biomedical applications of synthetic biodegradable polymers. Boca Raton, FL: CRC Press, 1995. p. 103-128

[62] Farrar DF, Gillson RK. Hydrolytic degradation of polyglyconate B: the relationship between degradation time, strength and molecular weight. Biomaterials 2002; (23): 3905-3912

[63] Zhu JH, Shen ZR, Wu LT, Yang SL. In vitro degradation of polylactide and poly(lactide-co-glycolide) microspheres. J. Appl polym Sci 1991; (43): 2099-2106

[64] Scott G, Gilead D. Degradable polymers: principles and applications. London: Chapman & Hall, 1995. p. 1-40

[65] Reed AM, Gilding DK. Biodegradable polymers for use in surgery – Poly(glycolic)/Poly(lactic acid) homo- and copolymers. 2. In vitro degradation. Polymer 1981; (22): 494-498

[66] Schliecker G, Schmidt C, Fuchs S, Wombacher R, Kissel T. Hydrolytic degradation of poly(lactide-co-glycolide) films: effect of oligomers on degradation rate and crystallinity. Int. J. Pharmaceut. 2003; (266): 39-49

[67] Eldsater C, Erlandsson B, Renstad R, Albertsson AC, Karlsson S. The biodegradation of amorphous and crystalline regions in film-blown poly(ε-caprolactone). Polymer 2000; (41): 1297-1304

[68] Vert M, Li SM, Garreau H. More about the degradation of LA/GA-derived matrices in aqueous media. J Contr. Rel. 1991; (16): 15-26

[69] Grizzi I, Garreau H, Li SM, Vert M. Biodegradation of devices based on poly(DL-lactic acid): size dependence. Biomaterials 1995; (16): 305-311

[70] Grijmpa DW, Pennings AJ. (Co)polymers of L-lactide. 1. Synthesis, thermal properties and hydrolytic degradation. Macromol. Chem. Phys. 1994; (195): 1633-1647

[71] Li S, McCarthy S. Further investigations on the hydrolytic degradation of poly(DL-lactide). Biomaterials 1999; (20): 35-44

[72] Gautier L, Mortaigne B, Bellenger V, Verdu J. Osmotic cracking nucleation in hydrothermal-aged polyester matrix. Polymer 2000; (41): 2481-2490

[73] Huh SJ, Park W, Ju SG, Lee JE, Han Y. Small-bowel displacement system for the sparing of small bowel in three-dimensional conformal radiotherapy for cervical cancer. Clin Oncol (R Coll Radiol) 2004; (16):467-473

[74] Blankenberg FG, Mari C, Strauss HW. Development of radiocontrast agents for vascular imaging: progress to date. Am J Cardiovas Drugs 2002; (2): 357-365

[75] Kotov YA, S. Sokovnin Y, Balezin ME. A review of possible applications of nanosecond electron beams for sterilization in industrial poultry farming. Trends in Food Science & Technology 2003; (14): 4-8

[76] Moran LM, Rodriguez R, Calzado A, Turrero A, Arenas A, Cuevas A, Garcia-Castano B, Gomez N, Moran P. Image quality and dose evaluation in spiral chest CT examinations of patients with lung carcinoma. Br J Radiol. 2004; (77): 839-846

[77] Katsura I. Current status and future prospect of electron beam sterilization in Japan. Radiation Physics and Chemistry 1998; (52): 599-601

[78] De Lara J, Fernández PS, Periago PM and Palop A. Irradiation of spores of Bacillus cereus and Bacillus subtilis with electron beams. Innovative Food Science & Emerging Technologies 2002; (3): 379-384

[79] Bly JH. Electron beam processing. Radiation sources. International Information Associates, Pennsylvania: Yardley, 1988, p. 9-15

[80] Kelen T. Oxidative degradation. Polymer degradation. New York: VNR, 1983, p. 107-136

[81] Spadaro G, Dispenza C, Giammonaa G, Pitarresia G Cavallaro G. Cytarabine release from α, β-poly(N-hydroxyethyl)-aspartamide matrices cross-linked through γ-radiation. Biomaterials 1996; (17): 953-958

[82] Fisher JP, Dean D, Engel PS, Mikos AG. Photoinitiated polymerization of biomaterials. Annual Review of Materials Res. 2001; (31): 171-181

[83] Janik I, Kasprzak E, Al-Zier A, Rosiak JM. Radiation crosslinking and scission parameters for poly(vinyl methyl ether) in aqueous solution. Nucl. Instr. and Meth. Phys. Res. B 2003; (208): 374-379

[84] Schnabel W, in: Guven O (Ed.). Cross-linking and scission in polymer. NATO ASI series. The Netherlands: Kluwer Academic Publishers, 1988, p. 15

[85] Kelen T. Photodegradation. Polymer degradation. New York: VNR, 1983, p. 137-151

[86] Carlsson DJ, Chmela S, in: Scott G, editor. Polymers and high-energy irradiation: Degradation and stabilization. Mechanism of polymer degradation and stabilization. New York: Elsevier, 1990, p. 109-134

[87] Partridge RH. J Chem Phys 1970; (52): 2485

[88] Tsuda M, Oikawa S. J Polym Sci, Polym Chem Ed 1979; (17): 3759

[89] Falconer WE, Salovey R. J Chem Phys 1966; (44): 3151

[90] Franck J, Rabinowitch E. Some remarks about free radicals and the photochemistry of solutions. Trans. Faraday. Soc. 1934; (30): 120-131

[91] Montanari L, Costantini M, Signoretti EC, Cilurzo F, Valvo L, Onori S, Faucitano A, Genta I, Conti B, Genta I. Gamma irradiation effects on poly(DL-lactide-co-glycolide) microspheres. J. of Contr. Rel. 1998; (56): 219-229

[92] Suljovrujic E, Ignjatovic N, Uskokovic D. Gamma irradiation processing of hydroxyapatite/poly-L-lactide composite biomaterial. Rad. Phys. and Chem. 2003; (67): 375-379

[93] Montanari L, Cilurzo F, Selmin F, Conti B, Genta I, Poletti G, Orsini F, Valvo L. Poly(lactide-co-glycolide) microspheres containing bupivacaine: comparison between gamma and beta irradiation effects. J. of Contr. Rel. 2003; (90): 281-290

[94] Kantoglu O, Guven O. Radiation induced crystallinity damage in poly(L-lactic acid). Nuclear Instruments & Methods in Physics Research B 2002; (197): 259-264

[95] Chu CC, Zhang L, Coyne, LD. Effect of gamma irradiation and irradiation temperature on hydrolytic degradation of synthetic absorbable sutures. J. Appl. Polym. Sci. 1995; (56): 1275-1294

[96] Louwe C. Certificate of Analysis for PLGA(80:20) and PLLA. Purac Biochem.

[97] Smith D. Electron accelerator radiation protection – Lecture 10, New product lecture series, 1963. Burlington, Mass.: High Voltage Engineering Corp, 1963

[98] British Standard. Practice for dosimetry in an electron-beam facility for radiation processing at energies between 80 keV and 300 keV. International Standard ISO 15573 1998; 1st Ed.

[99] Pappas SP. EB curing – General Principles. Radiation curing – Science and technology. New York & London: Plenum Press, 1992, p. 16-18

[100] Blake DE. Radiation processing: Principles and applications of EB and UV processors. Finishing-Society of Manufacturing Engineers 1985; FC85-743

[101] Energy Science Inc (ESI). Electrocure / Electrocurtain systems operations and maintenance manual. United Kingdom, 1997

[102] Loo SCJ, Ooi CP, Boey YCF. Radiation effects on poly(lactide-co-glycolide) (PLGA) and poly(L-lactide) (PLLA). Polym Degrad Stab 2004; (83): 259-265

[103] Cowie JMG. Polymers: Chemistry & physics of modern materials. New York: Chapman and Hall, 1991. p. 184-222

[104] Lee TH, Boey FYC, Khor KA. On the determination of polymer crystallinity for a thermoplastic PPS composite by thermal analysis. Composites Sci. & Technol. 1995; (53): 259-274

[105] Sosnowski S. Poly(L-lactide) microspheres with controlled crystallinity. Polymer 2000; (42): 637-643

[106] Cullity BD. Elements of X-ray diffraction. Philippines: Addison-Wesley Publishing Company Inc, 1978 (2nd ed). p. 284-285

[107] Alexander LE. X-ray diffraction methods in polymer science. New York: John Wiley & Sons, 1969. p. 285-293

[108] Lin-Vien D, Colthup NB, Fateley WG, Grasselli JG. The handbook of infrared and Raman characteristic frequencies of organic molecules. Boston: Academic Press, 1991

[109] Bruice PY, in: Challice J, editor. Organic chemistry. New Jersey: Prentice Hall, 2001 (3rd ed). p. 534-577

[110] Bakhtiar C, Hardy DT. Lectures on organic chemistry. London: Imperial College Press & World Scientific Publishing, 1997. p. 409-411

[111] Loo JSC, Ooi CP, Boey FYC. Degradation of poly(lactide-co-glycolide) (PLGA) and poly(L-lactide) (PLLA) by electron beam radiation. Biomaterials 2005; (26): 1359-1367

[112] Lapin LL, in: Payne M, editor. Probability and statistics for modern engineering. Boston: PWS-Kent, 1990 (2nd ed). p. 388-435

[113] Schumacher BW. A review of the (macroscopic) laws for the electron penetration through matter. Electron and ion beam science and technology: First international conference. Toronto, Canada, 1964. New York: John Wiley, 1965, p. 5-70

[114] Loo SCJ, Ooi CP, Wee SHE, Boey YCF. Effect of isothermal annealing on the hydrolytic degradation rate of poly(lactide-*co*-glycolide) (PLGA). Biomaterials 2005; (26): 2827-2833

[115] Loo SCJ, Ooi CP, Boey YCF. Influence of electron-beam radiation on the hydrolytic degradation behaviour of poly(lactide-*co*-glycolide) (PLGA). Biomaterials 2005; (26): 3809-3817

[116] Venkatraman S, LP Tan, V Tjong, HM Koon, F Boey. Collapse pressures of biodegradable stents. Biomaterials 2003; (24): 2105-2111